

Electric Power Grid Resilience Against Electromagnetic Pulse (EMP) Disturbances

by Dingwei Wang

B.S. in Electrical Engineering, May 2018, Marquette University

A Thesis submitted to

The Faculty of
The School of Engineering and Applied Science
of The George Washington University
in partial satisfaction of the requirements
for the degree of Master of Science

May 17, 2020

Thesis directed by

Payman Dehghanian
Assistant Professor of Electrical and Computer Engineering

© Copyright 2020 by Dingwei Wang
All rights reserved

Dedication

This MS Thesis is lovingly dedicated to my parents (Yongliang Wang and Limin Ma), without whom my achievements so far could never be accomplished. They are the ones always nursing me with affections and love. Their support and encouragement have sustained me throughout my university life.

Acknowledgments

I would like to express my sincere gratitude to my advisor, Prof. Payman Dehghanian, for his guide, understanding, wisdom, patience, encouragements, and for supporting me reach this point. His guidance and feedback helped me in all the time of courses, research and writing of this thesis. Thanks also to my committee members, Prof. Milos Doroslovacki and Prof. Shahrokh Ahmadi, for their time and patience.

Appreciation goes to my friends and the member of the Smart Grid Laboratory for making my time at the George Washington University a wonderful experience.

Most of all, I am fully indebted to my parents for their terrific support, without which, the pursuit of this advanced degree would never have been started and accomplished.

Abstract

Electric Power Grid Resilience Against Electromagnetic Pulse (EMP) Disturbances

Electromagnetic pulse (EMP) disturbances have been received, along with other cyber and physical attacks, as a potential threat to modern digitized power grids and the national security. While the EMP attacks are not lethal to human being, they bring extremely harmful and unrecoverable damages to electronics. Irrespective of the type of the EMP attacks, either nuclear or nonnuclear, EMPs are considered among the high-impact low-probability (HILP) weapon of mass destruction (WMD) and weapon of mass effect (WME) events. While such severe events cause electronics melt down with prolonged and extensive electric outages, the conventional reliability view is insufficient to coping with such challenges on the modern power systems. The detection technology on such weapons is in lack of advanced developments and the attack forewarning is extremely hard to predict. Therefore, detection techniques, modeling frameworks, and mitigation plans against which is a necessity to ensure and further improve the resilience of the power grids against such HILP events.

This thesis firstly focuses on investigating damages caused by EMP attacks of different patterns and realizations. Individual component in power grids such as coaxial wires and transmission towers will be analyzed under EMP attack scenarios to evaluate their vulnerability and electromagnetic compatibility (EMC). Grid scale system vulnerability to EMP threats is next pursued on various networks of different size and complexity such as 4-bus, 150-bus, and 2000-bus systems. Eventually, some protection and mitigation plans against EMP attacks will be studied, where simulations support the protection effectiveness and resilience in power grids against EMP attacks.

Table of Contents

Dedication	iv
Acknowledgments	v
Abstract	vi
List of Figures	ix
List of Tables	xi
1 Introduction	1
1.1 Problem Statement	1
1.2 On The Concept of Resilience	4
1.3 Thesis Outline	9
2 Literature Review	11
2.1 Introduction	11
2.2 EMP Classification	11
2.2.1 Nuclear EMP (NEMP)	11
2.2.2 Nonnuclear EMP (NNEMP)	13
2.3 Potential Impacts of EMP Attacks on Power Grids	14
2.4 Typical EMP Simulation Approach	16
2.5 EMP Simulation Algorithms	18
2.6 EMP Threat Detection in Power Systems	20
2.7 Power Grid Resilience to EMPs	21
3 EMP Attack Characterization in Power Systems	24
3.1 Introduction	24
3.2 Simulations on Bare Wire and Coaxial Cable	24
3.3 Simulations on Cell Tower	28
3.4 Simulations on Overhead Transmission Line Tower	29
3.5 Conclusion	32
4 Grid Scale Vulnerability Assessment to EMP Attacks	33
4.1 Introduction	33
4.2 Simulations on the 4-Bus Test System	33
4.3 Simulations on the 150-Bus Test System	38
4.4 Simulations on the 2000-Bus Test System	43
4.5 Conclusion	55
5 Protection and Mitigation Plans Against EMP Attacks on Power Systems	56
5.1 Introduction	56
5.2 Contemporary Protection Plans Against EMP Attacks	56
5.3 Evaluation of Time Domain Test of EMP Shielding Effectiveness	59

5.4 Contemporary Mitigation Plan Against EMP Attacks	62
5.5 Future Protection and Mitigation Trends	64
5.6 Conclusion	64
6 Conclusion	65
6.1 Conclusion	65
6.2 Future Research	66
Bibliography	67

List of Figures

1.1	Elements of Resilience by Electric Power Research Institute (EPRI)	7
1.2	The Conceptual Resilience Curve Related to A HILP Event	8
2.1	Nuclear EMP Waveform [1].	12
2.2	Explosive Pumped Coaxial Flux Compression Generator [2].	13
3.1	Bare Cable Designed in CST Studio Suite	25
3.2	Electric Field Propagation in Bare Wire	26
3.3	Structure of Coaxial Cable	27
3.4	EMP Excitation Signal in CST Studio Suite	27
3.5	Current Induced in Bare Wire and Coaxial Wire	28
3.6	EMP Waveform Incident on Cell Tower	30
3.7	Residual Energy Left on Cell Tower After the Incident	31
3.8	EMP Incident on Overhead Transmission Line Tower	32
4.1	Four Bus System	34
4.2	4-Bus Test System with GICs Visualized for 24 V/km Eastward E-Field . . .	35
4.3	4-Bus Test System Sensitivity Analysis	37
4.4	The 150-Bus Test System in the State of Tennessee	38
4.5	Electric Field Contour Map at Time Step $t= 0$ Second	39
4.6	Electric Field Contour Map at Time Step $t= 28800$ Seconds	39
4.7	Electric Field Contour Map at Time Step $t= 68000$ Seconds	40
4.8	Electric Field Contour Map at Time Step $t= 150000$ Seconds	40
4.9	Electric Field Contour Map at Time Step $t= 172790$ Seconds	41
4.10	Effective GIC Plot for Each Transformers in the 150-Bus Test System	42
4.11	The Total GIC-Induced Mvar Losses Plot for All Transformers in the 150-Bus Test System	42
4.12	Distribution of the Total GIC Reactive Power Loss for Each Transformers in the 150-Bus Test System	42
4.13	Texas 2000-Bus Test System	43
4.14	The 2000-Bus Test System Electric Field Contour Map at $t = 0$ Second . . .	45
4.15	The 2000-Bus Test System Electric Field Contour Map at $t = 20$ Seconds . .	46
4.16	The 2000-Bus Test System Electric Field Contour Map at $t = 30$ Seconds . .	47
4.17	The 2000-Bus Test System Electric Field Contour Map at $t = 50$ Seconds . .	48
4.18	The 2000-Bus Test System Electric Field Contour Map at $t = 60$ Seconds . .	49
4.19	The 2000-Bus Test System Substations Electric Field at $t = 0$ Second to $t = 80$ Seconds	50
4.20	The 2000-Bus Test System Transformer Effective GIC at $t = 0$ second to $t = 80$ Seconds	50
4.21	The 2000-Bus Test System Substation Reactive Power Loss at $t = 0$ Second to $t = 80$ Seconds	50
4.22	The 2000-Bus Test System Transformer Effective GIC Ranking	51

4.23	The 2000-Bus Test System Transformer Effective GIC Sensitivity Analysis .	52
4.24	The 2000-Bus Test System Line Amp Input Sensitivity Analysis	53
5.1	Contemporary Protection Plan Against EMP Attacks	59
5.2	A Turnkey Solution Against EMP for Industries	60
5.3	Simulation Model Setup	61
5.4	Probe Reading Under Unprotected Condition	61
5.5	Probe Reading Under Protected Condition	62

List of Tables

1.1	Statistics of Outage Events in the U.S. Between 1984-2006	1
1.2	The Conceptual Contrast Between Reliability and Resilience	4
2.1	Potential Impacts of HILP EMPs on Critical Infrastructures [3]	15

Chapter 1: Introduction

1.1 Problem Statement

In the recent years, more frequent realization of the high-impact low-probability (HILP) hazards and catastrophe have resulted in prolonged electricity outages, excessive equipment damages, and even more severe economic loss and disruptions in our modern society [4–6]. The HILP events include two categories of external events that may hit the power grid at anytime and anywhere: (i) natural disasters, such as hurricanes, earthquakes tornadoes, windstorms, wildfires, ice storms, etc [7–18]; (ii) man-made disasters, such as cyber attacks or physical attacks on power system infrastructure [19–22].

Table 1.1: Statistics of Outage Events in the U.S. Between 1984-2006 [23]

Statistics for Outage Cause Categories			
	% of events	Mean size in MW	Mean size in customers
Earthquake	0.8	1,408	375,900
Tornado	2.8	367	115,439
Hurricane/Tropical Storm	4.2	1,309	782,695
Ice Storm	5	1,152	343,448
Lightning	11.3	270	70,944
Wind/Rain	14.8	793	185,199
Other cold weather	5.5	542	150,255
Fire	5.2	431	111,244
Intentional attack	1.6	340	24,572
Supply shortage	5.3	341	138,957
Other external cause	4.8	710	246,071
Equipment Failure	29.7	379	57,140
Operator Error	10.1	489	105,322
Voltage reduction	7.7	153	212,900
Volunteer reduction	5.9	190	134,543

Table 1.1 shows the statistics of 933 electric outage events, reported by the North American Electric Reliability Corporation (NERC), between 1984 to 2006 [23]. Extreme weathers and natural disasters have relatively low frequencies, but a greater impact on the electric power supply and a larger size of the affected electricity customers, among the

introduced outage cause categories.

Different from other types of HILP events a power grid may be vulnerable to, a weapon of mass destruction (WMD) is a type of weapon inflicting mass casualties and/or destroying or rendering high-value assets as useless. Typical WMD include chemical, biological, nuclear, and radiological weapons. This became painfully true from the 9/11 attacks [24]. The term weapon of mass effect (WME) describes the human reactions and events surrounding the use of a WMD that may result in limited, no casualties or physical damage on human. The mass effects may be sensationalized media reporting, panic, and social and political change after WMD is used [21, 24].

Electromagnetic pulse has recently attracted a lot of attention from the society and the national homeland security department. Electromagnetic pulse abbreviated as EMP, is a type of weapon that fall into the category of HILP events, WMD, and WME mentioned above. EMP is a set of burst of electromagnetic radiations generated by a rapid explosion. Broadly defined, an EMP is any transient burst of electromagnetic energy, with a very sharp leading edge building up quickly to a maximum level. Its frequency ranges from direct current (DC), zero Hz, to some upper limits depending on the source [21, 25, 26]. Characterized by their magnitudes, frequencies, footprint, and type of energy, there are many different types, such as static electricity sparks, interference from nuclear EMP and non-nuclear EMP weapons, gasoline engine sparks, lightning, electric switching, and geomagnetic disturbances (GMD) caused by solar corona mass ejections (CME) [27], [28].

The EMP is, in fact, an electromagnetic shock wave [29]. This pulse of energy produces a powerful electromagnetic field, particularly within the vicinity of the weapon burst. The field can be sufficiently strong to produce short lived transient voltages of thousands of volts on exposed electrical conductors, such as wires or conductive tracks on printed circuit boards, where exposed. It is this aspect of the EMP consequence which is of military concern, as it can result in irreversible damages to a wide range of electrical and electronic equipment, particularly computers, radios, or radar receivers. Subject to the electromagnetic

hardness of the electronics, a measure of the equipment's resilience to this effect, and the intensity of the field produced by the weapon, the equipment can be irreversibly damaged or in effect electrically destroyed. The damage inflicted is not unlike that experienced through exposure to close proximity lightning strikes, and may require complete replacement of the equipment, or at least substantial portions thereof.

The first found of EMP related project is the discovery of Compton Effect. In 1925, Physicist Arthur H. Compton found unexpected electromagnetic radiation during the study of the nuclear reaction, laying the foundation for its use as an offensive weapon [30]. To nuclear EMPs, there can be found two real nuclear damage incidents in history. In 1961, The Soviet Union hosted an air-explosive nuclear test at an attitude of 35 km over the Novaya island. It was unexpected that the hydrogen bomb not only destroyed almost everything near the explosion, but also caused an impact on electronic systems thousands of kilometers away. Communication systems around that area were interrupted, and the military equipment on the island could not function for a year [30]. In 1962, The United States tested a 1.4 million tons hydrogen bomb over the middle of Pacific Ocean. It radiated a huge amount of gamma rays, damaging the oxygen and nitrogen in that area, and releasing huge amount of electrons. The weapon damaged the Hawaiian street lamp which was 3,000 kilometers away. Even the radio navigation system that far away in Australia was in chaos for 18 hours [30].

Much of the knowledge and understanding of the EMP threat is based upon testing a prior generation of devices and components, some of which are being replaced with newer technologies that have not been yet adequately tested and protected against EMP impacts. Therefore, a full analyses of the impacts caused by various types of EMP attacks and an estimate of the power system economical and physical losses in facing such threats are becoming necessary and urgent. In the mean time, the task of enhancing power system resilience against such modern attack mechanisms should also be on the federal, industrial, and academic agenda.

1.2 On The Concept of Resilience

Unlike the widely adopted terminology "reliability" in many traditional principles, power system resilience is an emerging concept and its definition is unclear and unfocused thus far; nonetheless, the definition has a common comprehension. "Resilience" and "Reliability" seem to have a similar but essentially distinct meanings. The key characteristic difference between the terms resilience and reliability is presented in Table 1.2 [4, 31].

Table 1.2: The Concept Contrast Between Reliability and Resilience [31]

Reliability	Resilience
High-probability, low-impact	Low-probability, high-impact
Static	Adaptive, ongoing, short- and long-term
Evaluates the power system states	Evaluates the power system states <i>and</i> transition times between states
Concerned with customer interruption time	Concerned with customer interruption time <i>and</i> the infrastructure recovery time

The existing reliability metrics do not concentrate on the consequence of individual HILP events. Instead, the reliability principals focus primarily on the maintainability of the electric equipment [32–52] as well as the system supply adequacy and security in facing the high-probability credible contingencies, and in presence of renewable variations [53–78] and integration of other modern technologies in the grid [15, 79–107]. Beyond minimizing the probability of extensive and prolonged outages, resilience also takes the following into account: acknowledgment of the occurrence of such outages, preparation to cope with them, minimization of the outage effect, rapid service restoration and learning from the experience to enhance the future performance [4–6, 108–111].

National Academies of Sciences, Engineering, and Medicine [108] provides a definition in 2017 for resilience as follows: "*Resilience is not just about lessening the likelihood that these outages will occur. It is also about limiting the scope and impact of outages when they do occur, restoring power rapidly afterwards, and learning from these experiences to better deal with events in the future.*"

PJM Interconnection provides a definition in March 2017 as follows [112]: "*Resilience, in the context of the bulk electric system, relates to preparing for, operating through and recovering from a high-impact, low-frequency event. Resilience is remaining reliable even during these events*". This definition is more specific to the HILP events.

In former President Barack Obama's Presidential Policy Directive [113], the term "resilience" refer to "*the ability to prepare for and adapt to changing conditions and withstand and recover rapidly from disruptions. Resilience includes the ability to withstand and recover from deliberate attacks, accidents, or naturally occurring threats or incidents*".

A definition of resilience for energy system is provided by UK Energy Research Center [114] as follows: "*Resilience is the capacity of an energy system to tolerate disturbance and to continue to deliver affordable energy services to consumers. A resilient energy system can speedily recover from shocks and can provide alternative means of satisfying energy service needs in the event of changed external circumstances.*"

Among the existing definitions of resilience, four aspects of the system resilience are summarized in [115] as follows:

- The state of electricity services of a power system can be described by resilience when confronting an interruption or outage. The description of resilience contains the extent of the service degradation, the rapidity of service recovery, and the recovery extent of the service. As can be seen, resilience does not only reveal a discrete state of whether a disturbance has happened, but also demonstrates the level of disturbance.
- The system resilience is determined by its design and its operation. These affect the degradation degree during a disturbance, the swiftness of the recovery and the completion of the recovery. For instance, a more redundant system that considers recovery strategies and additional contingency operation modes might undergo fewer and shorter interruptions. On the other hand, such a redundant system is more strenuous to reconstruct.

- Different resilience levels of the system can be resulted from different response at different costs. For instance, the system rebuilt with additional resources and a more efficient set of equipment can provide higher quality of service than the original level after the disaster recovery.
- The system resilience changes over time. The service of a system could be enhanced with regular maintenance and upgrade but at a cost. On the other hand, the service of a system without regular maintenance and upgrade has a lower operating cost but it can be anticipated that the quality of service and will lessen in the future. Accordingly, identifying the system critical components for maintenance, the ones for which a maintenance actions could result in the highest improvement in system reliability could potentially be a promising direction.

The National Infrastructure Advisory Council (NIAC), USA provided comes up with four main features of resilience in [116]:

- **Robustness:** The capability to maintain operation or withstand when disaster occurs, especially HILP events. Besides the system structure or design, it also relates to the system redundancy in case of some important components damages, along with the investment and maintenance of the critical infrastructure.
- **Resourcefulness:** The capability to expertly handle the occurred disaster. It incorporates determining the strategies and priority of the action that should be taken to both control and diminish the hazard, convey the decision to the people to execute. This feature mainly relates to the human, and not the adopted technology.
- **Rapid Recovery:** The capability to restore the system to its normal operating condition as soon as possible following the hazards. It relates to elaborately prepared contingency plans, capable emergency operations and strategic resources distribution and crews dispatch.

- **Adaptability:** The manner to learn from a hazard. It relates to the enhancement of the robustness, resourcefulness and recovery abilities of the system for the future hazards via new tools and technologies.

The Cabinet Office, U.K. also provides four main characteristics of infrastructure resilience in [117] as follows:

- **Resistance:** provides the strength or protection to withstand the disaster and its main effect to further mitigate the damage or disturbance.
- **Reliability:** the infrastructure components make sure to be inherently designed to maintain operation under certain conditions.
- **Redundancy:** the availability of backup equipment or spare capacity to allow the operation to be switched or redirected to alternative routes.
- **Response and Recovery:** rapid and effective response to and recovery from the hazards.

Additionally, Electric Power Research Institute (EPRI) in the U.S. also determines the three elements of resilience which are prevention, survivability, recovery for distribution system in [118] as demonstrated in Figure 1.1:

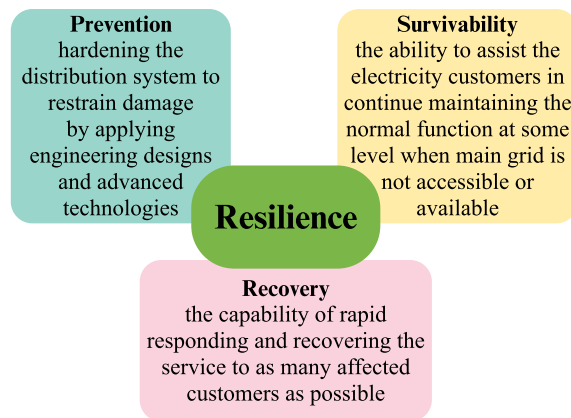


Figure 1.1: Elements of Resilience by Electric Power Research Institute (EPRI) [118]

Notice that these elements and aspects of the system resilience can also lead to its measurement (or metrics). Most of the existing definitions of resilience refer to the capability of the system to withstand and rapidly recover from HILP events [6, 111].

A conceptual resilience curve is proposed in [31] to describe the variations in the system resilience level over time with regards to a HILP event, as illustrated in Figure 1.2, where R represents the resilience level of the system. With respect to a HILP event, the power system experiences the following states [31, 119]:

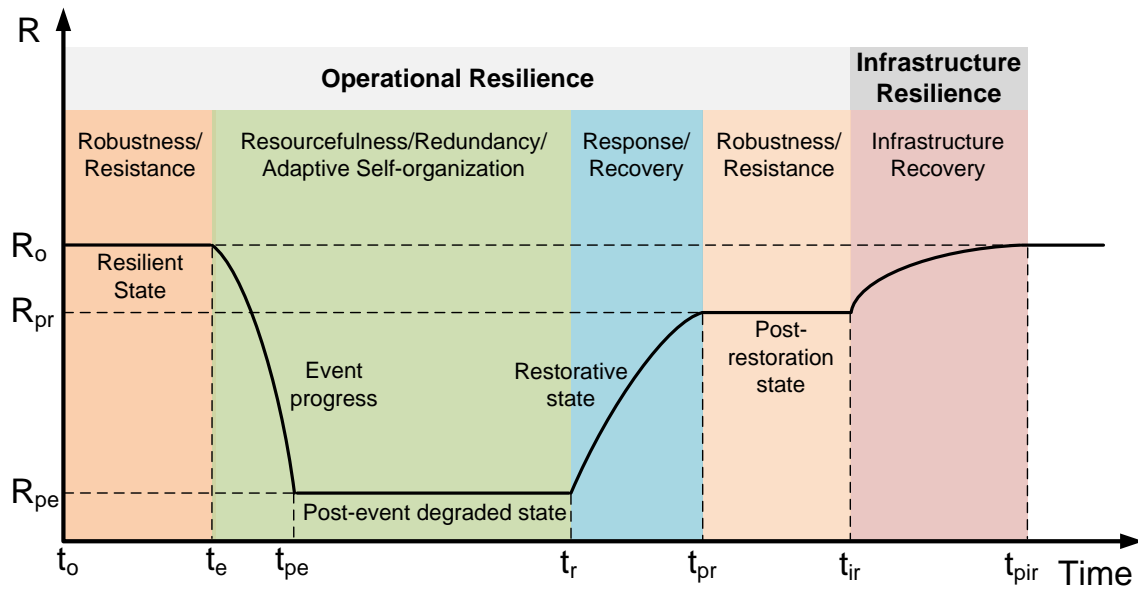


Figure 1.2: The Conceptual Resilience Curve Related to A HILP Event [31]

- **Resilient State** $t_0 \sim t_e$: before the HILP event happens at t_e , the power system should be robust and resistant to withstand the first strike of the HILP event by sufficiently predict the time and location of the external disturbance and preventive actions (e.g. preventive generation rescheduling) taken by the system operator, aiming to enhance the disturbance resilience of the infrastructure.
- **Event Progress** $t_e \sim t_{pe}$: during the HILP event progress, the system is degraded to post-event degradation state, where the system resilience decrease to R_{pe} . Emergency or corrective actions (e.g. generation re-dispatch alone or generation re-dispatch

coordinating with dynamic-boundary microgrid operation) can be taken to reduce the effect of the external disturbance.

- **Post-Event Degraded State** $t_{pe} \sim t_r$: after the event strike, the system enters the post-event degraded state. At this stage, the key resilience features are the *resourcefulness*, *redundancy*, *adaptive self-organization*, they offer the necessary *corrective operational flexibility* to accommodate and cope with the changing situation. This assists in minimizing the consequence of the event and the degradation in the system resilience level (e.g. $R_0 - R_{pe}$) while appropriate and effective coordination and preparation enable rapid beginning of the restoration state.
- **Restorative State** $t_r \sim t_{pr}$: the system should manifest fast *response* and *recovery* ability to recover the system resilience level from R_{pe} to R_{pr} . R_{pr} may be the pre-event resilience level R_0 or a desired resilience level that is not as high as R_0 .
- **Post-Restoration State** $t_{pr} \sim t_{ir}$ **and Infrastructure Recovery** $t_{ir} \sim t_{pir}$: Following the restorative state, the consequence of the event on the system resilience and its performance during the event need to be evaluated and analyzed to enhance the infrastructure resilience for future similar or unpredictable events. Depending on the severity of the event, the system may need longer time to recover the infrastructure in $t_{ir} \sim t_{pir}$.

1.3 Thesis Outline

The remainder of the thesis is organized as follows:

Chapter 2 provides a literature review on EMP attacks, backgrounds about EMP, such as EMP classification and intensity; and EMP attack theories such as damage principle, chain effect, and consequence. It will also describe the EMP-engendered damages to power grid while the current infrastructure is not well prepared for such intensive WMDs.

Chapter 3 evaluates the response of common electric components in power system such as coaxial wires and transmission towers under the scenarios of EMP attacks. Each component is under evaluation of electromagnetic compatibility (EMC) and the worst direction of attacks. The result will demonstrate how electric field caused by EMP attacks propagates through components and how the induced voltage/current harm the infrastructure.

Chapter 4 investigates the grid-scale impacts of the EMP attacks in power systems. Three different power systems of different size and complexity and attack scenarios of different patterns and realizations will be evaluated using the suggested parameters. These attack scenarios will demonstrate the impacts on system reliability and resilience performance by observing the electric field, reactive power loss, and induced currents on the model's one-line diagrams and contour maps.

In **Chapter 5**, the current protection and mitigation methods against EMP attacks will be introduced. Results from **Chapter 3** and **Chapter 4** will be leveraged to evaluate the protection effectiveness by comparing the device circumstances with/without protection. Some studies on protection and mitigation guidance against the EMP attacks from industry and national perspective will be also presented.

Chapter 6 presents the research conclusions and summarizes the main findings of this thesis. Possible future work plan is also provided in this chapter.

Chapter 2: Literature Review

2.1 Introduction

While the EMP attacks are becoming a new threat to power grids and electronics, the society in general should plan ahead for any type of EMP attacks to the grid and home electronics. This chapter investigates previous research, provides a literature review on the EMP threats, and contains a background on the EMP weapons, EMP attack theories, EMP-engendered damages, and EMP detection mechanisms.

2.2 EMP Classification

The EMP attacks can be categorized into two different classes: nuclear EMP (NEMP) and nonnuclear EMP (NNEMP), both of which can damage or destroy electronic devices, but are typically not lethal to human and animals [1].

2.2.1 Nuclear EMP (NEMP)

The nuclear type EMP attacks mainly contains high-altitude electromagnetic pulses (HEMP), resulting from a nuclear burst at a very high altitude [120]. The HEMP from a high-yield gamma ray weapon can in principle impact the functionality of power grids, communication infrastructures, computing and electronic processing systems, and ground transportation systems dependent on microprocessors or embedded electrical systems that are susceptible to the disruptive effects of large electromagnetic perturbations. A HEMP comprised of three components defined by an international standard—the International Electrotechnical Commission (IEC) [26]. Such an NEMP waveform is demonstrated in Fig. 2.1 divided into the following segments:

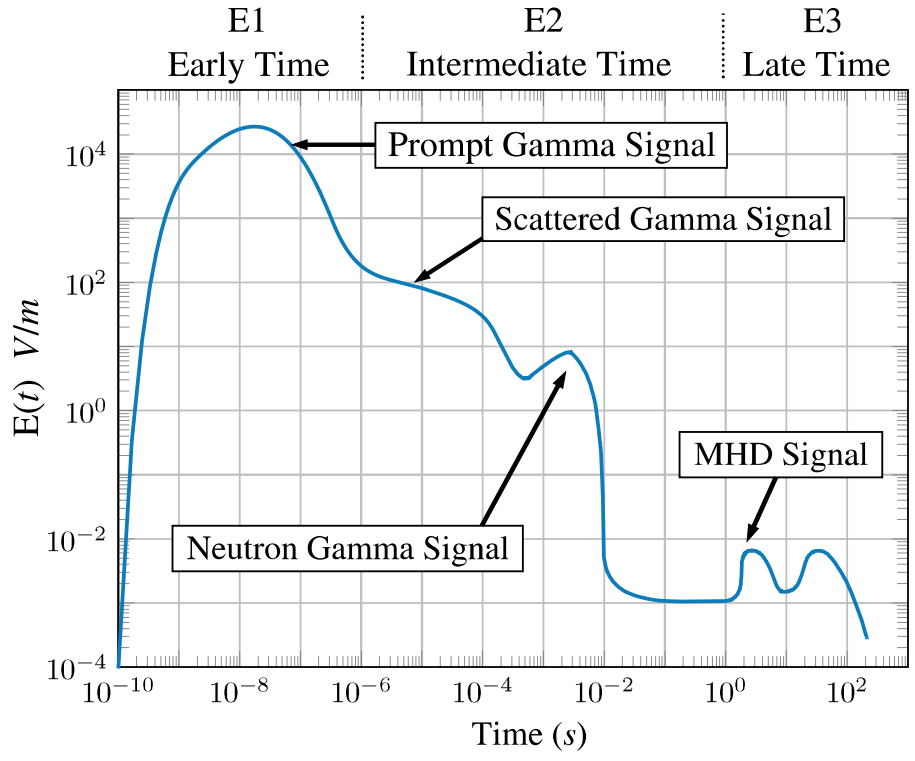


Figure 2.1: Nuclear EMP Waveform [1].

- E1 pulse is a very rapid and intense electromagnetic field that can induce very high voltages in electrical conductors.
- E2 pulse is generated by scattered gamma rays that produced by neutrons. The E2 wave is similar to lightning strikes and can cause the electric equipment to exceed its designed breakdown current.
- E3 pulse is a slow but lasting pulse, and can last about ten to hundred seconds after the explosion [121, 122].

Another effect of an NEMP attack could be intentional electromagnetic interference (IEMI), which is caused by repeating pulses generated by antennas, with a much smaller intensity and area affected compared to HEMP [123].

2.2.2 Nonnuclear EMP (NNEMP)

Nonnuclear EMP is an EMP characterized with no nuclear elements. Devices that can be a NNEMP weapon include a large low-inductance capacitor bank discharged into a single-loop antenna, a microwave generator, and an explosively pumped flux compression generator [120]. An example of NNEMP is EMP bomb. An EMP bomb contains armature cylinder, a stator winding and high explosive inside the tube. Once the bomb is triggered, the armature cylinder and stator winding will produce huge amount of magnetic field rapidly radiating to surroundings [124]. Compared to NEMP, the NNEMP device (i) is easier to carry and detonate, and (ii) has lower cost [125]. One structure of a NNEMP bomb is shown in Fig. 2.2 [2, 21].

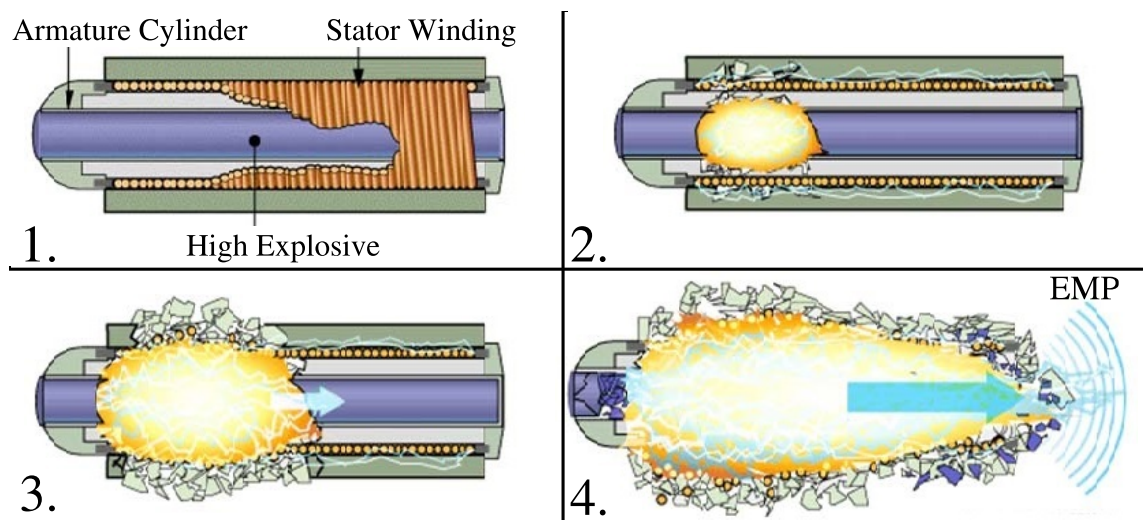


Figure 2.2: Explosive Pumped Coaxial Flux Compression Generator [2].

Another EMP effect is originated from the solar corona mass ejections (CMEs), which can cause changes in the earth's magnetic field (i.e., dB/dt). These changes in turn produce a non-uniform electric field at the surface that usually slowly varies dependent on the deep earth (hundreds of kilometers) conductivity. The electric fields can be modeled as a DC voltage source superimposed on the lines, and cause quasi-DC geomagnetically induced currents (GIC) flowing in high voltage power transmission grid [28]. This concept will be

used to analyze the impacts of EMP attacks on electric components and power grid in the following Chapter 3 and Chapter 4 of this thesis.

2.3 Potential Impacts of EMP Attacks on Power Grids

Generally, the EMP attack damage level is classified into four degrees: deny, degrade, damage, and destroy. *Deny level* usually happens at the occasions of small attacks and the device can be self or manually restored to the initial operating state as the inner part of the device is not damaged. *Degrade level* requires the device to restart or manually reset in order to get back to the healthy operating state. The *damage level* and *destroy level* reflect that the devices are temporally or permanently damaged or destroyed and the circuits or printed circuit board (PCB) need to be replaced.

Table 2.1 describes the equipment status under several types of high-impact low-probability (HILP) EMP attacks. NNEMP attacks have direct and permanent effects on all electric equipment including power grids and grid-dependent devices. Compared to physical attacks, although power grid equipment such as transformers and generators are identically vulnerable, the EMP can bring more dangerous chained effects to infrastructures that are connected to the grid such as water supply, internet, and GPS [1, 3, 126]. These chained effects analysis have not done in this thesis but may include in future research.

Nuclear EMPs (NEMP) may result in damages to power grid elements at the standard damage level of E1, E2, and E3 [3, 121]. E1 damages exceed the device breakdown voltages, E2 results in high induced current running through the wires and the E3 waveform is a long-term low-amplitude pulse lasting 10 to hundred seconds and can induce high levels of currents in long power and communication lines, destabilize or damage the equipment such as transformers and solid state communication line drives [121]. NEMP attacks can bring serious damages to power grid equipment such as generator stations, supervisory control and data acquisition (SCADA) control systems, power grid control centers; it also has long term effects on internet, cell phone systems, and military services [26]. Although critical

Table 2.1: Potential Impacts of HILP EMPs on Critical Infrastructures [3]

Equipment At Risk	EMP (Nuclear)	Solar Storm	Cyber	Physical Attacks	Radio Frequency Weapons
Generator Stations	DPE	DEU	DPE	DPE	DPE
SCADA/Industrial Controls	DPE	DPE	DPE	DPE	DPE
Utility Control Centers	DPE	DPE	DPE	DPE	DPE
Transformers	DPE	DPE	PPE+CE	DPE	DPE
Telecommunications Including Cellphones	DPE	DPE	DPE	CE	CE
Internet	DPE	DPE	DPE	CE	CE
Radio Emergency Communications	DPE	TE	CE	CE	CE
Emergency SATCOM Communications	DPE	TE	CE	CE	CE
GPS	DPE	TE	CE	CE	CE
Transportation	DPE	CE	CE	CE	CE
Water	DPE	CE	PPE+CE	CE	CE

DPE = Direct Permanent Effects.

DEU = Direct Effects Uncertain.

CE = Cascading Effects (if no backup power).

DPE+CE = Potential Permanent Effects plus Cascading Effects.

TE = Temporary Effect (0.5-36 hours) assuming backup power.

electronic elements in power system are usually contained within some sort of metallic box, they are not designed to protect the electronics from high-energy electromagnetic pulses that may infiltrate either from the free field or from many cable connections that may compromise electromagnetic integrity. The major concern for SCADA vulnerability to EMP is focused on the early time E1 component of the EMP signal. This is because, even in the power industry, SCADA systems are not directly coupled electrically to the very long cable runs that might be expected to couple to a late-time E3 signal [26].

The strength and effects of NEMP attack depends on the warhead type and yield, and the altitude and latitude of the detonation. An NEMP device can be detonated at altitudes between 30 and 400 kilometers and generates an electromagnetic pulse with amplitudes around tens of kilo-volts per meter and radius of effects from hundreds to thousands of kilometers [127]. Taking E2 waveform as an example, a similar lightning current of 100 KA affects a circle with radius of 50 meters by inducing voltages of 15.75 KV on the conductors. This overflows all the breakdown voltage ratings designed for electronic devices. With this incredible over-voltage, the device will create extreme heat due to the inducted current, causing side effects such as burning and explosion [128].

2.4 Typical EMP Simulation Approach

Electromagnetic compatibility (EMC) helps identifying if a device is compatible with (i.e., no interference is caused by) its electromagnetic (EM) environment and it does not emit levels of EM energy that cause electromagnetic interference (EMI) in other devices in the vicinity [129]. In other words, EMC is the interaction of electrical and electronic equipment with its electromagnetic environment, and with other equipment. The problems such as crosstalk (XT) on the printed circuit board (PCB), interference (EMI) of frequency conversion power supply on radio, thermal effect under special absorption rate (SAR) of mobile phone on the human body, antenna placement, lightning strike, and electromagnetic pulse all belong to the research area of electromagnetic compatibility [130].

In order to better regulate the EMC, a series of international standards and restrictions have been formulated, including general international standards, industry standards, military standards and so on. In the United States, there are MIL-STD-188-125-1 (CS115), MIL-STD-461G (CS116), and MIL-STD-464C (CS117) as the main standards [131–133]. In Chapter 5, the MIL-STD-188-125-1 standard will be used to evaluate a shielding effectiveness approach against EMP attacks. The traditional EMC testing could be divided into four categories: conducted emission (CE), conducted susceptibility (CS), radiated emission (RE), and radiated susceptibility (RS). According to the size of the electrical dimension, the EMP simulation can be divided into the following four categories:

- ***PCB-Level Simulation*** [134]: considering the signal integrity (SI), power integrity (PI), electromagnetic interference (EMI), and electromagnetic susceptibility (EMS) of PCBs under normal working conditions, one can obtain the current distribution on the board, or the near-field equivalent current and the equivalent magnetic current distribution including the board;
- ***Cable-Level Simulation*** [135–138]: any electronic equipment includes various types of cable harness, single-wire, twisted-pair, wiring arrangement, single-core and multi-core shielding wire harness and any combination of these lines and shielding. Once there exist cable harness in the system, EMC becomes very uncertain and shows strong stochastic statistical characteristics in simulation or measurement. In order to solve the problem of SI, EMI and EMS in simulation, and obtain a common-mode current or equivalent electromagnetic current, transfer impedance based on measurements and with certain statistical significance is usually used;
- ***Cabinet-Level Simulation*** [139–143]: it mainly talks about the metal cabinet or case. PCB and cable are electromagnetic radiation sources, which can be addressed in the above two levels. For the cabinet itself, the most difficult challenge is the small heat sink, lap, fastening screw, conductive rubber, shielding film, metal wire mesh

and other structures whose size is far smaller than the wavelength and can not be ignored, because such problems must be addressed by full-wave electromagnetic field simulation algorithms. Such algorithms need to divide the network to be able to distinguish these small structures. Hence, the resulting sharp increase in the number of grids, simulation speed and accuracy decline;

- ***Subsystem- and System-Level Simulation*** [144–149]: subsystems refer to subsystem devices that can work independently; systems refer to terminal products. EMC sources are obtained by simulation of PCB and cable harness. EMC characteristics of the system are obtained by having these sources into the cabinets and systems for electromagnetic simulations.

2.5 EMP Simulation Algorithms

Circuit simulation is mainly used for the analysis of inter-port characteristics, when the electromagnetic field in the port has no effect on other parts of the network or can be neglected; the necessary condition for circuit simulation is that the physical size of the circuit is much smaller than that of the wavelength. In other words, when the size of the circuit board can be compared with the wavelength corresponding to the highest frequency in the circuit, the electromagnetic field theory must be used to analyze the circuit board [150].

The circuit algorithm mainly aims at the network composed of linear passive lumped elements and non-linear active devices, and is simulated in frequency domain using pure transient equation models. Such simulation (i) does not need three-dimensional solid models, (ii) can include linear and non-linear device time-domain or frequency-domain models (SPICE and IBIS, etc.), (iii) features fast simulation speed, and (iv) enables time-domain signal and spectrum of voltage and current as the primary solutions [150].

Quasi-static magnetic and electric algorithm needs three-dimensional structure models. The so-called "quasi-static" means that the system must support the existence of electrostatic field and steady current, which is represented by the field pattern of electrostatic field

and static magnetic field. More precisely, the flux change rate or displacement current is very small. Therefore, the partial derivatives of B and D in time can be ignored in Maxwell's equations. The corresponding Maxwell's equations are called quasi-electrostatic and quasi-magneto-static, respectively. The derived algorithm is called quasi-electrostatic algorithm and quasi-magneto-static algorithm. This kind of algorithm is mainly used for EMC simulations in low frequency power systems or motor equipment. The quasi-static magnetic and electric algorithm is subdivided into quasi-electrostatic frequency domain, quasi-magneto-static frequency domain, quasi-electrostatic time domain and quasi-magneto-static time domain. The appropriate algorithm is selected according to the frequency and application characteristics of the equipment. It is obvious that quasi-static approximation can be used for high voltage insulation devices, while quasi-static magnetic algorithm is preferable for high current devices [150].

Full-wave electromagnetic algorithm is simply an algorithm for solving the complete form of Maxwell equation. Full-wave algorithm is divided into time-domain and frequency-domain algorithms. Finite difference method (FD), finite integral method (FI), transmission line matrix method (TLM), finite element method (FEM), boundary element method (BEM), moment method (MoM) and multilayer fast multipole method (MLFMM) are all full wave algorithms [151]. All full-wave algorithms require volume or surface mesh segmentation of the simulation area. The first three methods (FD, FI and TLM) are mainly explicit algorithms in time domain, and the sparse matrix, simulation time and memory are proportional to the first power of grid number; the last four methods (FEM, BEM, MoM and MLFMM) are implicit algorithms in frequency domain. FEM is also a sparse matrix, and simulation time and memory are proportional to the square of the grid number; while BEM and MoM are dense matrices, so time and memory are proportional to the cubic of the grid number. FD, FI, TLM and FEM are suitable for arbitrary structure and arbitrary medium, BEM and MoM are more suitable for arbitrary structure but uniform non-rotating medium distribution, while MLFMM is mainly suitable for metal convex structure, although MLFMM has superlinear

mesh convergence, i.e. well-known $N \log N$ computation. Full-wave algorithm, also known as low-frequency or accurate algorithm, is an accurate method for solving electromagnetic compatibility problems. For a given computer hardware resource, there is an upper limit on the electrical size that can be simulated by this method. Generally speaking, TLM and FI can simulate the largest electrical size without any restrictions, that is, any structure or material, followed by FD, FEM, MoM and BEM. For metal convex structures, MLFMM is a full-wave algorithm that can simulate the largest electrical size. The inherent advantage of time domain algorithm is that it is very suitable for UWB simulation, and EMC itself is an UWB problem. In addition, the time domain algorithm is natural, efficient and accurate for the simulation of transient electromagnetic effects, such as the transient impulse voltage induced on the cable harness under strong electromagnetic pulse irradiation [150, 152].

In summary, the time domain algorithm is to solve Maxwell's equations in an iterative way from the excitation source, that is, to simulate the propagation process of the wave, and to propagate from the source to the surroundings. Frequency domain algorithm is to solve Mack's thinking equations directly by matrix method, whether it is FEM's variational algorithm or MoM's electric field integral equation.

2.6 EMP Threat Detection in Power Systems

Since corona mass ejections (CME) caused EMP can lead to Quasi-DC GICs in high voltage transmission grid, the flow of such currents into power transmission lines can potentially cause "half-cycle saturation" of high-voltage bulk power transformers. This phenomenon can lead to relay miss-operations, voltage dips, elevated reactive power demand, transformer overheating, disruptive harmonics, aging or malfunction of the electric power devices, and even a total collapse of the grid in the worst case scenarios [153–157].

Strategies to enhance electric power grid resilience must accommodate both a diverse set of technical and institutional arrangements and response to a wide variety of hazards. There is no "one-size-fits-all" solution to avoiding, planning for, coping with, and recovering

from major outages [108]. A sensor developed in [108] contains parts of asymptotic conical antenna, an active integrator and the electro-optical converting circuit that can be used to detect EMP. The sensor uses an asymptotic conical antenna to sense Electric field, and the derivative signal from the antenna is encoded by an active integrator based on a high speed operational amplifier [158]. The CME caused EMP impact is detected through estimating the GICs in a current transformer. The authors in [159] proposed an approach to measure the absorbed reactive power. In [160], the existing current transformers are converted to flux-gate DC current (GIC) sensors by injecting AC excitation currents into their secondary winding; A detection method on the impact of CME caused EMP is developed in [161] by measuring the quasi-DC GIC flowing in the neutral earth points. Machine learning-based detection techniques for GICs resulted from GMD events in power systems are recently developed, tested, and verified in [8, 10, 14].

2.7 Power Grid Resilience to EMPs

Citizens are constantly dependent on reliable and continuous electric power for daily life. If electric power is not accessible even for an hour, the devastating impacts could be catastrophic to multiple infrastructures such as water/food supply and production, financial systems, transportation, and health care [6–9, 109–111]. No infrastructure other than electric power has the potential for nearly complete collapse in the event of a sufficiently robust EMP attack. While a less robust attack could result in less catastrophic outcomes, such outcomes would still have serious consequences that threaten the national security.

The continuous evolution of electronic devices into systems—that once were exclusively electromechanical—enabling computer control instead of direct human intervention and use of broad networks like the Internet, results in even greater reliance on microelectronics and thus the presence and sharply growing vulnerability of the power grid to EMP attacks. Just as the computer networks have opened the possibility to cyber assaults on the power grid or to electrical power system collapse associated with software failure (as during the August

14, 2003, blackout), they have enabled a pathway for EMP attack that is likely to be far more widespread, devastating, and difficult to assess, as it is a magnetic signal that can cause induced currents overrunning in electrical conductors, destroy power transformers [121,122], and would make it a challenging power restoration [25].

A nuclear device detonates at a precise point in our atmosphere, producing an electromagnetic pulse that can destroy our national grid. Literally, this is the plot of William Forstchen's novel "One Second After", in which, a hostile government attacks the United States by detonating a guided nuclear missile over North Carolina, creating a large-scale electromagnetic pulse. Chaos ensued, including the collapse of nuclear power plants, hunger, disease and collective hysteria [30]. In 1979, President Carter issued an order requiring that every weapon developed by the United States since then must take full account of EMP protection capabilities. The Critical Infrastructure Protection Act passed by the U.S. Congress in 2016 directs the Department of Homeland Security to develop plans to prioritize EMP survivability and recovery capabilities. And on March 26, 2019, President Trump signed an executive order instructing several federal agencies to study the risks of EMP damages to national technology and energy infrastructure and to enhance our ability to respond to such incidents [30].

According to the Washington Examiner, if the U.S. suffered an EMP hit, electricity would be lost, the military's weapons would be downed, 99 nuclear reactors would likely melt down without electricity for cooling, and 4.1 million people living near nuclear reactors would be displaced as radioactive cloud spreads. "An EMP would cause instantaneous and simultaneous loss of many technologies reliant on electrical power and computer circuit boards, such as cell phones and GPS devices," the report says. Military and commercial jets would be degraded, bases would be cut off, and power and GPS would go dark making defense and counter-attacks virtually impossible. The attack would dismantle or interfere with electricity, affecting transportation, food processing and health care. In fact, 90 percent of the population on the East Coast would die in a year of the attack. "Failures may include

long-term loss of electrical power (due to loss of emergency generators), sewage, fresh water, banking, land lines, cellular service, vehicles," the report says. Civil unrest is predicted to start within just "hours" of the attack.

The power system has been undergoing dramatic changes in technology and governance for several decades. In most parts of the United States, power is still supplied by regulated, vertically integrated utilities that generate electricity in large power generators, moving power out from power plant over high-voltage transmission lines, and distribute it to customers and end-consumers. In other parts of the country, electric utilities have been reconstructed to adapt more competitive markets such as wholesale power sales between generators and electricity distribution companies. In the more market-oriented parts of the country, transmission lines between utility buyers and sellers are regulated or publicly owned, as are most distribution systems that provide the poles, wires, and equipment to serve retail customers. However, the flows over such wires and customers' responses are increasingly determined by market forces. Efforts to improve resilience must accommodate institutional and policy heterogeneity across the country. In many countries, minor power grid system components and programs such as distributed generation, demand response, energy efficiency, customer-owned storage, microgrids, and electric vehicles are a rapidly growing part of the overall grid resource that must be planned and managed to maintain overall grid reliability, resilience, and security. Despite such developments, for at least the next two decades, most customers will continue to depend on the functioning of the large-scale, interconnected, tightly organized, and hierarchically structured electric grid. With the vulnerability to EMP attacks, efforts should be made on building in resilience in power grids is becoming more and more critical to every aspect of our economy [108]. Resilience is not just about reducing the probability that power outages will occur, it is also about limiting and lowering down the scope and impact of outages when they actually occur, restoring power rapidly after the event, and learning from the experiences to have more resistant to similar events in the future.

Chapter 3: EMP Attack Characterization in Power Systems

3.1 Introduction

In Chapter 2, different categories and characteristics of EMP attacks have been studied. In order to be able to quantify the impacts of EMP attacks in power grids, this chapter will demonstrate the analysis of typical EMP attacks on individual components in power systems. The EMP source used in this chapter was modeled as a *plane wave incident* and controlled by a user-defined excitation signal. Bare wire, coaxial cable, transmission line tower, and cell tower models were designed first and then simulated in Computer Simulation Technology (CST) Studio Suite in order to measure the electromagnetic compatibility (EMC) of these models Section 2.4. These simulations help better understanding of the characteristics of EMP attacks, how they influence the power system components, and how electric field and induced current propagate in these attack scenarios.

3.2 Simulations on Bare Wire and Coaxial Cable

Prior to the simulations, it is important to determine which workflow, domains, and parameters are suitable for EMP simulations. Described in [162] support section, CST Studio Suite has a workflow setting exclusively for EMP simulations. In this case, EMC/EMI template with radiated susceptibility (RS) workflow, introduced in Section 2.4, was selected to perform EMP modeling and simulations. The solver operates in time domain and uses transmission line matrix method (TLM) algorithm discussed briefly in [151] and Section 2.4. References [163] and [164] suggest the standard electric field peak magnitudes of 24 V/km in EMP simulations, also applied in simulations in both Chapter 3 and Chapter 4.

The most basic and important component in power systems is cable. Cables are used to connect every buses (substations) in the network, and transmit power to anywhere in the

world. It is necessary to analyze the EMC of a cable in order to indicate its vulnerability to EMP attacks. In the United States, Aluminum conductor steel reinforced (ACSR) product is a bare electric conductor grade hard-drawn aluminum conductors stranded around an inner core of galvanized steel wire [165]. ACSR wires are widely used in transmission lines. In this chapter, one of the commonly used cables with code word “Raven” is selected and modeled as demonstrated in Figure 3.1.

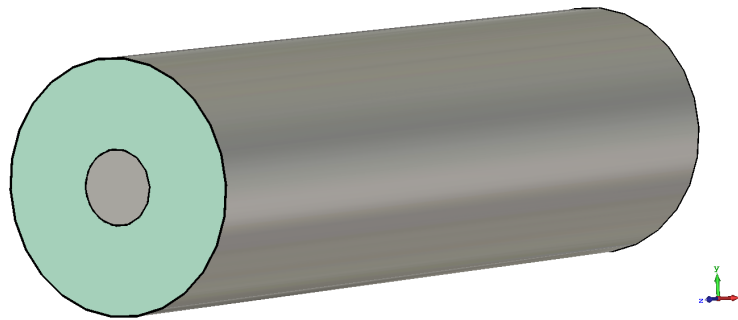


Figure 3.1: Bare Cable Designed in CST Studio Suite

Figure 3.1 shows a bare cable with a size of 1/0 AWG, diameter of 0.398 inches, resistance of 0.159 ohms per 1000 feet, and allowable ampacity of 242 Amps. For simulation purposes, the six inner stranding cores are composite to one core. The inner core is aluminum and wrapped with poly tetra fluoroethylene (PTFE), which is an insulator. Let the electric field with an intensity of 24 V/km propagates from one side of the wire and travels to the other side. The propagation direction is parallel to the wire. By running a time domain TLM simulation using the wave guide port input in CST, the resulting electric field on the conductor is illustrated in Figure 3.2. According to the arrows shown in Figure 3.2, the electric field in the bare wire is radiated from the center of the core toward the outside insulator. Also, the strength of the field is decreasing as it moves from the inner to the outer directions. The induced current travels back and forth through the inner core with maximum intensity of 852 Amps. The intensity of the electric field on the core has an average uniform value of 24 V/km. Therefore, this bare wire has almost no protection against an incoming

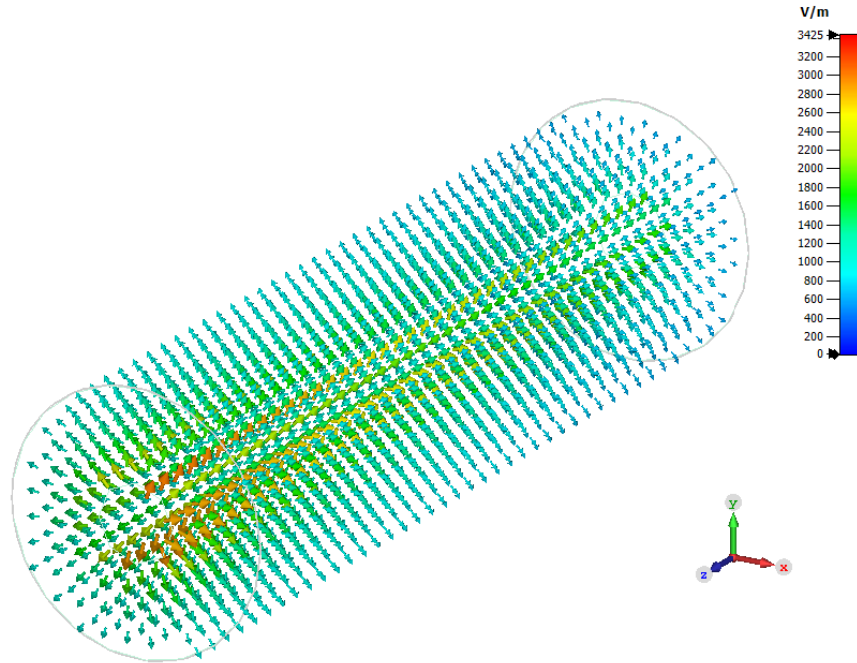


Figure 3.2: Electric Field Propagation in Bare Wire

electric field, and the maximum intensity of the induced current is exceeding the wire's allowable ampacity of 242 Amps.

However, bare wires are hardly ever used as transmission lines nowadays; instead, coaxial cables are widely applied in power systems. Figure 3.3 shows the configuration of a typical coaxial cable. Compared to a bare wire, a coaxial cable has a conductor shielding, insulation shielding, and copper strip shielding for every strand cores. In order to compare the two types of cables resilience to the electric field, an excitation signal shown in Figure 3.4 with a maximum E-field intensity of 24 V/km and rise time of 3 ns was used in the simulations. In a total run time of 100 ns, the frequency is also uniformly changing from 0 to 1000 MHz in this scenario.

Figure 3.5 shows the current induced (in unit of dB) versus frequency when the electric field is at the maximum, and the interference of the cable is obtained (this is called the disturbance induced current in lines). Obviously, the shielding efficiency of the coaxial line

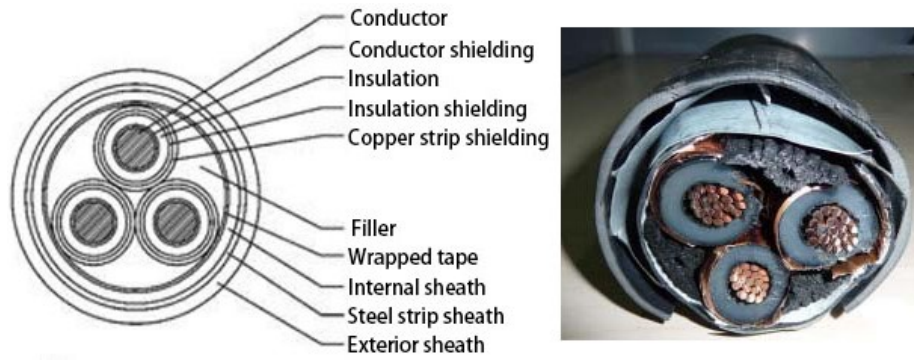


Figure 3.3: Structure of Coaxial Cable

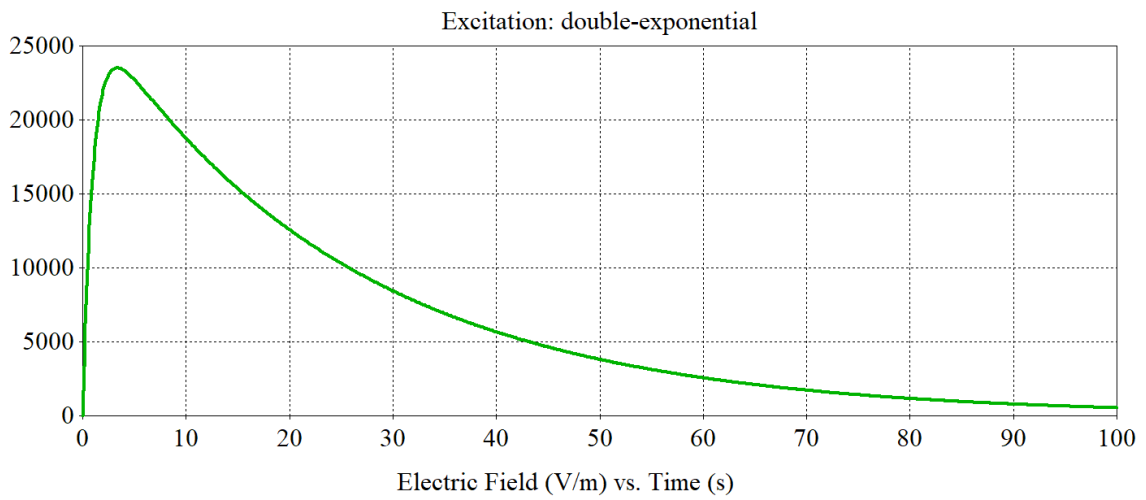


Figure 3.4: EMP Excitation Signal in CST Studio Suite.

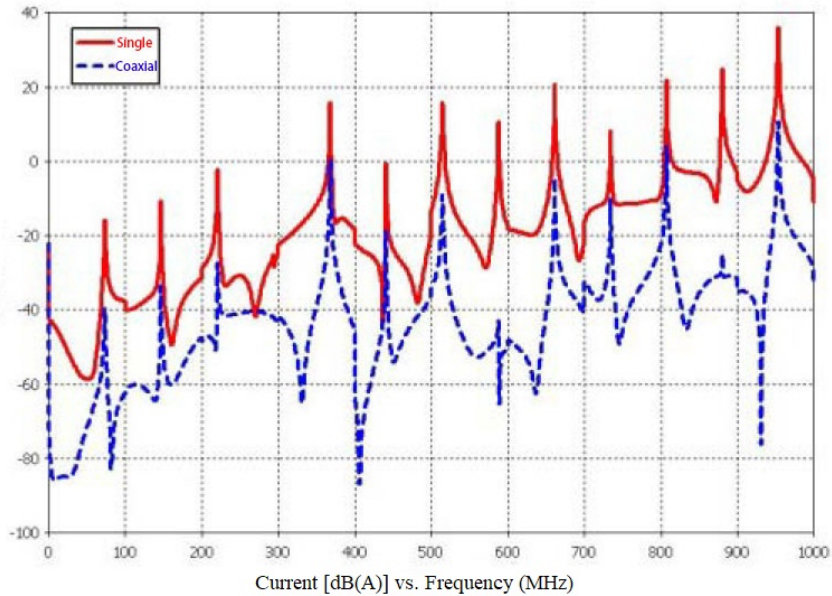


Figure 3.5: Current Induced in Bare Wire and Coaxial Wire

is much higher than the bare line. However, coaxial cable, as an individual component, still suffers from the large intensity of electric field, meaning that the cable needs further developments and protections against EMP weapon grade level attacks.

3.3 Simulations on Cell Tower

A very important type of facility in our modern societies that we rely on nowadays are cell towers. People are relying on communications heavily and these cell towers perform a very important function to keep the people connected. Also, 5G technology is growing rapidly, thereby highlighting the importance to understand the characteristics and response of the cell towers against EMP attacks to ensure that they can function properly when facing such HILP events.

Figure 3.6 shows an EMP source coming in at the 45 degree angle on the top right side of the cell tower. A coaxial cable connects the ground shielded box and antennas at the top of the tower. The cable picks up the current around 600 amps on the coax shield and the bulk current monitor around the cell tower detected about 2000 amps of current. As time

passes when the plane wave arrives and paths through from the top right to the lower left, the wave front shows a double exponential signal profile. It first hits the tower and then continues on to reflect off the ground plane, and later times the tower picks up the energy and basically acts as an antenna. The residual energy stays a while after the plane wave has completely passed through, shown in Figure 3.7. This type of energy can propagate to other parts of the tower through cable connections and temporarily disable or permanently destroy the nearby electronic equipment and accessories [166].

3.4 Simulations on Overhead Transmission Line Tower

Overhead transmission line is crucial to power systems as electricity needs to travel and get delivered to every household and industries. This section demonstrates how an overhead transmission line tower can be affected by an EMP attack. One section of the three-phase overhead transmission line model was built in CST Studio Suite, where each line is separated by a metallic tower and by insulators at the top of the tower. The insulators are modeled as high resistance elements that isolate the line and tower itself. The three phase transmission line wires can be analyzed by monitoring the current flowing through them. Using a similar approach in Section 3.3, the EMP waveform travels in parallel to the ground plane shown in Figure 3.8 [166].

The surface current contour plot in Figure 3.8 shows the wires were induced with the most of the currents. And the currents flowing on the tower itself can be seen propagating from the top to the bottom direction. The insulators on the tower have not been affected by neither of the electric field nor the induced current as appeared in blue color throughout the test. Therefore, the current induced on the tower itself did not get transmitted to the transmission lines. All these results and observations can provide some insights into the structure behaviors and response when exposed to an EMP attack.

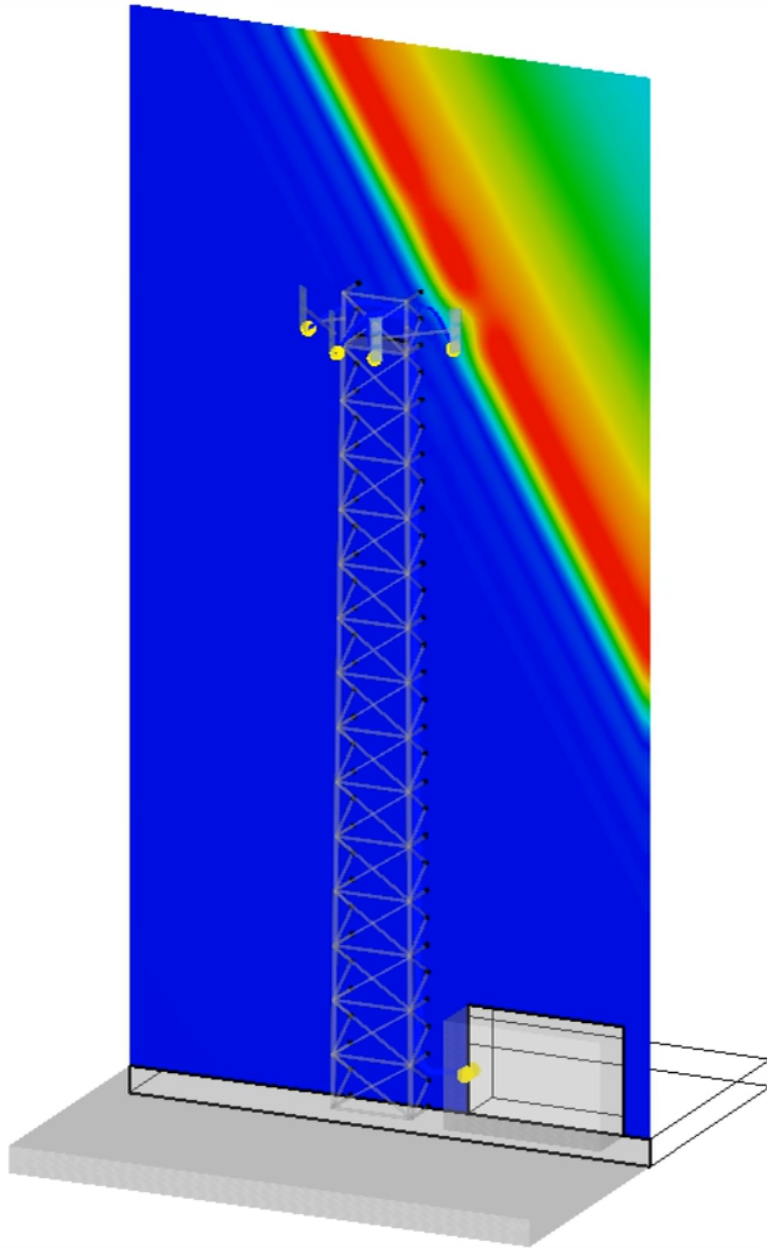


Figure 3.6: EMP Waveform Incident on Cell Tower

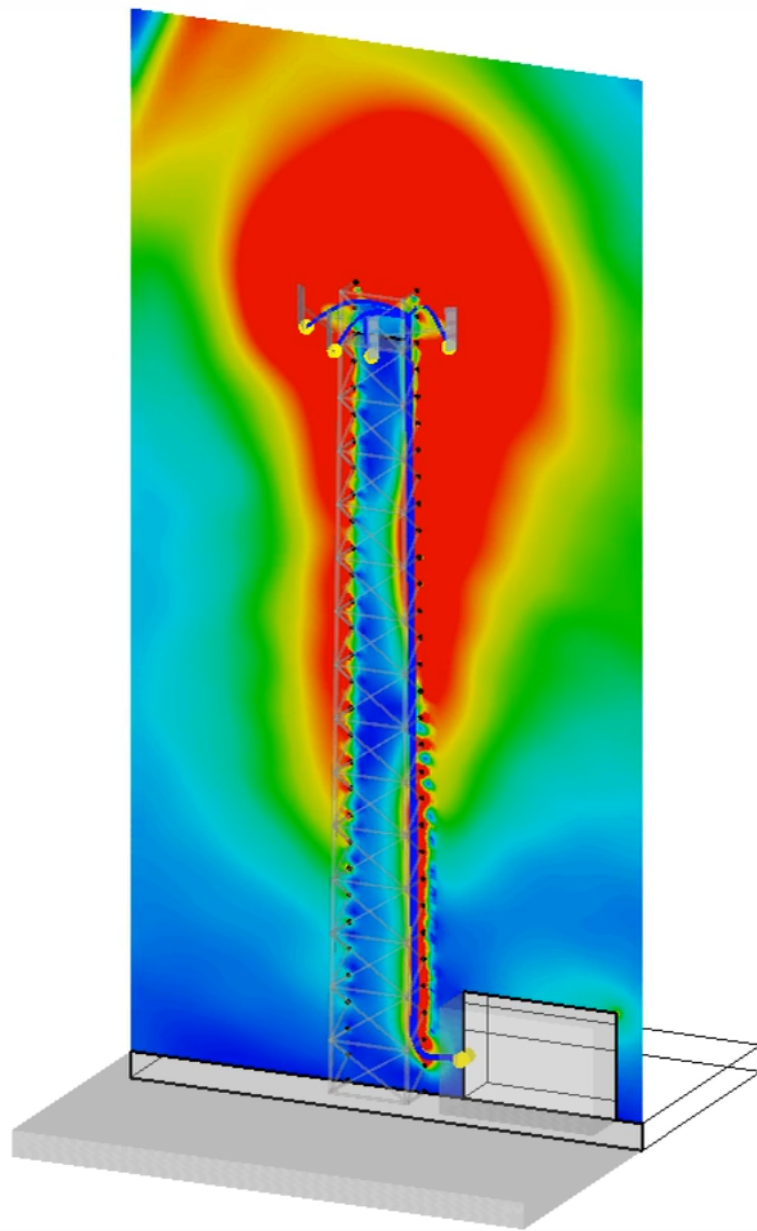


Figure 3.7: Residual Energy Left on Cell Tower After the Incident

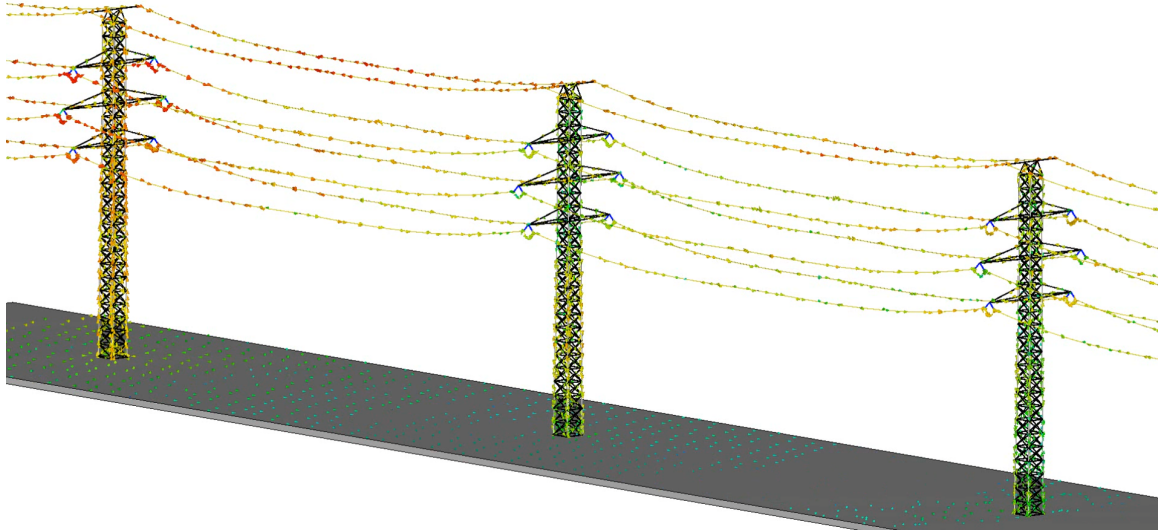


Figure 3.8: EMP Incident on Overhead Transmission Line Tower.

3.5 Conclusion

In this chapter, bare cable, coaxial cable, cell tower, and overhead transmission line tower were simulated in CST Studio Suite in order to visualize and evaluate the impacts of EMP attacks and the corresponding electric field incidents on power systems' individual components. Several parameters such as electric field direction and magnitude, current direction and magnitude induced in the equipment, and animated contour map were evaluated. By summarizing and analyzing how EMP attacks influences the individual components in power grids, the EMP attacks behavior and the overall impact in large-scale power grids can be researched accordingly.

Chapter 4: Grid Scale Vulnerability Assessment to EMP Attacks

4.1 Introduction

In Chapter 3, several components that appeared frequently in modern power systems were analyzed and evaluated under the scenario of EMP attacks. Next, it is necessary to research the EMP threat to larger scale power systems. In this chapter, 4-bus, 150-bus, and 2000-bus systems are used to simulate their performance under various EMP attack scenarios. Similar to Chapter 3, the electric field, effective GIC and reactive power loss are the main factors which are importantly concerned. The EMP source used in this chapter include the static single snapshot inputs, time-varying electric field inputs, and time-varying series voltage inputs. The simulations in this chapter encompass the electric field, GIC and reactive power loss calculations, contour mapping, and sensitivity analysis. The purpose of these simulations are to better understand the characteristics of EMP attacks in power systems, and how GICs affect the power flows, buses, and transformers in power systems. All simulations in this chapter are performed in PowerWorld simulator software package.

4.2 Simulations on the 4-Bus Test System

Before moving onto a relatively large-scale power system, it is helpful to apply an EMP attack scenario to a smaller system. A four bus test system shown in Figure 4.1 consists of 2 generators with generator step-up (GSU) transformer, and a 765 kV transmission line. Bus 1 and Bus 3 belong to substation A and Bus 2 and Bus 4 belong to substation B. We assume that all substations have grounding resistance of 0.2 ohm, Bus 1 generator has an implicitly modeled GSU transformer with the resistance of 0.3 ohm/phase on the high (wye-grounded) side, and Bus 4 generator has a similar GSU transformer with 0.3 ohm/phase resistance. The 765 kV transmission line between Bus 1 and Bus 2 is characterized with a resistance

of 3 ohm/phase. The transmission line length between Bus 1 and Bus 2 is set to 170.8 km long [167].

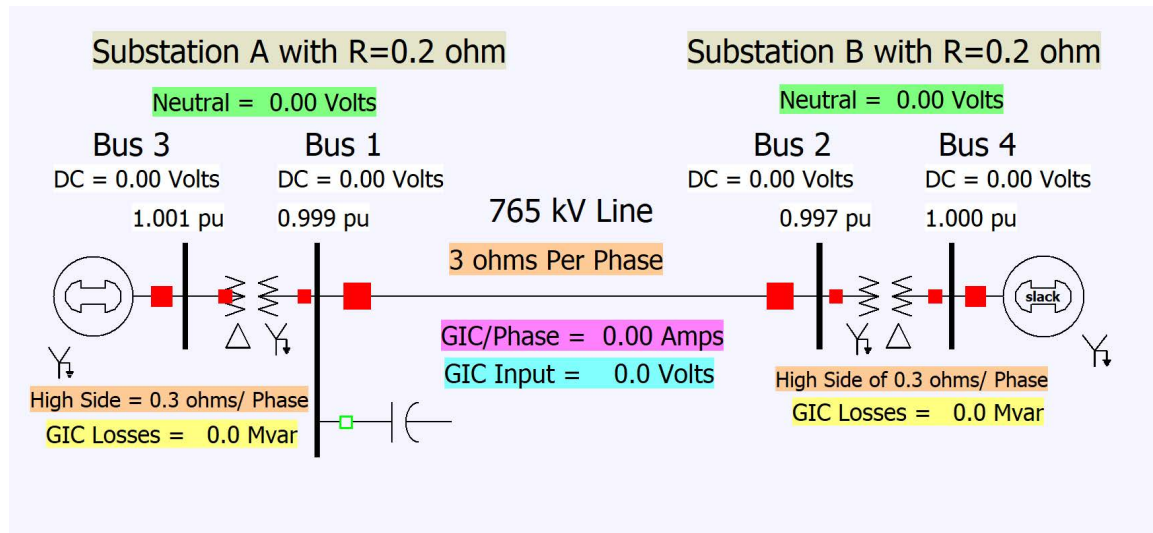


Figure 4.1: The Studied 4-Bus Test System

In order to model a uniform single snapshot electric field, two input parameters are required: the magnitude and direction. In this simulation, the maximum electric field is 24 V/km, same as the parameter employed in Chapter 3, and the direction is 90 degrees. The direction indicates that the electric field propagates in the west-to-east direction (from left to right in Figure 4.1). By using the GIC add-on in PowerWorld Simulator with the aforementioned set-up, the GIC and substation reactive power loss have been calculated in Figure 4.2.

For this 24 V/km eastward electric field, the GIC input is 4098.9 Volts. This is dependent on the transmission line length between Bus 1 and Bus 2. Longer transmission lines may have larger GIC input voltages. From the GIC input voltage, it is easy to assess the actual GIC for the system. The DC resistance values for the transmission line, transformers, and substations have been given in Figure 4.1. The three phase transmission line and transformers are in parallel, so the total 3 phase resistance of the one-line diagram is 1 ohm for the transmission line and 0.1 ohm for each of the transformers. Note that the low-voltage side is delta connected, so the resistance is connected in series with two substations, which

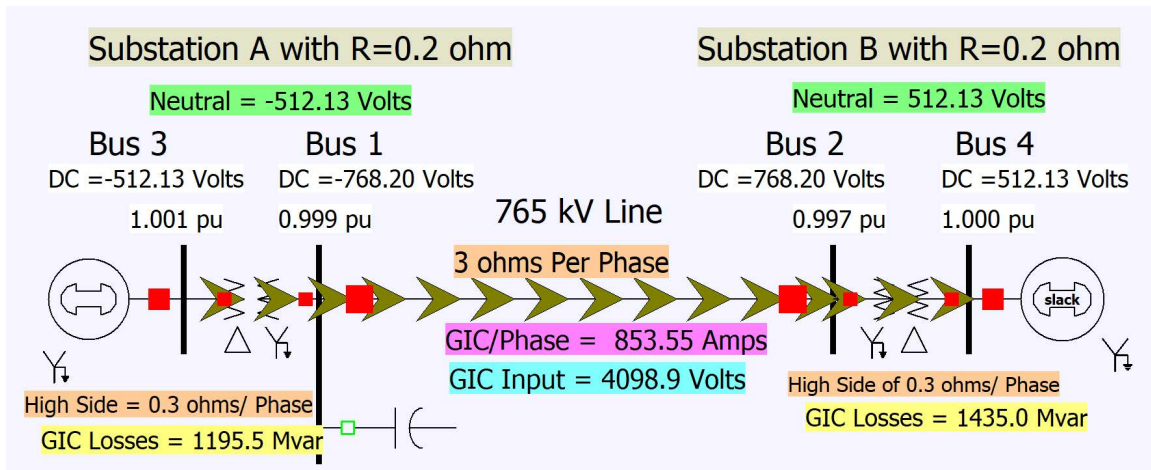


Figure 4.2: 4-Bus Test System with GICs Visualized for 24 V/km Eastward E-Field

are 0.2 ohms each. The GIC per phase is calculated as 853.55 Amps, with the direction from Bus 1 to Bus 2. The total three phase GIC is just three times of the per phase value because these phase are connected in parallel.

In this simulation, an eastward electric field was chosen, but it is always good to know what the direction is that achieves the minimum and maximum induced current and reactive power loss. System summary shows the minimum direction is zero degree (Northward, orthogonal to the transmission line) and maximum direction is 90 degrees (Eastward, align with the transmission line). Since the test chooses the maximum direction, the total reactive power loss in the specified direction and maximum direction are both 2630.5 Mvar.

Another important concern is to find out whether the system is sensitive to electric field caused GIC. In this case, a sensitivity analysis was executed in PowerWorld simulator. A parameter called line Amp input sensitivity can show the sensitivity of GIC quantities such as current and DC bus voltages to a selected GIC injection on a transmission line. PowerWorld Simulator has an automatic sensitivity analysis calculations, where the detailed algorithm is introduced in [168]. Figure 4.3 shows the sensitivity analysis setting in GIC analysis form in the simulation package. In this case, the assumed GIC injection is 1 Amps on transmission line from Bus 1 to Bus 2. The results show the transformer per phase effective GIC from Bus 1 to Bus 3 and Bus 2 to Bus 4 are about 0.208 Amps. This means

with every 1 V/km increase in the electric field, the transmission line will receive an induced current of 0.208 Amps per phase effective GIC.

In conclusion, the GIC on the transmission line is found 853.55 Amps with the electric field intensity of 24 V/km. This number is huge enough to generate excess heats and the line is likely to burn out. The electric field caused 2630.5 Mvar reactive loss, which is also relatively large because the case is just simulated a four bus example with limited original generation capacity.

Sensitivity Analysis

Type of Sensitivity Calculation
 Line Amp Input Sensitivity
 Transformer Ieffective GIC Sensitivity

Sensitivity Options
 Assumed Line Injection (Amps)

Assumed Field Direction
 Parallel to Line
 Specified Direction

Recalculate Sensitivities
 Calculate Sub Driving Point Values

Choose the Transmission Line (for input sensitivities) or Transformer (for Ieffective Sensitivites)
 Sort by Name Number
 Filter:
 Use Area/Zone Filters

Search For Near Bus Select Far Bus, CKT

1 (Bus 1) [765.0 kV]	2 (Bus 2) [765.0 kV] CKT 1
2 (Bus 2) [765.0 kV]	3 (Bus 3) [20.00 kV] CKT 1
3 (Bus 3) [20.00 kV]	
4 (Bus 4) [20.00 kV]	

Buses Lines Substations Transformers

	From Number	From Name	To Number	To Name	Circuit	Neutral Current (Amps)	Transformer Per Phase Effective GIC, Amps	Transformer Per Unit Effective GIC	dIeffective/dEF
1	1	Bus 1	3	Bus 3	1	-0.625	0.208	0.00195	
2	2	Bus 2	4	Bus 4	1	0.625	0.208	0.00195	

Figure 4.3: 4-Bus Test System Sensitivity Analysis

4.3 Simulations on the 150-Bus Test System

The purpose of this simulation is to analyze the effect of continuous, time varying sources of EMP attacks on the power system mentioned in Chapter 2. In this case, a 150-bus test system located in the state of Tennessee is evaluated. The system consists of 27 generators, 98 substations, 60 transformers and 157 transmission lines. A similar approach to the one implemented on the 4-bus test system is pursued here with an exception that the input EMP source has changed to time varying electric field. The PowerWorld Simulator supports the binary and text file formats for time and spatially-varying surface electric field inputs; this format allows development of detailed attack scenarios based on historic events. The 150-bus test system is illustrated in Figure 4.4, where a binary format file based on the June 22, 2015 event over this area was injected into the simulator [169]. The file contains times points and geo-spatial (longitude and latitude) grid with the corresponding eastward and northward E-field for each point.

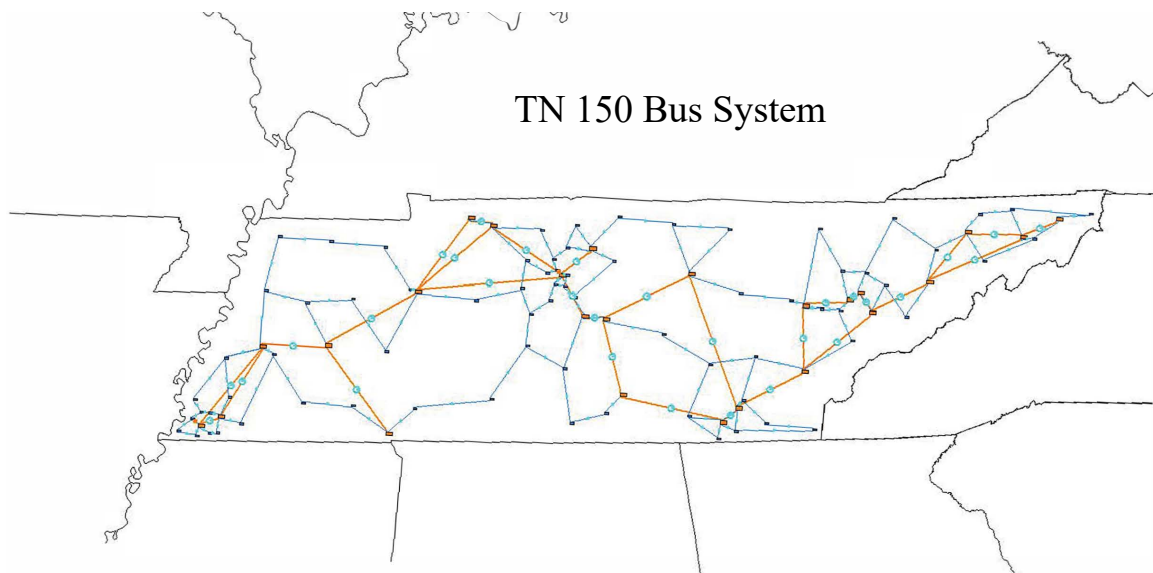


Figure 4.4: The 150-Bus Test System in the State of Tennessee

The event injected to the simulator contains a total time period of 172790 seconds (48 hours), and time varying surface electric field input from 0 to 3 V/km. By specifying the

“current time” in the “GIC analysis form” dialog box, the GIC can be calculated for single time points. To visualize the overall changes from the starting time to the end time, transient stability simulation was used in this case. Properly setting up a time period and sampling time step, the results can be shown in the one line diagram using the contour mapping.

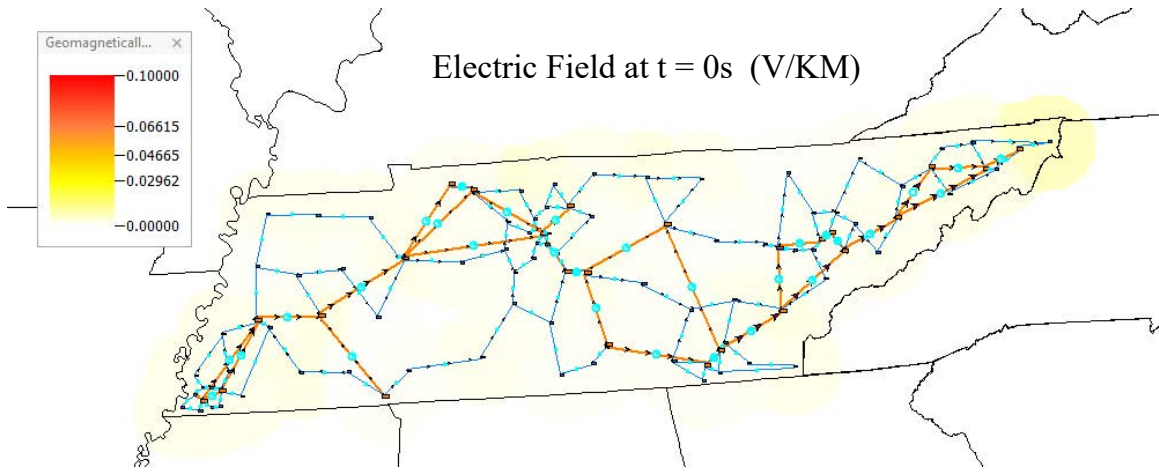


Figure 4.5: Electric Field Contour Map at Time Step $t= 0$ Second

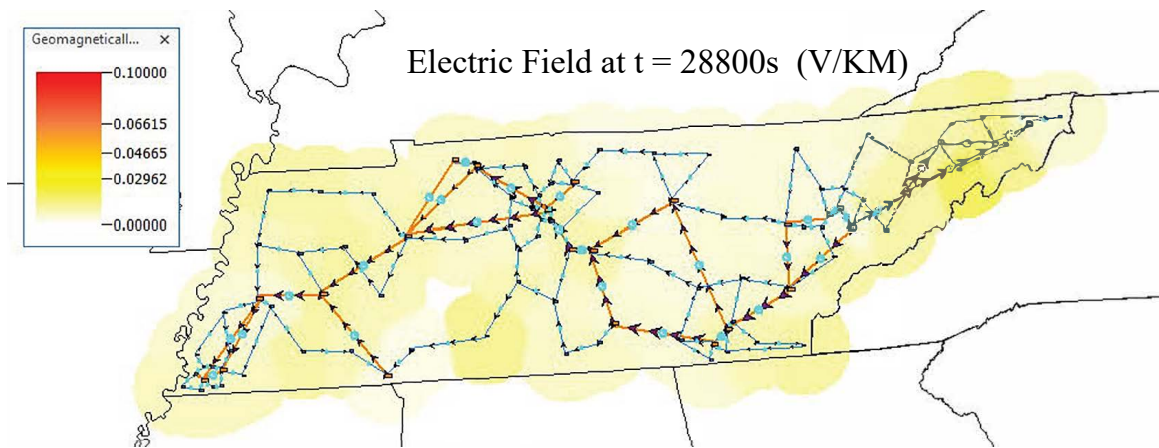


Figure 4.6: Electric Field Contour Map at Time Step $t= 28800$ Seconds

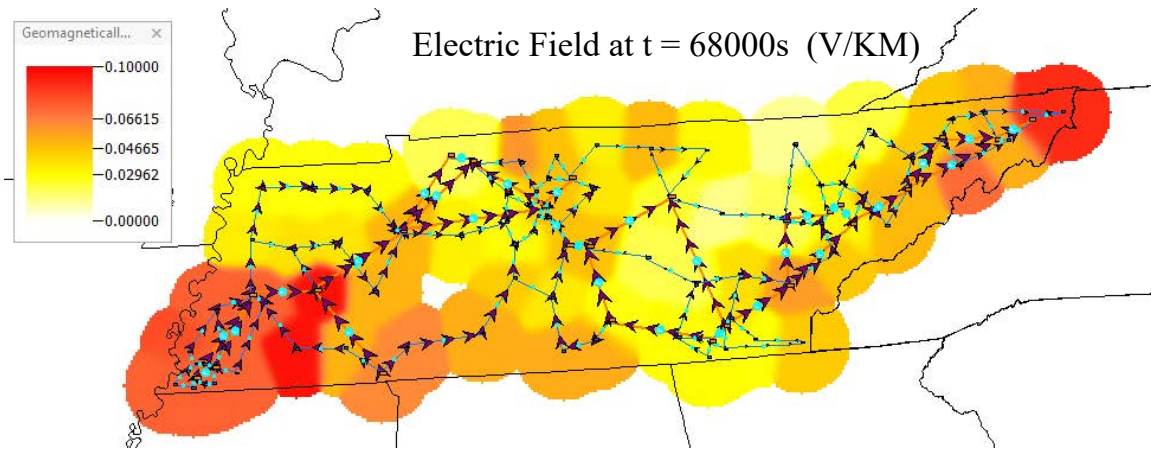


Figure 4.7: Electric Field Contour Map at Time Step $t= 68000$ Seconds

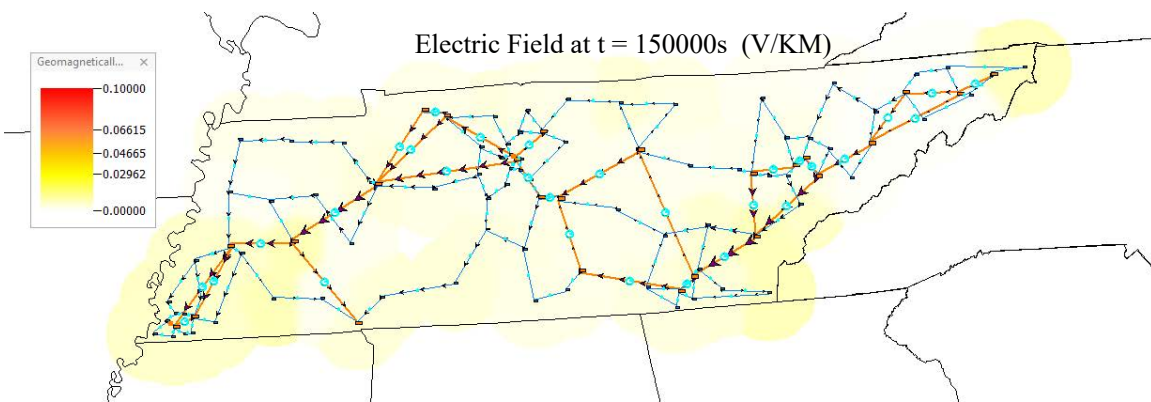


Figure 4.8: Electric Field Contour Map at Time Step $t= 150000$ Seconds

From Figure 4.5 to Figure 4.9 are several time steps of the electric field variations over the entire event time period. At the initial state, substations are not affected by GICs, but as the event time elapses, several substations have experienced an electric field around them. Note that the source of the event is a time varying surface electric field with the magnitude changing from 0 to 3 V/km; hence, at some points or a short time period, the transformer may have some “relief” from the electric field converge; as captured in Figure 4.8, the E-field decreased from the time stamp 68000 seconds to the time stamp at 150000 seconds, while it increased again until the event ends (time stamp 172790 seconds). By running the GIC simulations in the transient stability platform, the GIC data for each transformer and the recorded reactive power loss are saved in separate files. The system summary indicates that

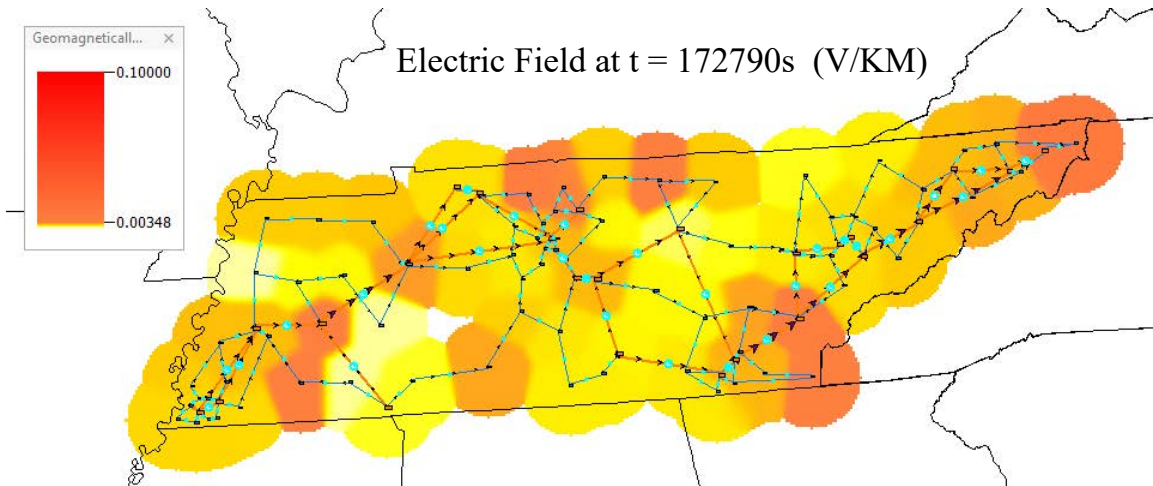


Figure 4.9: Electric Field Contour Map at Time Step $t= 172790$ Seconds

the highest cumulative electric field for all transformers are collected at $t= 68000$ seconds, shown in Figure 4.7. By running the transient stability simulations from the initial time stamp all the way to the end, the GIC induced in each transformer and the total reactive power loss for all transformers in the event period have been plotted in Figure 4.10 and Figure 4.11, respectively.

In Figure 4.10, each line in different color represents each of the system transformers. According to the figure, the highest GIC induced in transformer appears at $t = 68000$ seconds, which confirmed the earlier results in the system summary and contour map. Also, by observing Figure 4.11, the highest total reactive power loss appears synchronously with the highest GIC, at $t = 68000$ seconds. The reported plot Figure 4.12 illustrates the distribution of the total reactive power for each transformers at $t = 68000$ seconds on the one-line diagram contour.

In conclusion, the GIC induced on each transformer is changing over the time varying electric field. The effective GIC plot for each transformer and the total reactive power loss for all transformers have been generated. Contour mapping for electric field intensity during the EMP event period have been executed and the consequences at several time points of interest have been analyzed.

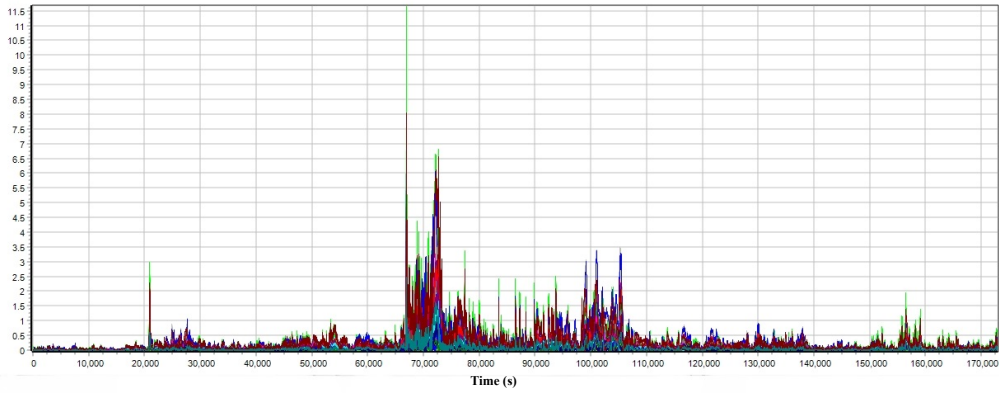


Figure 4.10: Effective GIC Plot for Each Transformers in the 150-Bus Test System

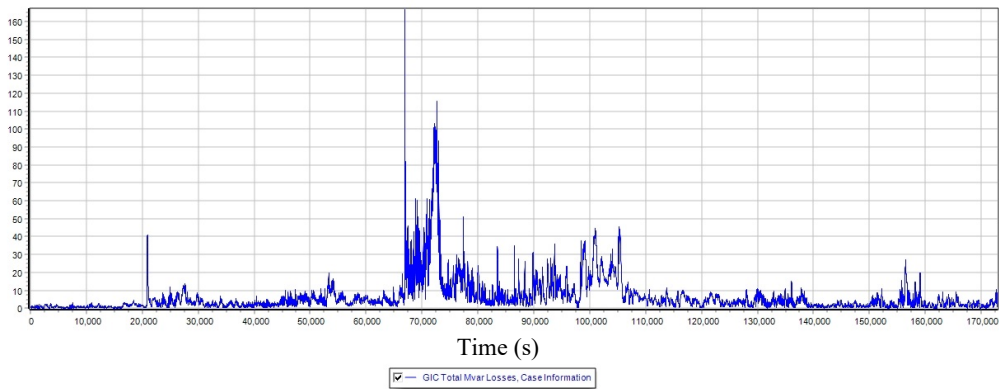


Figure 4.11: The Total GIC-Induced Mvar Losses Plot for All Transformers in the 150-Bus Test System

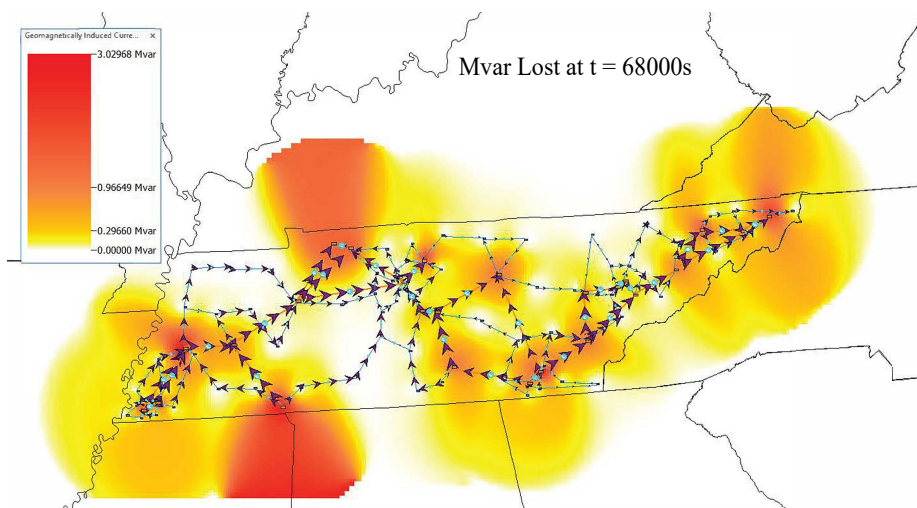


Figure 4.12: Distribution of the Total GIC Reactive Power Loss for Each Transformers in the 150-Bus Test System

4.4 Simulations on the 2000-Bus Test System

The purpose of this simulation is to analyze the E3 effects of a high-altitude electromagnetic pulse (HEMP) attack on the power system mentioned in Chapter 2. Algorithms are borrowed from the public Oak Ridge National Laboratory (ORNL) research [170]. In this case, a 2000-bus test system located in the state of Texas is evaluated under EMP attack scenarios. Similar approach as the one applied to the 150-bus test system is pursued here with the exception that the input source impacts a concentrated small area rather than a constant direction. PowerWorld Simulator can auto-create time and spatially-varying electric fields associated with the de-classified EMP waveform based on the location, time functions, and spatial functions [171].

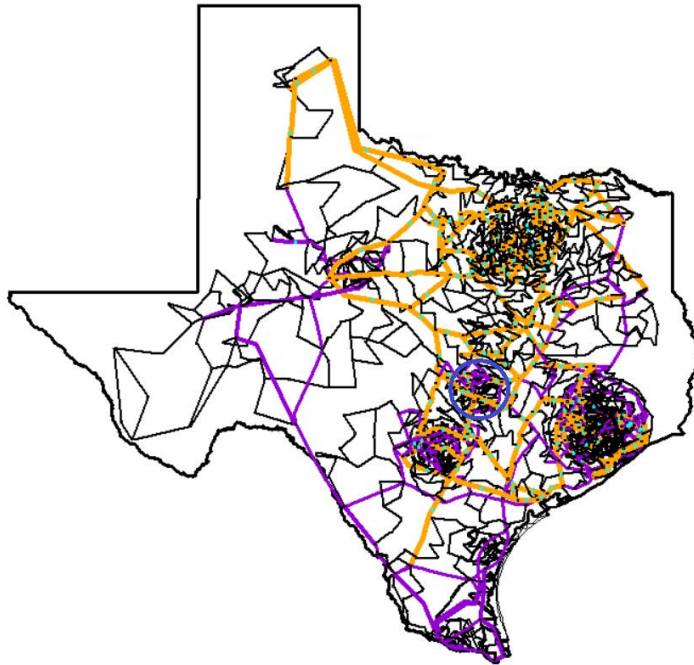


Figure 4.13: Texas 2000-Bus Test System

The 2000-bus test system in PowerWorld Simulator is demonstrated in Figure 4.13. The bold lines and the black dots represent the main transmission lines and substations, respectively. Using the time varying series voltage input calculation mode, and the EMP as the input, a time-series of the transmission line GIC DC input voltages are inserted to the

GIC analysis platform. The EMP source location is illustrated in Figure 4.13 at the center of the blue circle. The simulation lasts for 60 seconds according to the ORNL research [170], and the wave shape is characterized based on the March 1989 Quebec event described in [172], with the maximum electric field of 24 V/km. By setting the time period from 0 to 60 seconds with the time step of 10 seconds, the electric field propagates across the system and can be recorded through contour maps. Figure 4.14 to Figure 4.18 represent the electric field across the system captured at several selected time points. From these figures, the observations are: (i) the electric field continues to increase and spread from the center of the impact position, then reaching the highest value around the center at 60 seconds; (ii) some substations which are observed heavy impacted by other areas will also spread the electric field around themselves.

Similar to Section 4.3, the transient stability has been executed to collect the electric field data for each substation during the event time period, effective GIC for each transformer (total of 562 transformers) during the event time period, and the total reactive power loss for each substation (total of 1500 substations) during the event time period, as shown in Figure 4.19, Figure 4.20, and Figure 4.21, respectively. The transient stability test has been extended to 80 seconds in order to observe the value variations following the event.

In Figure 4.19, Figure 4.20, and Figure 4.21, each line in different color represents each of the transformers/substations. According to the figures, the highest electric field intensity appears at $t = 60$ seconds, which confirmed the earlier results in Figure 4.18. Also, by observing the results in Figure 4.21, the highest total reactive power loss appears synchronously with the highest GIC, at $t = 60$ seconds. Plot Figure 4.20 shows the highest effective GIC induced in transformer that appears at $t = 60$ seconds, concurrently at the time stamp when the highest E-field is recorded. Similar to the analyses in Section 4.2, a sensitivity analysis has been performed for the 2000-bus test system. Besides the line Amp input sensitivity, an option called transformer effective GIC sensitivity analysis can identify the transmission lines with the greatest impacts on the transformer GIC.

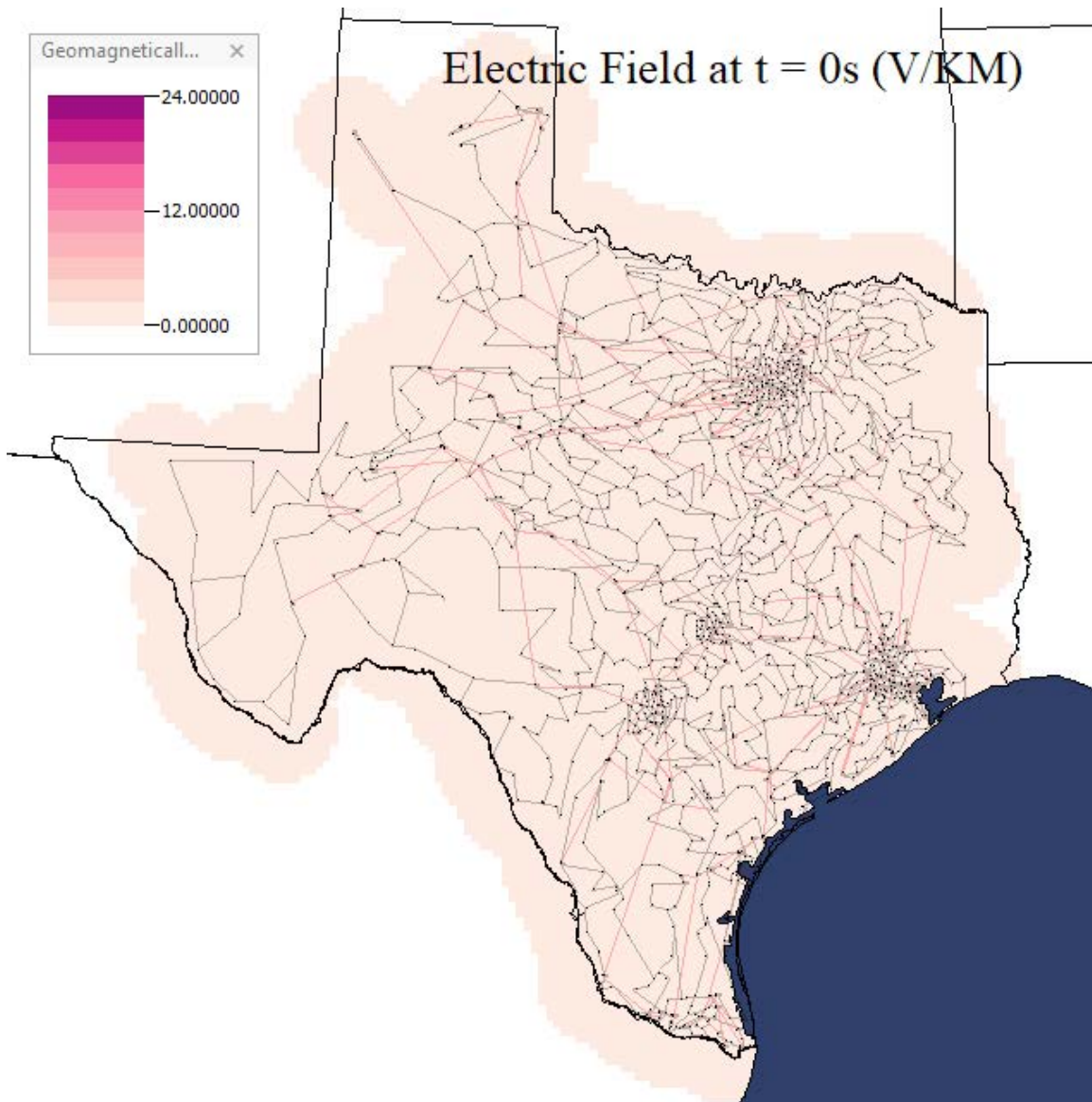


Figure 4.14: The 2000-Bus Test System Electric Field Contour Map at $t = 0$ Second

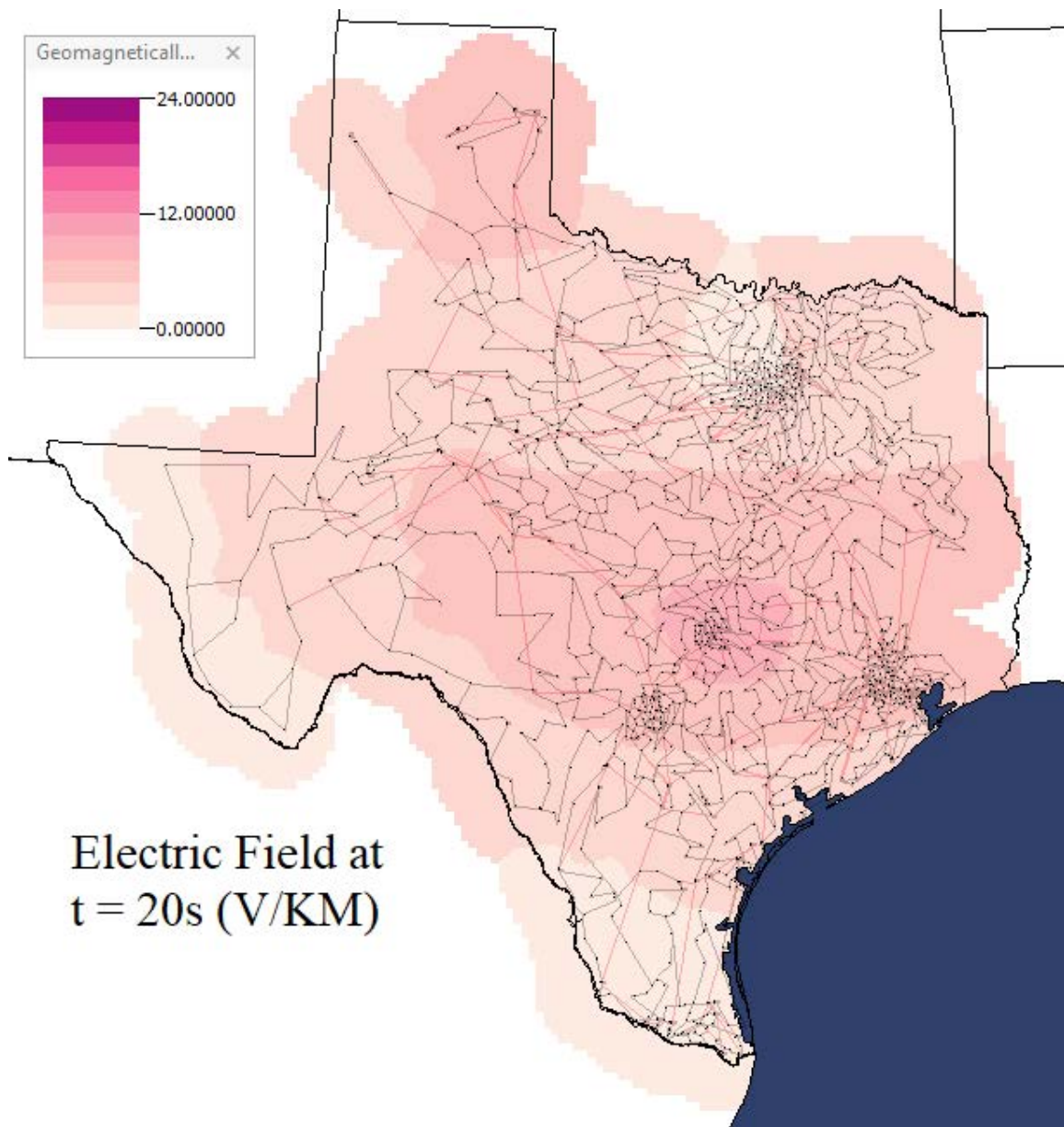


Figure 4.15: The 2000-Bus Test System Electric Field Contour Map at $t = 20$ Seconds

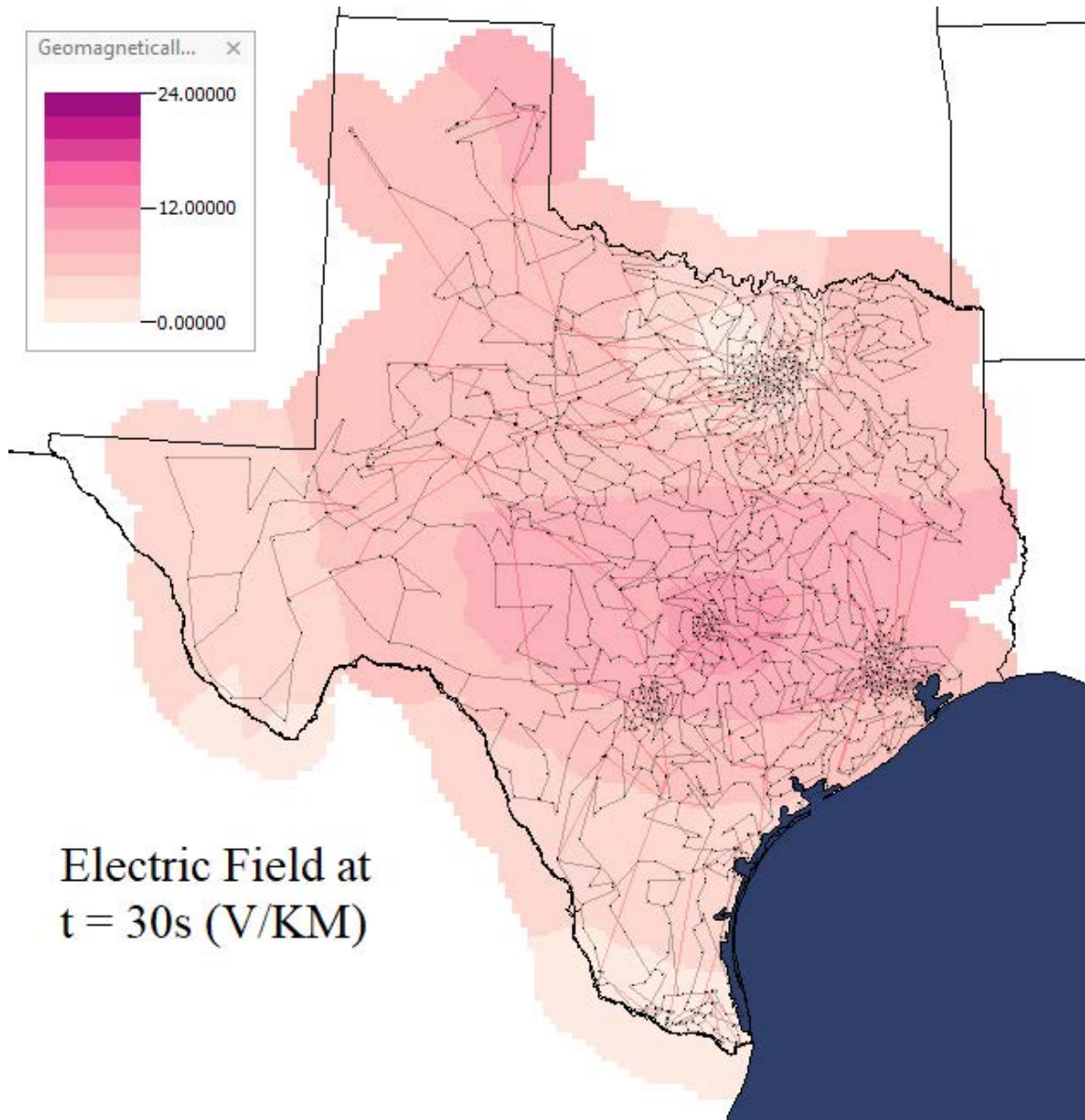


Figure 4.16: The 2000-Bus Test System Electric Field Contour Map at $t = 30$ Seconds

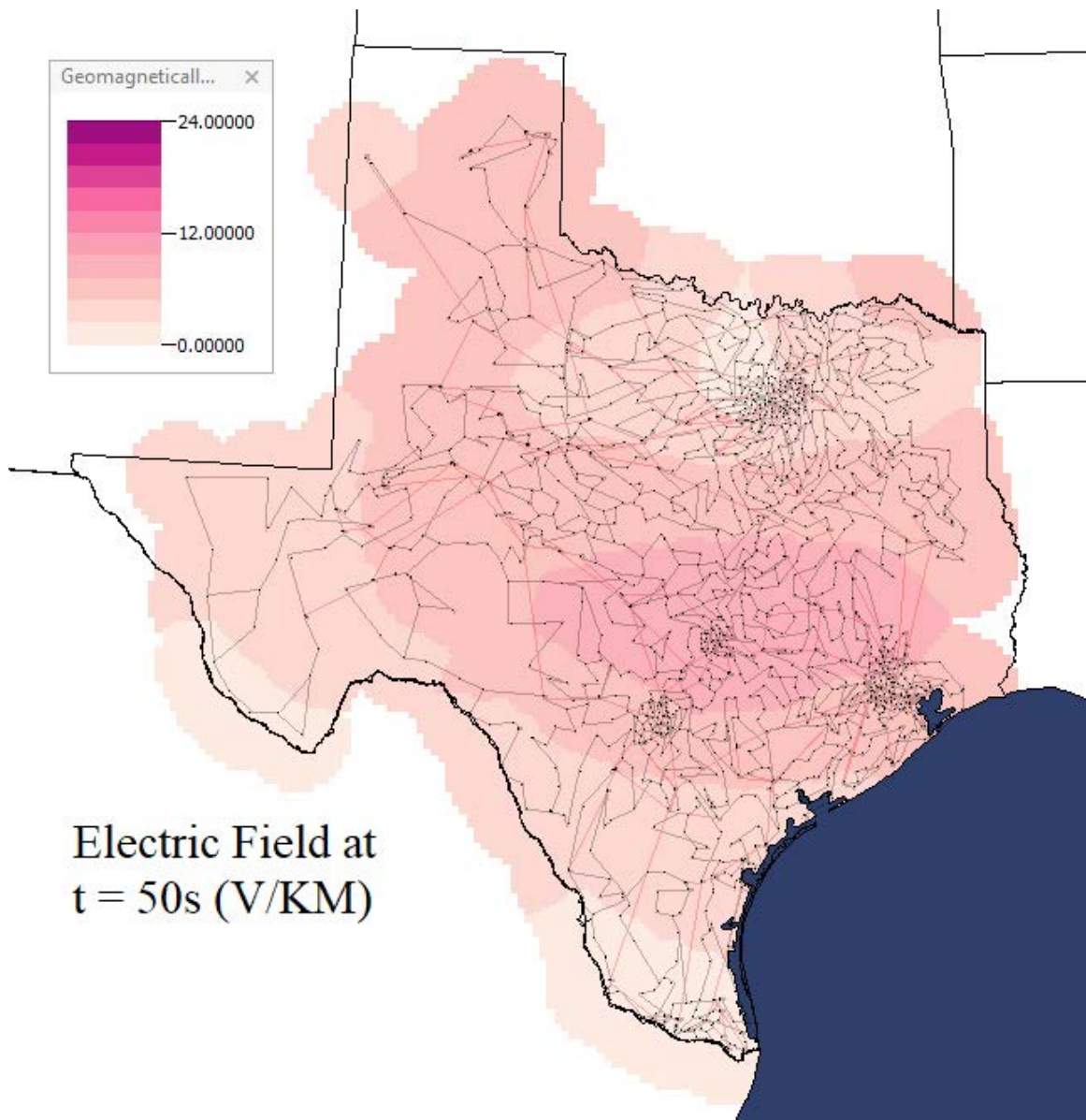


Figure 4.17: The 2000-Bus Test System Electric Field Contour Map at $t = 50$ Seconds

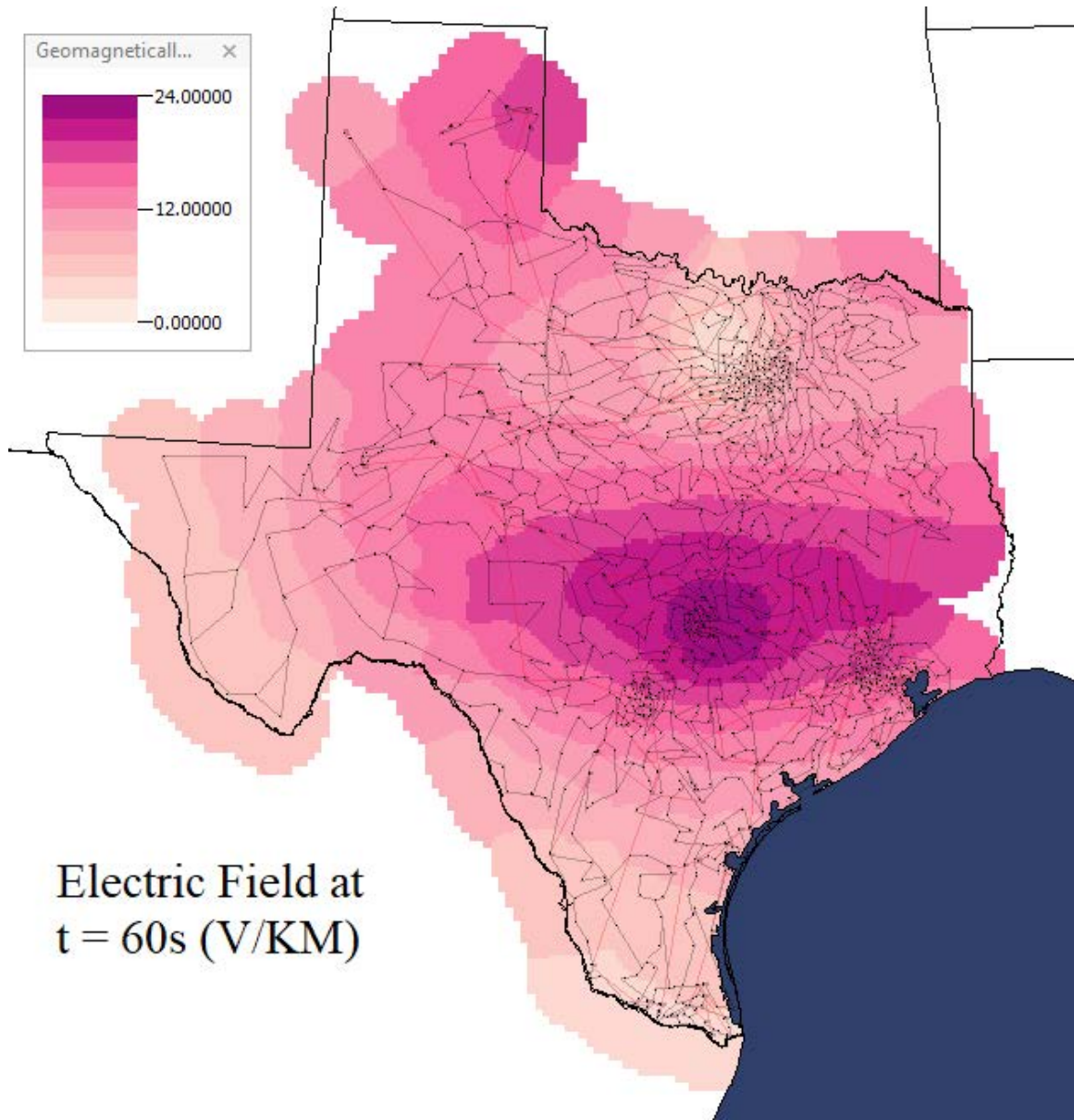


Figure 4.18: The 2000-Bus Test System Electric Field Contour Map at $t = 60$ Seconds

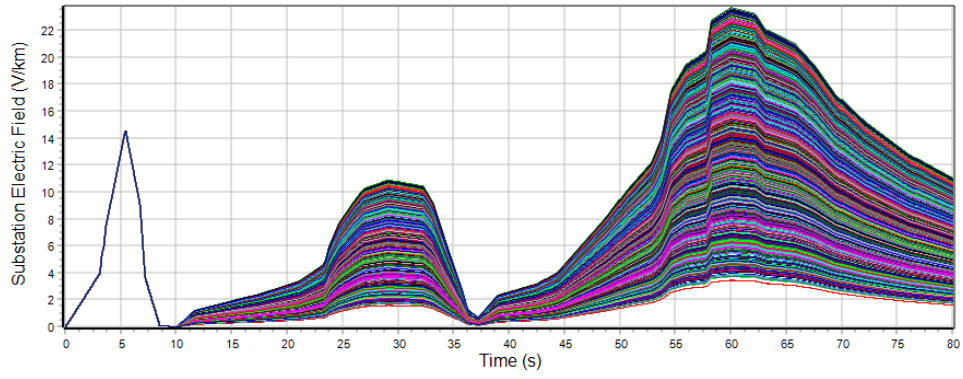


Figure 4.19: The 2000-Bus Test System Substations Electric Field at $t = 0$ Second to $t = 80$ Seconds

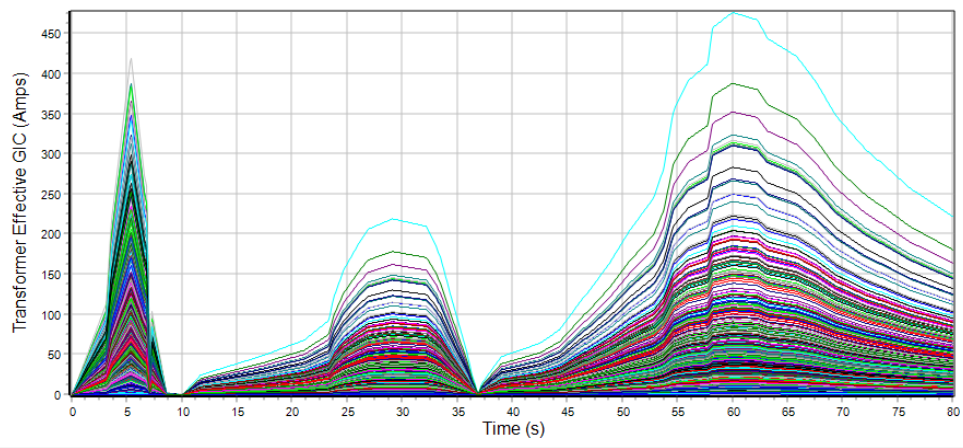


Figure 4.20: The 2000-Bus Test System Transformer Effective GIC at $t = 0$ second to $t = 80$ Seconds

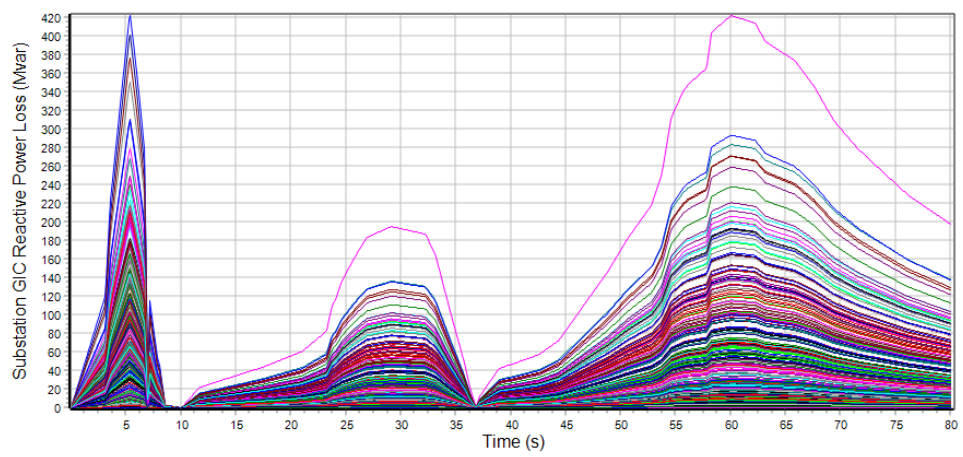


Figure 4.21: The 2000-Bus Test System Substation Reactive Power Loss at $t = 0$ Second to $t = 80$ Seconds

Tables and Results

Areas Buses Generators DC Lines Lines Line Shunts Loads Switched Shunts Substations Transformers System Summary G-Matrix Multi-Terminal DC Lines VSC DC Lines

Records Set Columns Options

	Bus Num High	Bus Name High	Bus Num Med	Bus Name Med	Bus Num Ter	Bus Name Ter	Circuit	Transformer Per Phase Effective GIC Amps	Transformer Per Unit Effective GIC	GIC Mvar Losses	Maximum Mvar Losses	Maximum Effective Direction (Degrees)	Neutral Current (Amps)	Maximum Neutral Amps	Maximum Neutral Current Degrees	Ignore GIC Losses	GIC Blocked for Transformer Neutral	Tr
1	1900	North Richland	290	North Richland	0		1	28.631	0.121	17.84	18.08	83.5	33.145	33.21	89.4	NO	NO	
2	1802	Throckmorton	447	Throckmorton	0		1	24.995	0.106	16.31	16.44	85.7	-68.117	68.54	86.6	NO	NO	
3	2006	Dallas 18 345	115	Dallas 18 115	0		1	22.694	0.096	14.16	14.20	97.5	34.738	35.00	86.0	NO	NO	
4	1882	Lytle 345	921	Lytle 115	0		1	22.110	0.093	14.24	14.66	106.8	-42.803	44.31	108.0	NO	NO	
5	1788	Cooper 345	1676	Cooper G0	0		1	20.291	0.086	13.37	15.81	60.7	60.872	71.98	60.7	NO	NO	
6	2007	De Leon 345	421	De Leon 115	0		1	20.215	0.085	13.19	15.35	123.7	45.187	53.14	124.8	NO	NO	
7	1993	Terrell 2 345	87	Terrell 2 115	0		1	18.611	0.079	11.85	19.21	144.9	48.944	71.75	140.0	NO	NO	
8	2003	Lopeno 345	1095	Lopeno 115	0		1	17.614	0.074	11.57	13.61	61.3	-43.443	51.35	60.8	NO	NO	
9	1959	Garland 3 345	23	Garland 3 115	0		1	17.461	0.074	10.86	11.07	104.2	31.933	31.94	94.2	NO	NO	
10	1924	Plano 1 345	13	Plano 115	0		1	16.922	0.072	10.61	13.70	53.8	30.673	33.10	70.9	NO	NO	
11	1938	Tivoli 3 345	883	Tivoli 3 115	0		1	16.458	0.070	10.83	11.68	70.9	-40.526	43.16	72.9	NO	NO	
12	1885	Plano 2 345	14	Plano 2 115	0		1	16.046	0.068	10.04	13.49	51.1	27.612	29.89	70.5	NO	NO	
13	1891	Houston 12 345	638	Houston 12 115	0		1	15.989	0.068	10.16	14.29	48.3	15.893	17.85	65.9	NO	NO	
14	1934	Carrollton 1 345	4	Carrollton 115	0		1	15.987	0.068	9.99	11.48	122.5	33.953	33.96	93.8	NO	NO	
15	1995	Beeville 1 345	942	Beeville 115	0		1	15.555	0.066	10.21	10.75	111.2	44.027	46.63	112.2	NO	NO	
16	1896	Lufkin 2 345	258	Lufkin 2 115	0		1	15.194	0.064	9.92	10.27	77.9	44.586	46.22	77.7	NO	NO	
17	2005	Prosper 345	42	Prosper 115	0		1	14.596	0.062	9.17	10.11	117.9	-12.143	20.70	147.1	NO	NO	
18	1992	Rotan 345	1340	Rotan 115	0		1	14.395	0.061	9.49	9.49	93.5	31.763	31.78	94.8	NO	NO	
19	1939	Houston 43 345	671	Houston 43 115	0		1	14.077	0.059	8.99	9.99	67.1	10.475	11.64	67.1	NO	NO	
20	1860	Jacksboro 2 345	1442	Jacksboro 2 115	0		1	13.796	0.058	8.92	9.20	78.9	-38.967	40.61	76.6	NO	NO	
21	2001	Palmer 345	79	Palmer 115	0		1	13.763	0.058	8.76	9.96	64.6	31.922	34.65	70.1	NO	NO	
22	1786	Dallas 10 345	107	Dallas 10 115	0		1	13.536	0.057	8.39	8.39	93.6	27.899	28.10	86.1	NO	NO	
23	1890	Dallas 3 345	100	Dallas 3 115	0		1	13.509	0.057	8.44	9.52	65.5	32.696	33.84	78.1	NO	NO	
24	1802	Throckmorton	1697	Throckmorton	0		1	13.211	0.056	8.71	8.78	85.5	-39.633	39.98	85.5	NO	NO	
25	1922	Donna 345	1078	Donna 115	0		1	12.922	0.055	8.18	9.43	63.1	-23.775	31.93	51.1	NO	NO	
26	1842	Floydada 1 345	1286	Floydada 115	0		1	12.760	0.054	8.27	9.27	66.2	-32.935	36.17	68.6	NO	NO	
27	1910	Blum 345	501	Blum 115	0		1	12.458	0.053	8.09	10.64	52.5	-33.355	44.10	52.1	NO	NO	
28	1990	Memphis 345	1290	Memphis 115	0		1	12.085	0.051	7.83	17.83	157.0	-31.322	73.79	157.9	NO	NO	
29	1901	Alice 1 345	1017	Alice 115	0		1	11.288	0.048	7.42	8.13	117.1	-22.773	23.59	108.1	NO	NO	
30	1879	O'Donnell 345	1485	O'Donnell 115	0		1	10.700	0.045	7.02	7.17	81.5	-36.731	36.83	88.7	NO	NO	
31	1967	Richmond 2 345	713	Richmond 2 115	0		1	10.673	0.045	6.85	7.75	120.9	3.215	10.09	21.6	NO	NO	
32	1965	Mexia 345	533	Mexia 115	0		1	10.508	0.044	6.87	6.91	98.7	-26.918	27.16	100.6	NO	NO	
33	1816	Baytown 3 345	788	Baytown 3 115	0		1	10.485	0.044	6.78	6.87	83.4	27.725	27.92	86.2	NO	NO	
34	1932	Dallas 8 345	105	Dallas 8 115	0		1	10.419	0.044	6.52	8.95	49.8	30.571	31.35	80.2	NO	NO	
35	1945	Fort Worth 15 345	339	Fort Worth 15 115	0		1	10.367	0.044	6.52	7.52	122.9	20.686	24.16	124.1	NO	NO	
36	1911	Houston 48 345	677	Houston 48 115	0		1	10.304	0.044	6.53	7.00	71.8	-2.046	7.79	18.2	NO	NO	
37	1966	Conroe 4 345	683	Conroe 4 115	0		1	10.259	0.043	6.56	7.37	120.2	27.928	29.82	113.5	NO	NO	
38	1901	Carrollton 345	1697	Carrollton G0	0		1	10.183	0.043	6.66	8.38	48.3	30.386	31.78	48.3	NO	NO	

Figure 4.22: The 2000-Bus Test System Transformer Effective GIC Ranking

Sensitivity Analysis

Type of Sensitivity Calculation

- Line Amp Input Sensitivity
- Transformer Effective GIC Sensitivity

Sensitivity Options

Assumed Direction (Degrees, 0 to 360)

93.00

Assumed Field Direction

- Parallel to Line
- Specified Direction

Recalculate Sensitivities

Calculate Sub Driving Point Values

Choose the Transmission Line (for input sensitivities) or Transformer (for ineffective sensitivities)

	Bus Num High	Bus Name High	Bus Num Med	Bus Name Med	Bus Num Ter	Bus Name Ter	Circuit	Include in Sensitivity Calculation	Transformer Per Phase Effective GIC Amps	Transformer Per Unit Effective GIC	Neutral Current (Amps)
1	1900	North Richland	290	North Richland	0		1	YES	28.631	0.12098	33.145
2	1802	Throckmorton	447	Throckmorton	0		1	NO	24.995	0.10561	-68.117
3	2006	Dallas 18 345	115	Dallas 18 115	0		1	NO	22.694	0.09589	34.738
4	1882	Lytle 345	921	Lytle 115	0		1	NO	22.110	0.09342	-42.803
5	1788	Cooper 345	1676	Cooper G0	0		1	NO	20.291	0.08574	60.872
6	2007	De Leon 345	421	De Leon 115	0		1	NO	20.215	0.08542	45.187
7	1993	Terrell 2 345	87	Terrell 2 115	0		1	NO	18.611	0.07864	48.944
8	2003	Lopeno 345	1095	Lopeno 115	0		1	NO	17.614	0.07443	-43.443
9	1959	Garland 3 345	23	Garland 3 115	0		1	NO	17.461	0.07378	31.933
10	1924	Plano 1 345	13	Plano 115	0		1	NO	16.922	0.07150	30.673
11	1938	Tivoli 3 345	883	Tivoli 3 115	0		1	NO	16.458	0.06954	-40.526
12	1885	Plano 2 345	14	Plano 2 115	0		1	NO	16.046	0.06780	27.612

Lines

	From Number	From Name	To Number	To Name	Circuit	dIeffective/dE	dIeffective/dVoltage	Distance Between Substations (km)	Compass Angle Between Substations
1	1900	North Richland	1797	Weatherford 4 2			0.255	67.66	266.71
2	1900	North Richland	1797	Weatherford 4 1			0.255	67.66	266.71
3	1953	Weatherford 2	1905	Weatherford 3 1			0.056	8.05	174.13
4	1797	Weatherford 4	1860	Jacksboro 2 34 1			0.042	53.34	308.01
5	1797	Weatherford 4	1801	Gordon 345 2			0.035	49.64	234.37
6	1797	Weatherford 4	1801	Gordon 345 1			0.035	49.64	234.37
7	330	Haltom City 115	338	Fort Worth 14 1			0.029	7.67	0.81
8	285	Bedford 115	290	North Richland 1			0.025	7.15	298.82
9	1905	Weatherford 3	1798	Fort Worth 10 1			0.023	26.67	101.24
10	321	Weatherford 4	450	Poolville 115 1			0.015	13.85	5.21
11	335	Fort Worth 11	341	Fort Worth 17 1			0.014	10.89	17.73
12	341	Fort Worth 17	361	Keller 2 115 1			0.014	9.80	125.52
13	324	Fort Worth 115	330	Haltom City 115 2			0.013	9.70	70.21
14	324	Fort Worth 115	330	Haltom City 115 1			0.013	9.70	70.21
15	1947	Aledo 345	1799	Fort Worth 16 1			0.012	56.43	75.40
16	1933	Coppell 345	1799	Fort Worth 16 1			0.010	14.47	204.20
17	1953	Weatherford 2	1914	Santo 345 1			0.010	39.69	244.43
18	1953	Weatherford 2	1914	Santo 345 2			0.010	39.69	244.43
19	450	Poolville 115	451	Whitt 115 1			0.010	12.45	255.92
20	318	Weatherford 1	337	Fort Worth 13 1			0.009	20.08	91.82
21	318	Weatherford 1	337	Fort Worth 13 2			0.009	20.08	91.82
22	327	Fort Worth 4 1	335	Fort Worth 11 1			0.008	7.35	9.95

Figure 4.23: The 2000-Bus Test System Transformer Effective GIC Sensitivity Analysis

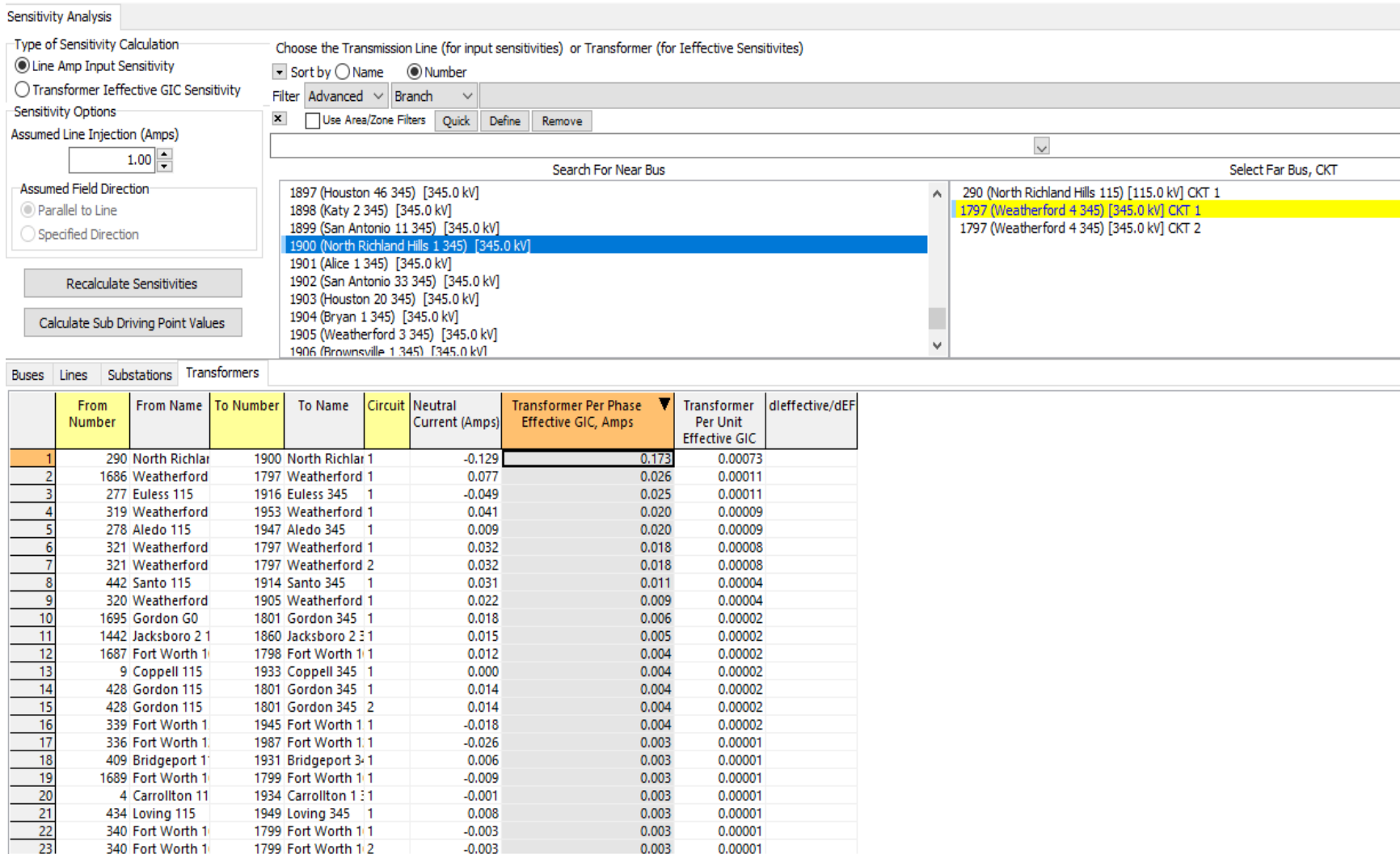


Figure 4.24: The 2000-Bus Test System Line Amp Input Sensitivity Analysis

In the 2000-bus test system case, a concept of local geomagnetic latitude and earth resistivity were taken into account. Unlike the 4-bus test system, when a large system tile over a state, the geographical factors will affect the propagation of the electric field or GIC. Therefore, an earth resistivity file and the latitude scaling was loaded into the PowerWorld Simulator. In order to perform the sensitivity analysis, the peak surface electric field magnitude is set to 8 V/km at a reference location in Quebec at 60 degree North geomagnetic latitude (shown as the blue circle in Figure 4.13). The worst direction is found 93 degree by running a GIC calculation under a single snapshot input mode. Figure 4.22 is to sort which transformer suffered the most from the GIC; in this case, the transformer in between Bus 1900 to Bus 290 has observed the most GIC of 28.6 Amps. Under the transformer dIeffective GIC sensitivity tab, we set the assumed direction to 93 degrees, and include Bus 1900 to Bus 290 in the sensitivity calculation; the results are demonstrated in Figure 4.23. The dIeffective/dVoltage value indicates the change in the effective GIC for a 1 Volt variation in the induced voltage on the transmission line; it is observed in this case that the line from Bus 1900 to Bus 1797 is responsible for most of the GIC.

Switching to line Amp input sensitivity tab, we assume the line injection is 1 Amps and we select the two lines obtained from the transformer Ieffective GIC sensitivity analysis. Figure 4.24 shows the result that indicates same lines, shown in the transformer Ieffective GIC sensitivity analysis, were identified the most sensitive to the effective GIC. Hence, the line Amp input sensitivity analysis and the transformer Ieffective GIC sensitivity analysis are corresponded.

In conclusion, the electric field impacting a small area was simulated and propagated throughout a time period. Contour mapping for the electric field intensity during the event period have been executed and several time points of interest have been analyzed. The effective GIC plot for each transformer and the reactive power loss for each transformer have been generated. The line Amp input sensitivity analysis and the transformer Ieffective GIC sensitivity analysis were performed and extensively evaluated.

4.5 Conclusion

In this chapter, 4-bus, 150-bus, and 2000-bus test systems were simulated in PowerWorld Simulator in order to better understand the EMP impacts in power systems under various EMP attack scenarios. Several important parameters such as substations electric field, effective GIC induced in lines, and reactive power loss were evaluated and the sensitivity analysis for line Amp input and transformer effective GIC were also performed. By summarizing and analyzing these results, effective protection and mitigation plans against EMP attacks could be decided accordingly.

Chapter 5: Protection and Mitigation Plans Against EMP Attacks on Power Systems

5.1 Introduction

According to the results achieved in Chapter 3 and Chapter 4, we observed that individual components and substations, transformers, and transmission lines in power systems are relatively vulnerable; hence, the protection and mitigation plans against EMP attacks need to be investigated. In this Chapter, we first introduce the common practice and then a protection approach applied on wires and small scale systems will be elaborated. In order to be able to compare, we use the same data, model parameters and characteristics used in the analyses of the Chapter 3 and Chapter 4.

5.2 Contemporary Protection Plans Against EMP Attacks

The main criteria to evaluate the priority of EMP protection are as follows: (1) assessing the risk to society if the infrastructure is disrupted and (2) comparing the role of infrastructure in basic functions defined in national policies, together with the amount of downtime that can be tolerated. Such policies can be employed to determine which level of EMP protection should be achieved for a particular infrastructure. It is recommended that for any infrastructure supporting life or safety or the economic well-being of the society, at least a Level 1 EMP protection capability should be attained as a near-term goal. If the loss of a particular infrastructure will likely result in a significant loss of life or health or economic well-being, then an EMP protection Level 2 or 3 is recommended. Few infrastructure owners/operators will need to meet EMP protection Level 4 guidelines, as these protections are more expensive and are developed mainly for Presidential support or strategic military missions [127].

A basic scheme for protecting the electronic devices against EMP attacks are to encapsulate the equipment in a Faraday cage. A Faraday cage or Faraday shield is an enclosure structure used to block the electromagnetic fields outside the cage. Invented in 1836, a Faraday cage may be formed by a continuous coverage of conductive metal materials. The Faraday cage should be grounded directly [173]. Some implementation examples for protection against EMP are as follows:

1. **Antenna Protection:** Some standard protectors can be installed on wires to protect against EMP attacks. A device called coaxial surge protection (CSP) is a protector for coaxial lines against lightning and also NEMP [174].
2. **Power Supply Cable Protection:** A protector can be used onto mobile installation or fixed applications. These protector series are optimized to protect sensitive devices and systems against the effects of over-voltages and fast transients and especially suited to be used in sensitive and mission-critical defense systems [174].
3. **Surge Protector:** The protector is intended to protect one wire of an analog telephone line or control signals of sensitive telecommunication, sensor or other electronic equipment against destructive over-voltage effects. It can protect earth-free AC or DC power supply lines, which are short-circuit current limited to less than 0.5 A against over-voltage effects caused by NEMP, HEMP or lightning strikes [174].
4. **Modular Attachment Kit:** Abbreviated as MAK, it is an innovative protection concept against lightning strikes and NEMP attacks. The MAK module is commonly used for mobile or transportable systems such as containers, trucks or tanks that require power supply from external wires and transportable shelters, remote signal, and antenna lines. A MAK box frame is a seamless part of the shield—so it is a Faraday cage—that can block EM waveforms. Mostly, the MAK can protect people from working in the shielded room against the effects of lightning and can simultaneously protect

electronic devices against surges due to EMP attacks or conducted electromagnetic interference (EMI) [175].

5. **EMP Shield:** EMP Shield is the world's only public military tested EMP protection technology. The EMP Shield is installed in homes and can detect and protect all the equipment connected to the electrical systems. This equipment can shunt (short) the overflow voltage coming in from the grid and the voltage surges collected within homes. This device is designed to protect an entire home from lightning, CME, power surges, and EMPs [176].

Another approach to protect the equipment from EMP attacks is to shunt the overflow current over the wires [177]. Several companies have developed EMP protectors that can be installed either on power grid substations or home power lines [127, 178]. One detailed example is about the CSP simulation of RF front end EMP protection [179]. From the simulation results, three response processes of the protection module are shown as follows: spike leakage, flat top leakage, and reverse pulse. With an input 4 kV square wave pulse signal, the protective module has a fast response and can be operated first; the front stage outputs a spike leakage voltage of less than 200 V, withstanding a large impulse voltage. Following a multi-level step-down process, the protection module controls the spike leakage voltage below 30 V in less than 1 ns, which reveals a promising protection on the later circuit. In addition, if the results are to be further improved, the transmission time of the pulse spikes can be slowed down by changing the circuit board and using microstrip lines of dielectric substrates between each level to achieve the goal of matching between poles.

From the hardware perspective, the following could be pursued to improve the resistance against EMP attacks:

- Design of devices with multi-layer stack and installation of high-speed devices with shortened connections.
- The use of isolated transformer inputs, where at the same time, a common mode choke

coil to be connected in series on the input power line of the power chip, and a plurality of small capacitors to be connected in parallel at the output end.

- The use of high-speed optocoupler devices to isolate the system in the grounding metal box where the feeders are wrapped in tin foil.
- Increase in the aperture of the line and install the electromagnetic sealing gasket. For the hole seam that can not be deepened, several small holes can be used instead of punching or adding metal wire mesh.

For industries and governments, the contemporary protection plan against EMP attacks can be summarized in four steps: Plan, Do, Act, and Check, shown in Figure 5.1 [180], and a turnkey solution for EMP protection construction shown in Figure 5.2 [181].

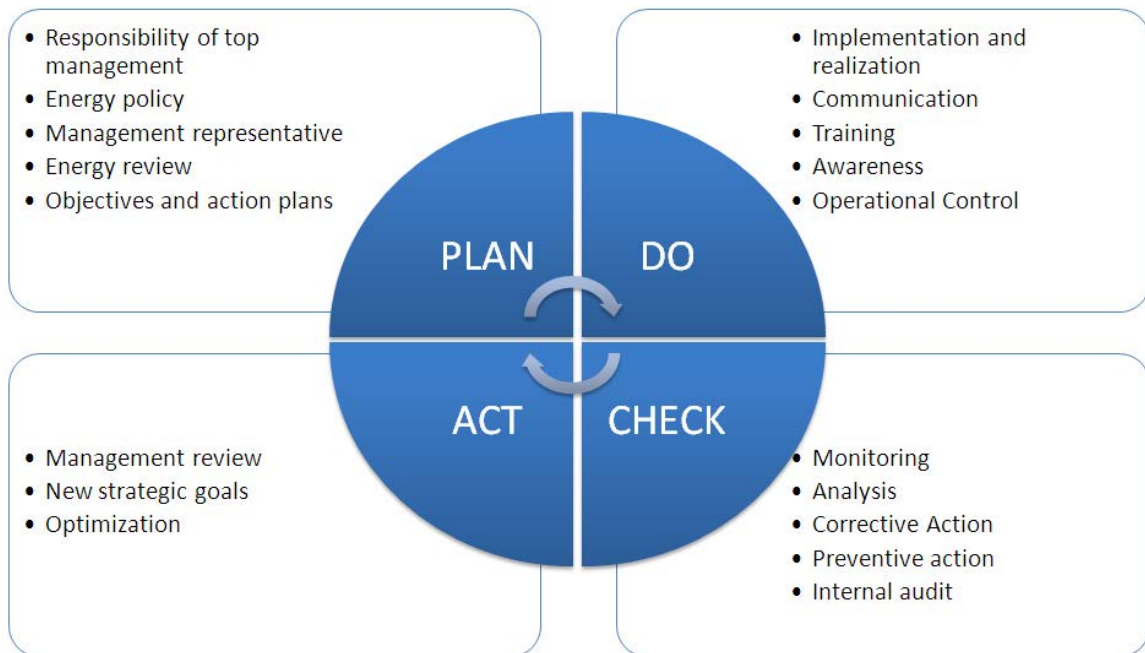


Figure 5.1: Contemporary Protection Plan Against EMP Attacks [180]

5.3 Evaluation of Time Domain Test of EMP Shielding Effectiveness

According to the results presented in the previous Sections, a test of EMP shielding effectiveness on the electric equipment is studied in this Section. A military standard MIL-STD-188

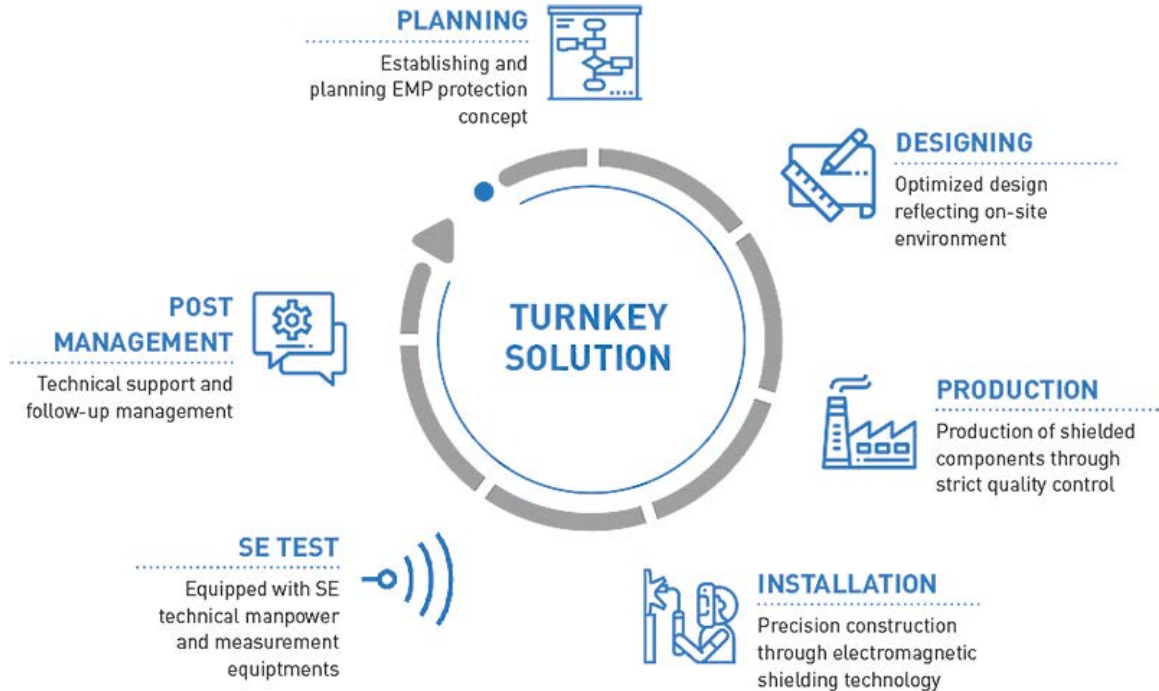


Figure 5.2: A Turnkey Solution Against EMP for Industries [181]

125-1 published by the US Department of Defence specifies the protection instruction against EMP. The standard mainly focuses on the shielding approach and surge protection concepts [131]. The test was executed in CST Studio Suite software. Figure 5.3 shows a setup for shielding effectiveness simulation. A perfect electric conductor plane was placed in the middle with shielding material at the center. We set up the boundary conditions while the wave incident is located on the left side and E-field probe on the right side. The wave incident was pointed rightward, orthogonal to the plane. The shielding material parameters are specified as follows: conductivity of 5000000 S/m, relative permeability of 1 [182].

The excitation signal used in this test is a Gaussian signal with the highest amplitude of 1 V/m at 1.7 ns, and the total simulation time period of 3.5 ns [182]. Figure 5.4 shows the probe's feedback when the excitation signal is applied under unprotected condition. The maximum probe electric field reading is 0.8 V/m at 4.1 ns and opposite direction of electric field reading 0.6 V/m at 5.2 ns. Results show that the peak value of the probe for the unprotected condition is very close to the peak value of the excitation signal. The probe

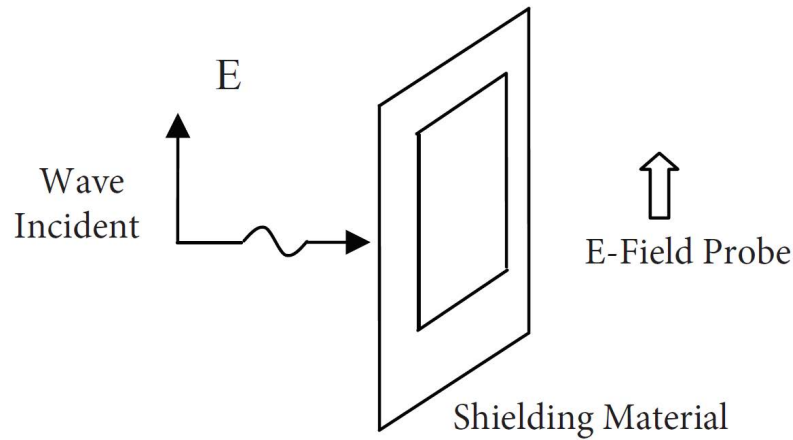


Figure 5.3: Simulation Model Setup

detected almost all the excitation signal with very little loss [182].

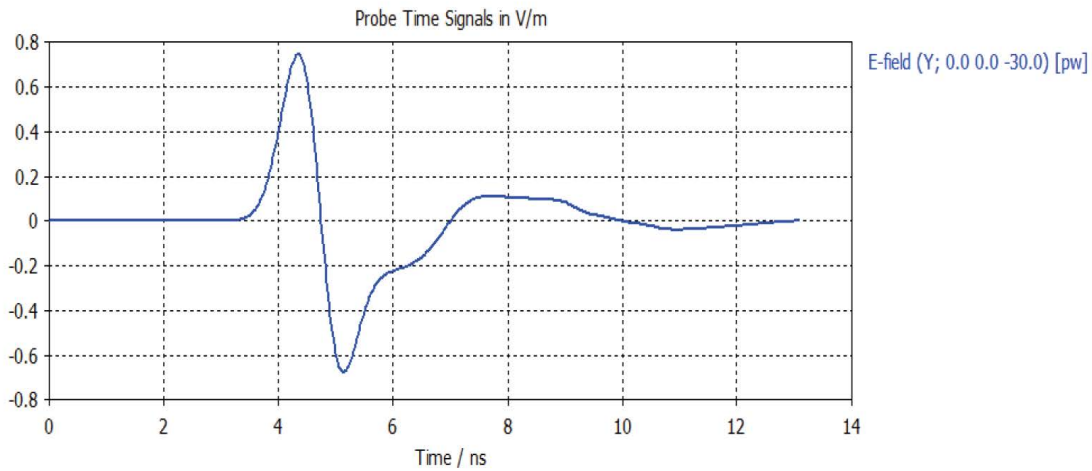


Figure 5.4: Probe Reading Under Unprotected Condition

Figure 5.5 shows the probe's feedback when the excitation signal is applied under protected condition. The maximum probe electric field reading is $8e-6$ V/m at 4.3 ns and opposite direction of electric field reading $4e-6$ V/m at 5.1 ns. The results show that the peak value of the probe for protected condition is heavily reduced compared to the excitation signal. Also, comparing Figure 5.5 with Figure 5.4, not only the amplitude of the detected electric field was strongly decreased, but also the time for the first signal rise and the

total signal period are also delayed and shortened. The probe detected almost none of the excitation signal compared to the unprotected condition [182].

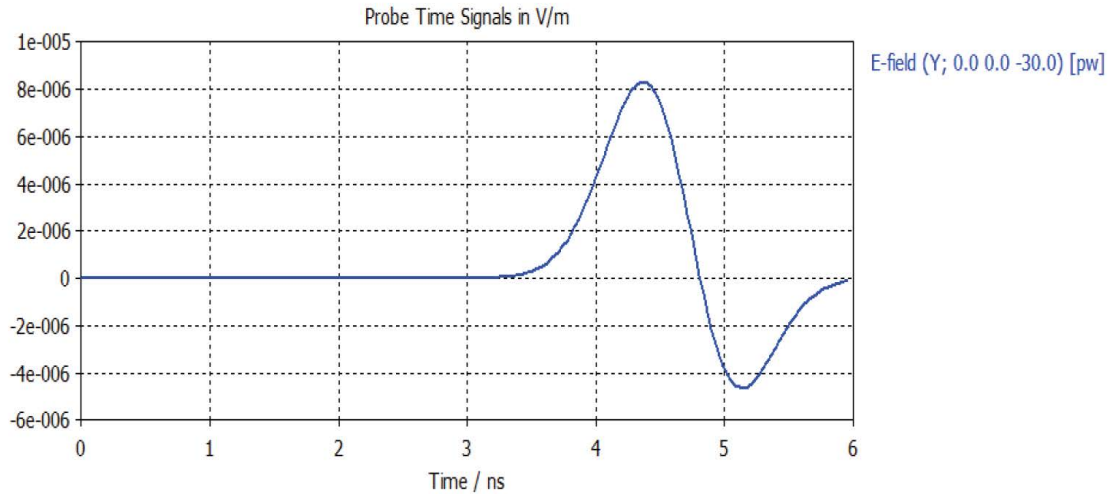


Figure 5.5: Probe Reading Under Protected Condition

In conclusion, the results show that the protection material played a crucial role to reducing the electric field pathing through the device. Without proper protection, such as a bare wire mentioned in Chapter 3 exposed to the environment, it may easily get destroyed by just a small intensity of the electric field and the generated GIC to substations and generators. With the protection material applied, the E-field detected by the probe was significantly reduced. The test and the results have successfully reflected the coaxial wire simulation results reported earlier in Chapter 3.

5.4 Contemporary Mitigation Plan Against EMP Attacks

While large failures in bulk power grids are rare, and there is no available record related to EMP attacks, it is essential that the society is prepared for periods of prolonged outage as many vital public infrastructures such as heating and cooling, water and sewage pumping, traffic control, financial systems, and many aspects of emergency response and public security depend on the electric power supply. The effects of power outages vary with weather,

for different types and locations of end-users, and over different outage duration [108]. In the event of a HEMP attack and in order to reduce the number of affected systems, the scope of damage should be limited and the ability should be reinforced to bring the systems and infrastructures back online and to the normal operating conditions as soon as possible. In so doing, the following guidelines from [26] should be considered:

- Early detection and solid response plans are essential to preparedness. While detection or prevention of an attack is beyond the purview of private stakeholders, coordination between the military, the power industry, and other affected agencies and first responders are needed to limit the initial damages and initiate procedures for a swift recovery of impacted systems.
- Broader understanding within the private sector of the potential for HEMP threats should lead to the design of more resilient components and systems. In parallel to the hardening of existing systems, stakeholders should guarantee adequate supplies of spare components and emergency operation procedures.
- Post-HEMP plans should focus on swift repair, re-supply, and infrastructure recovery, as well as system-wide power coordination, from the local to national levels.

In order to mitigate the CME caused EMPs and the consequential GIC impacts, [183] proposed a GIC mitigation algorithm that uses linear sensitivity analysis to find the best switching strategy and minimize the GIC-saturated reactive power loss. In [184] and [185], strategies for placing the blocking devices in transformer neutrals to mitigate the negative GIC impacts in large-scale power systems are presented. The authors in [186] introduced a neutral switching solution consisted of connecting switching devices at the neutral grounding connection point of transformer banks to reduce the GIC impact during GMD events.

5.5 Future Protection and Mitigation Trends

The tasks for building more resilience power grids against EMP is still crucial and remain a long way to go [21]. Further plans against EMP attacks could focus on hardware (chips, power supplies, PCB), SCADA and grid control system protection. On the *devices level*, the following practices are suggested: (i) shielding and grounding processing, (ii) limiting the coupling frequency to a narrow band by using separating filters, (iii) using components which are not easily affected by EMP, like electronic tubes, (iv) considering the replaceability of vulnerable components. On a *system level*, the following actions are recommended: (i) electromagnetic protection to be embedded in the design practices, (ii) selection of frequency hopping spread spectrum communication mode as far as possible, (iii) addition of auto-closed systems to system design, (iv) design of communication networks considering N-1 scenarios. And on a *national level*, efforts should focus on (i) effective emergency plans, (ii) strategies to destroy the enemy's launch platforms, and (iii) appropriate development of EMP weapons to achieve strategic balance. Future research and developments should be focused on developing algorithms for detection of EMP threats, tools for blocking and protection against EMP attacks, i.e., structural resilience, and strategies for swift response and recovery following the EMP attacks, i.e., operational resilience. [1] [4, 126]

5.6 Conclusion

In this chapter, the protection strategies against EMP attacks were introduced and mitigation guidelines were studied. Based on a military standard published by the US Department of Defence, an EMP shielding effectiveness was evaluated. The result shows that an exterior isolation or insulation material is essential to electric components in order to survive the EMP attacks. According to the research, protection and mitigation plans against EMP, especially HEMP attacks, are not yet fully developed and applied, and the existing power grids are still vulnerable and not resilient to such threats.

Chapter 6: Conclusion

6.1 Conclusion

With the increasing trend of the physical and cyber attack on power grids being realized, the high-impact low-probability (HILP) events challenge the power system more frequently. The weapons of mass destruction (WMD) and weapons of mass effect (WME) engenders a significant threat to both the power grid and the modern society as a whole. When the prolonged electric outages caused by HILP, WMD, and WME events severely influence the society and economics, the conventional reliability view is not sufficient to build in system survivability against such HILP events. It is significant to understand the theory behind the means of the attacks, and develop sufficient detection, protection and mitigation plans accordingly. While the EMP attacks are becoming a new threat to power grids and electronics, the society in general should plan ahead for any type of EMP attacks to the grid and home electronics. In order to analyze the damages and consequences following an EMP detonation and improve the power grid resilience against EMP attacks, this research investigated electromagnetic compatibility (EMC) of some common components in power grids; moreover, the analyses included a system-wide vulnerability assessment when facing EMP attacks of different size and intensity. In order to fully comprehend the simulation software principles, an electromagnetic algorithm was also studied in this research. Besides, the existing protection and mitigation methods were investigated, and a shielding protection method was introduced, tested, and verified through simulations.

In Chapter 3, in order to understand the characterization of EMP attacks on individual components, some common power grid components were analyzed in CST. The simulation gives preliminary electric field and induced current data, as well as the animated wave incident behavior. Those data later was used to compare and verify the results from the grid scale vulnerability simulations in PowerWorld software platform.

In Chapter 4, in order to explore the EMP attack scenario into larger scale power systems, 3 different systems with different size, complexity, and input methods were simulated and evaluated in PowerWorld software package. On each of these models, the electric field and GIC caused by an EMP attack were observed and analyzed. For some models, the time-varying effect on the entire system was presented through animated contour maps.

In Chapter 5, some existing protection and mitigation methods and guidelines were introduced. A protection method was tested in order to explore the effectiveness of a shielding approach against EMP threats. The future trends of defence against EMP attacks were also elaborated in detail.

6.2 Future Research

The data obtained from the individual component shielding effectiveness could be further utilized in the system-wide vulnerability assessments against EMP attacks. The future work may include implementation of the work on larger power grids to verify the scalability and effectiveness of the simulation results. Also, protection of the components through shielding effectiveness tests can help demonstrate how the improvements in individual components will affect the system-wide vulnerability to EMP attacks. This will guide on necessary investment on critical components in the grid, where the protection against EMP will results in the highest benefits system-wide.

Future research may also include investigating the EMP chained effect to the critical infrastructures that are connected to the power grid; for example, impacts on time-synchronized and GPS-connected devices such as Phasor Measurement Units.

Bibliography

- [1] U.S. Department of Energy, “U.S. department of energy electromagnetic pulse resilience action plan,” 2017.
- [2] T. Harris, “How e-bombs work,” 2003. [Online] Available at: <https://science.howstuffworks.com/e-bomb3.htm>, Accessed: 2019.
- [3] G. H. Baker and S. Vollandt, “Cascading consequences: Electrical grid critical infrastructure vulnerability,” May 2018.
- [4] P. Dehghanian, *Power System Topology Control for Enhanced Resilience of Smart Electricity Grids*. PhD thesis, Texas A&M University, 2017.
- [5] P. Dehghanian, B. Zhang, T. Dokic, and M. Kezunovic, “Predictive risk analytics for weather-resilient operation of electric power systems,” *IEEE Transactions on Sustainable Energy*, vol. 10, no. 1, pp. 3–15, 2019.
- [6] P. Dehghanian, S. Aslan, and P. Dehghanian, “Maintaining electric system safety through an enhanced network resilience,” *IEEE Transactions on Industry Applications*, vol. 54, no. 5, pp. 4927–4937, 2018.
- [7] Z. Yang, P. Dehghanian, and M. Nazemi, “Enhancing seismic resilience of electric power distribution systems with mobile power sources,” in *IEEE Industry Applications Society (IAS) Annual Meeting*, pp. 1–7, 2019.
- [8] S. Wang, P. Dehghanian, L. Li, and B. Wang, “A machine learning approach to detection of geomagnetically-induced currents in power grids,” in *IEEE Industry Applications Society (IAS) Annual Meeting*, pp. 1–7, 2019.
- [9] J. Su, P. Dehghanian, M. Nazemi, and B. Wang, “Distributed wind power resources for enhanced power grid resilience,” in *The 51st North American Power Symposium (NAPS)*, pp. 1–6, 2019.
- [10] M. Babakmehr, F. Harirchi, M. Nazir, S. Wang, P. Dehghanian, and J. Enslin, “Sparse representation-based classification of geomagnetically induced currents,” in *Clemson University Power Systems Conference*, pp. 1–6, 2020.
- [11] Z. Yang, M. Nazemi, P. Dehghanian, and M. Barati, “Toward resilient solar-integrated distribution grids: Harnessing the mobility of power sources,” in *IEEE Power and Energy Society (PES) Transmission and Distribution (T&D) Conference and Exposition*, pp. 1–5, 2020.
- [12] B. Shinde, S. Wang, P. Dehghanian, and M. Babakmehr, “Real-time detection of critical generators in power systems: A deep learning HCP approach,” in *The 4th IEEE Texas Power and Energy Conference (TPEC)*, pp. 1–6, 2020.

- [13] M. Nazemi and P. Dehghanian, "Seismic-resilient bulk power grids: Hazard characterization, modeling, and mitigation," *IEEE Transactions on Engineering Management*, pp. 1–17, 2020.
- [14] S. Wang, P. Dehghanian, L. Li, and B. Wang, "A machine learning approach to detection of geomagnetically-induced currents in power grids," *IEEE Transactions on Industry Applications*, vol. 56, pp. 1098–1106, March/April 2020.
- [15] S. Wang, P. Dehghanian, M. Alhazmi, and M. Nazemi, "Advanced control solutions for enhanced resilience of modern power-electronic-interfaced distribution systems," *Journal of Modern Power Systems and Clean Energy*, vol. 7, pp. 716–730, July 2019.
- [16] S. Wang, P. Dehghanian, M. Alhazmi, J. Su, and B. Shinde, "Resilience-assured protective control of DC/AC inverters under unbalanced and fault scenarios," in *The 10th IEEE Power and Energy Society (PES) Conference on Innovative Smart Grid Technologies-North America (ISGT-NA)*, pp. 1–5, 2019.
- [17] Z. Yang, P. Dehghanian, and M. Nazemi, "Seismic-resilient electric power distribution systems: Harnessing the mobility of power sources," *IEEE Transactions on Industry Applications*, pp. 1–10, 2020.
- [18] M. Nazemi, P. Dehghanian, M. Alhazmi, and F. Wang, "Multivariate uncertainty characterization for resilience planning in electric power systems," in *IEEE/IAS 56th Industrial and Commercial Power Systems (I&CPS) Technical Conference*, pp. 1–7, 2020.
- [19] B. Wang, J. A. Camacho, G. M. Pulliam, A. H. Etemadi, and P. Dehghanian, "New reward and penalty scheme for electric distribution utilities employing load-based reliability indices," *IET Generation, Transmission & Distribution*, vol. 12, no. 15, pp. 3647–3654, 2018.
- [20] B. Wang, P. Dehghanian, S. Wang, and M. Mitolo, "Electrical safety considerations in large-scale electric vehicle charging stations," *IEEE Transactions on Industry Applications*, vol. 55, no. 6, pp. 6603–6612, 2019.
- [21] D. Wang, Y. Li, P. Dehghanian, and S. Wang, "Power grid resilience to electromagnetic (EMP) disturbances: A literature review," in *The 51st North American Power Symposium (NAPS)*, pp. 1–6, 2019.
- [22] M. Babakmehr, F. Harirchi, P. Dehghanian, and J. Enslin, "Artificial intelligence-based cyber-physical event classification for islanding detection in power inverters," *IEEE Journal of Emerging and Selected Topics in Power Electronics*, pp. 1–11, 2020.
- [23] R. J. Campbell, "Weather-related power outages and electric system resiliency," Congressional Research Service, Library of Congress Washington, DC, 2012.
- [24] P. Purpura, "Security and loss prevention," pp. 349–389, 2008. Accessed: 2019.

- [25] J. S. Foster Jr and *et al.*, “Report of the commission to assess the threat to the united states from electromagnetic pulse (EMP) attack: Critical national infrastructures,” tech. rep., Electromagnetic Pulse (EMP) Commission Mclean VA, 2008.
- [26] Electric Power Research Institute, “Electromagnetic pulse (EMP) and the power grid,” August 2013. [Online] Available at: https://www.eiscouncil.org/App_Data/Upload/58a9c013-3188-41c8-8957-4a260ed248bc.pdf, Accessed: 2019.
- [27] “A basic primer in lightning effects and protection.” [Online] Available at: <https://studylib.net/doc/18869279/a-basic-primer-in-lightning-effects-and-protection>, Accessed: 2019.
- [28] T. J. Overbye, “PSERC Tutorial: High Altitude Electromagnetic Pulse (HEMP) Impacts on the Grid,” tech. rep., June 2016.
- [29] C. Kopp, “The electromagnetic bomb—a weapon of electrical mass destruction,” tech. rep., Monash Univ Clauton (Australia), 1996.
- [30] J. Emanuelson, “EMP history.” [Online] Available at: <http://www.future-science.com/emp/EMP-history.html>, Accessed: 2019.
- [31] M. Panteli and P. Mancarella, “The grid: Stronger bigger smarter?: Presenting a conceptual framework of power system resilience,” *IEEE Power Energy Mag*, vol. 13, no. 3, pp. 58–66, 2015.
- [32] P. Dehghanian, Y. Guan, and M. Kezunovic, “Real-time life-cycle assessment of high voltage circuit breakers for maintenance using online condition monitoring data,” *IEEE Transactions on Industry Applications*, vol. 55, no. 2, pp. 1135–1146, 2019.
- [33] P. Dehghanian, M. Kezunovic, G. Gurralla, and Y. Guan, “Security-based circuit breaker maintenance management,” in *IEEE Power and Energy Society (PES) General Meeting*, pp. 1–5, 2013.
- [34] Y. Guan, M. Kezunovic, P. Dehghanian, and G. Gurralla, “Assessing circuit breaker life cycle using condition-based data,” in *IEEE Power and Energy Society (PES) General Meeting*, pp. 1–5, 2013.
- [35] P. Dehghanian and M. Kezunovic, “Cost/benefit analysis for circuit breaker maintenance planning and scheduling,” in *The 45th North American Power Symposium (NAPS)*, pp. 1–6, 2013.
- [36] P. Dehghanian, Y. Guan, and M. Kezunovic, “Real-time life-cycle assessment of circuit breakers for maintenance using online condition monitoring data,” in *IEEE/IAS 54th Industrial and Commercial Power Systems (I&CPS) Technical Conference*, pp. 1–8, 2018.

- [37] P. Dehghanian, T. Popovic, and M. Kezunovic, "Circuit breaker operational health assessment via condition monitoring data," in *The 46th North American Power Symposium*, pp. 1–6, 2014.
- [38] S. Moradi, V. Vahidinasab, M. Kia, and P. Dehghanian, "A mathematical framework for reliability-centered asset management implementation in microgrids," *International Transactions on Electrical Energy Systems*, 2018.
- [39] H. Mirsaedi, A. Fereidunian, S. M. Mohammadi-Hosseininejad, P. Dehghanian, and H. Lesani, "Long-term maintenance scheduling and budgeting in electricity distribution systems equipped with automatic switches," *IEEE Transactions on Industrial Informatics*, vol. 14, no. 5, pp. 1909–1919, 2018.
- [40] M. Asghari Gharakheili, M. Fotuhi-Firuzabad, and P. Dehghanian, "A new multi-attribute support tool for identifying critical components in power transmission systems," *IEEE Systems Journal*, vol. 12, no. 1, pp. 316–327, 2018.
- [41] F. Pourahmadi, M. Fotuhi-Firuzabad, and P. Dehghanian, "Application of game theory in reliability centered maintenance of electric power systems," *IEEE Transactions on Industry Applications*, vol. 53, no. 2, pp. 936–946, 2017.
- [42] F. Pourahmadi, M. Fotuhi-Firuzabad, and P. Dehghanian, "Identification of critical generating units for maintenance: A game theory approach," *IET Generation, Transmission & Distribution*, vol. 10, no. 12, pp. 2942–2952, 2016.
- [43] H. Sabouhi, A. Abbaspour, M. Fotuhi-Firuzabad, and P. Dehghanian, "Identifying critical components of combined cycle power plants for implementation of reliability centered maintenance," *IEEE CSEE Journal of Power and Energy Systems*, vol. 2, no. 2, pp. 87–97, 2016.
- [44] H. Sabouhi, A. Abbaspour, M. Fotuhi-Firuzabad, and P. Dehghanian, "Reliability modeling and availability analysis of combined cycle power plants," *International Journal of Electrical Power and Energy Systems*, vol. 79, pp. 108–119, 2016.
- [45] R. Ghorani, M. Fotuhi-Firuzabad, P. Dehghanian, and W. Li, "Identifying critical component for reliability centered maintenance management of deregulated power systems," *IET Generation, Transmission, and Distribution*, vol. 9, no. 9, pp. 828–837, 2015.
- [46] P. Dehghanian, M. Fotuhi-Firuzabad, F. Aminifar, and R. Billinton, "A comprehensive scheme for reliability centered maintenance implementation in power distribution systems- part II: Numerical analysis," *IEEE Transactions on Power Delivery*, vol. 28, no. 2, pp. 771–778, 2013.
- [47] P. Dehghanian, M. Fotuhi-Firuzabad, F. Aminifar, and R. Billinton, "A comprehensive scheme for reliability centered maintenance implementation in power distribution systems- part I: Methodology," *IEEE Transactions on Power Delivery*, vol. 28, no. 2, pp. 761–770, 2013.

- [48] P. Dehghanian, M. Fotuhi-Firuzabad, S. Bagheri-Shoraki, and A. Razi-Kazemi, "Critical component identification in reliability centered asset management of distribution power systems via fuzzy ahp," *IEEE Systems Journal*, vol. 6, no. 4, pp. 593–602, 2012.
- [49] P. Dehghanian, M. Fotuhi-Firuzabad, and A. Razi-Kazemi, "An approach for critical component identification in reliability-centered maintenance of power distribution systems based on analytical hierarchical process," in *The 21st International Conference and Exhibition on Electricity Distribution (CIRED)*, pp. 1–4, 2011.
- [50] P. Dehghanian and M. Fotuhi-Firuzabad, "A reliability-oriented outlook on the critical components of power distribution systems," in *The 9th IET International Conference on Advances in Power System Control, Operation, and Management (APSCOM)*, pp. 1–6, 2011.
- [51] P. Dehghanian, M. Moeini-Aghtaie, M. Fotuhi-Firuzabad, and R. Billinton, "A practical application of the delphi method in maintenance-targeted resource allocation of distribution utilities," in *The 13th International Conference on Probabilistic Methods Applied to Power Systems (PMAPS)*, pp. 1–6, 2014.
- [52] F. Pourahmadi, M. Fotuhi-Firuzabad, and P. Dehghanian, "Identification of critical components in power systems: A game theory application," in *IEEE Industry Application Society (IAS) Annual Meeting*, pp. 1–6, 2016.
- [53] B. Zhang, P. Dehghanian, and M. Kezunovic, "Simulation of weather impacts on the wholesale electricity market," in *10th International Conference on Deregulated Electricity Market Issues in South Eastern Europe (DEMSEE)*, pp. 1–6, 2015.
- [54] T. Dokic, P. Dehghanian, P.-C. Chen, M. Kezunovic, Z. Medina-Cetina, J. Stojanovic, and Z. Obradovic, "Risk assessment of a transmission line insulation breakdown due to lightning and severe weather," in *The 49th Hawaii International Conference on System Science (HICSS)*, pp. 1–8, 2016.
- [55] B. Zhang, P. Dehghanian, and M. Kezunovic, "Spatial-temporal solar power forecast through gaussian conditional random fields," in *IEEE Power and Energy Society (PES) General Meeting*, pp. 1–5, 2016.
- [56] F. Pourahmadi and P. Dehghanian, "A game-theoretic loss allocation approach in power distribution systems with high penetration of distributed generations," *Mathematics*, vol. 6, no. 9, pp. 1–14, 2018.
- [57] F. Pourahmadi, S. H. Hosseini, P. Dehghanian, E. Shittu, and M. Fotuhi-Firuzabad, "Uncertainty cost of stochastic producers: Metrics and impacts on power grid operational flexibility," *IEEE Transactions on Engineering Management*, pp. 1–12, 2020.
- [58] F. Wang, B. Xiang, K. Li, X. Ge, H. Lu, J. Lai, and P. Dehghanian, "Smart households' aggregated capacity forecasting for load aggregators under incentive-based demand

response programs,” *IEEE Transactions on Industry Applications*, vol. 56, pp. 1086–1097, March/April 2020.

- [59] M. Zareian Jahromi, M. Tajdinian, J. Zhao, P. Dehghanian, M. Allahbakhshi, and A. Seifi, “An enhanced sensitivity-based decentralized framework for real-time transient stability assessment in bulk power grids with renewable energy resources,” *IET Generation, Transmission, and Distribution Systems*, vol. 14, pp. 665–674, February 2020.
- [60] M. Moeini-Aghtaie, P. Dehghanian, M. Fotuhi-Firuzabad, and A. Abbaspour, “Multi-agent genetic algorithm: An online probabilistic view on economic dispatch of energy hubs constrained by wind availability,” *IEEE Transactions on Sustainable Energy*, vol. 5, no. 2, pp. 699–708, 2014.
- [61] P. Dehghanian, S. H. Hosseini, M. Moeini-Aghtaie, and S. Arabali, “Optimal siting of dg units in power systems from a probabilistic multi-objective optimization perspective,” *International Journal of Electrical Power and Energy Systems*, vol. 51, pp. 14–26, 2013.
- [62] J. Lai, X. Lu, F. Wang, P. Dehghanian, and R. Tang, “Broadcast gossip algorithms for distributed peer-to-peer control in AC microgrids,” *IEEE Transactions on Industry Applications*, vol. 55, pp. 2241–2251, May/June 2019.
- [63] F. Wang, B. Xiang, K. Li, J. Lai, and P. Dehghanian, “Day-ahead forecast of aggregated loads for smart households under incentive-based demand response programs,” in *IEEE Industry Applications Society (IAS) Annual Meeting*, pp. 1–10, 2019.
- [64] S. Dehghan-Dehnavi, M. Fotuhi-Firuzabad, M. Moeini-Aghtaie, P. Dehghanian, and F. Wang, “Estimating participation abilities of industrial customers in demand response programs: A two-level decision-making tree analysis,” in *IEEE/IAS 56th Industrial and Commercial Power Systems (I&CPS) Technical Conference*, pp. 1–7, 2020.
- [65] F. Pourahmadi, H. Heidarabadi, S. H. Hosseini, and P. Dehghanian, “Dynamic uncertainty set characterization for bulk power grid flexibility assessment,” *IEEE Systems Journal*, vol. 14, pp. 718–728, March 2020.
- [66] R. Azizpanah-Abarghooee, P. Dehghanian, and V. Terzija, “A practical multi-area bi-objective environmental economic dispatch equipped with a hybrid gradient search method and improved jaya algorithm,” *IET Generation, Transmission & Distribution*, vol. 10, no. 14, pp. 3580–3596, 2016.
- [67] M. Khoshjahan, P. Dehghanian, M. Moeini-Aghtaie, and M. Fotuhi-Firuzabad, “Harnessing ramp capability of spinning reserve services for enhanced power system flexibility,” *IEEE Transactions on Industry Applications*, vol. 55, pp. 7103–7112, November/December 2019.

- [68] M. Zareian Jahromi, M. Tajdinian, J. Zhao, P. Dehghanian, M. Allahbakhshi, and A. Seifi, "An enhanced sensitivity-based decentralized framework for real-time transient stability assessment in bulk power grids with renewable energy resources," *IET Generation, Transmission, and Distribution Systems*, vol. 14, pp. 665–674, February 2020.
- [69] M. Tajdinian, M. Allahbakhshi, A. R. Bagheri, H. Samet, P. Dehghanian, and O. P. Malik, "An enhanced sub-cycle statistical algorithm for inrush and fault currents classification in differential protection schemes," *International Journal of Electrical Power and Energy Systems*, vol. 119, pp. 1–17, July 2020.
- [70] Z. Li, K. Li, F. Wang, Z. Mi, and P. Dehghanian, "An auto-encoder neural network approach to monthly electricity consumption forecasting using hourly data," in *IEEE/IAS 56th Industrial and Commercial Power Systems (I&CPS) Technical Conference*, pp. 1–7, 2020.
- [71] P. Dehghanian and M. Kezunovic, "Probabilistic decision making for the bulk power system optimal topology control," *IEEE Transactions on Smart Grid*, vol. 7, no. 4, pp. 2071–2081, 2016.
- [72] P. Dehghanian, Y. Wang, G. Gurralla, E. Moreno-Centeno, and P. Kezunovic, "Flexible implementation of power system corrective topology control," *Electric Power System Research*, vol. 128, pp. 79–89, 2015.
- [73] M. Alhazmi, P. Dehghanian, S. Wang, and B. Shinde, "Power grid optimal topology control considering correlations of system uncertainties," in *IEEE/IAS 55th Industrial and Commercial Power Systems (I&CPS) Technical Conference*, pp. 1–7, 2019.
- [74] M. Kezunovic, T. Popovic, G. Gurralla, P. Dehghanian, A. Esmailian, and M. Tasdighi, "Reliable implementation of robust adaptive topology control," in *The 47th Hawaii International Conference on System Science (HICSS)*, pp. 1–10, 2014.
- [75] P. Dehghanian and M. Kezunovic, "Impact assessment of power system topology control on system reliability," in *IEEE Conference on Intelligent Systems Applications to Power Systems (ISAP)*, pp. 1–6, 2015.
- [76] P. Dehghanian and M. Kezunovic, "Probabilistic impact of transmission line switching on power system operating states," in *IEEE Power and Energy Society (PES) Transmission and Distribution (T&D) Conference and Exposition*, pp. 1–6, 2016.
- [77] M. Alhazmi, P. Dehghanian, S. Wang, and B. Shinde, "Power grid optimal topology control considering correlations of system uncertainties," *IEEE Transactions on Industry Applications*, vol. 55, pp. 5594–5604, November/December 2019.
- [78] M. Nazemi, P. Dehghanian, and M. Lejeune, "A mixed-integer distributionally robust chance-constrained model for optimal topology control in power grids with uncertain renewables," in *13th IEEE Power and Energy Society (PES) PowerTech Conference*, pp. 1–6, 2019.

- [79] H. Tarzamni, E. Babaei, F. Panahandeh Esmaeelnia, P. Dehghanian, S. Tohidi, and M. B. Bannae Sharifian, "Analysis and reliability evaluation of a high step-up soft switching push-pull dc-dc converter," *IEEE Transactions on Reliability*, pp. 1–11, 2020.
- [80] H. Tarzamni, F. Panahandeh Esmaeelnia, M. Fotuhi-Firuzabad, F. Tahami, S. Tohidi, and P. Dehghanian, "Comprehensive analytics for reliability evaluation of conventional isolated multi-switch pwm dc-dc converters," *IEEE Transactions on Power Electronics*, vol. 35, pp. 5254–5266, May 2020.
- [81] T. Becejac and P. Dehghanian, "PMU multilevel end-to-end testing to assess synchrophasor measurements during faults," *IEEE Power and Energy Technology Systems Journal*, vol. 6, pp. 71–80, March 2019.
- [82] S. Wang, P. Dehghanian, and B. Zhang, "A data-driven algorithm for online power grid topology change identification with PMUs," in *IEEE Power and Energy Society (PES) General Meeting*, pp. 1–5, 2019.
- [83] S. Wang, P. Dehghanian, and Y. Gu, "A novel multi-resolution wavelet transform for online power grid waveform classification," in *The 1st IEEE International Conference on Smart Grid Synchronized Measurements and Analytics (SGSMA)*, pp. 1–6, 2019.
- [84] M. Kezunovic, A. Esmaeilian, T. Becejac, P. Dehghanian, and C. Qian, "Life-cycle management tools for synchrophasor systems: Why we need them and what they should entail," in *The 2016 IFAC CIGRE/CIRED Workshop on Control of Transmission and Distribution Smart Grids*, pp. 1–6, CIGRE, 2016.
- [85] T. Becejac, P. Dehghanian, and M. Kezunovic, "Analysis of PMU algorithm errors during fault transients and out-of-step disturbances," in *IEEE Power and Energy Society (PES) Transmission & Distribution (T&D) Conference and Exposition Latin America*, pp. 1–6, 2016.
- [86] T. Becejac, P. Dehghanian, and M. Kezunovic, "Probabilistic assessment of PMU integrity for planning of periodic maintenance and testing," in *International Conference on Probabilistic Methods Applied to Power Systems (PMAPS)*, pp. 1–6, 2016.
- [87] T. Becejac, P. Dehghanian, and M. Kezunovic, "Impact of PMU errors on the synchrophasor-based fault location algorithms," in *48th North American Power Symposium (NAPS)*, pp. 1–6, 2016.
- [88] M. Kezunovic, P. Dehghanian, and J. Sztipanovits, "An incremental system-of-systems integration modelling of cyber-physical electric power systems," in *Grid of the Future Symposium, CIGRE US National Committee*, pp. 1–6, CIGRE, 2016.
- [89] M. H. Rezaeian Koochi, P. Dehghanian, S. Esmaeili, P. Dehghanian, and S. Wang, "A synchrophasor-based decision tree approach for identification of most coherent generating units," in *The 44th Annual Conference of the IEEE Industrial Electronics Society (IECON)*, pp. 1–6, 2018.

- [90] S. Wang, P. Dehghanian, and L. Li, "Power grid online surveillance through PMU-embedded convolutional neural networks," *IEEE Transactions on Industry Applications*, vol. 56, pp. 1146–1155, March/April 2020.
- [91] S. Wang, P. Dehghanian, and Y. Gu, "A novel multi-resolution wavelet transform for online power grid waveform classification," in *The 1st IEEE International Conference on Smart Grid Synchronized Measurements and Analytics (SGSMA)*, pp. 1–6, 2019.
- [92] S. Wang, P. Dehghanian, and B. Zhang, "A data-driven algorithm for online power grid topology change identification with PMUs," in *IEEE Power and Energy Society (PES) General Meeting*, pp. 1–5, 2019.
- [93] S. Wang, L. Li, and P. Dehghanian, "Power grid online surveillance through PMU-embedded convolutional neural networks," in *IEEE Industry Applications Society (IAS) Annual Meeting*, pp. 1–7, 2019.
- [94] A. Razi-Kazemi and P. Dehghanian, "A practical approach to optimal RTU placement in power distribution systems incorporating fuzzy sets theory," *International Journal of Electrical Power and Energy Systems*, vol. 37, no. 1, pp. 31–42, 2012.
- [95] P. Dehghanian, A. Razi-Kazemi, and M. Fotuhi-Firuzabad, "Optimal RTU placement in power distribution systems using a novel method based on analytical hierarchical process (AHP)," in *The 10th International IEEE Conference on Environmental and Electrical Engineering (EEEIC)*, pp. 1–6, 2011.
- [96] M. Moeini-Aghaie, P. Dehghanian, and S. H. Hosseini, "Optimal distributed generation placement in a restructured environment via a multi-objective optimization approach," in *16th Conference on Electric Power Distribution Networks (EPDC)*, pp. 1–6, 2011.
- [97] A. Razi-Kazemi, P. Dehghanian, and G. Karami, "A probabilistic approach for remote terminal unit placement in power distribution systems," in *The 33rd IEEE International Telecommunications Energy Conference (INTELEC)*, pp. 1–6, 2011.
- [98] P. Dehghanian, A. Razi-Kazemi, and G. Karami, "Incorporating experts knowledge in RTU placement procedure using fuzzy sets theory- a practical approach," in *The 33rd IEEE International Telecommunications Energy Conference (INTELEC)*, pp. 1–6, 2011.
- [99] M. Shojaei, V. Rastegar-Moghaddam, A. Razi-Kazemi, P. Dehghanian, and G. Karami, "A new look on the automation of medium voltage substations in power distribution systems," in *17th Conference on Electric Power Distribution Networks (EPDC)*, pp. 1–6, 2012.
- [100] M. A. Saffari, M. S. Misaghian, M. Kia, Heidari, and P. Dehghanian, "Robust/stochastic optimization of energy arbitrage in smart microgrids using electric vehicles," *Electric Power Systems Research*, vol. 174, pp. 1–14, September 2019.

- [101] M. Moeini-Aghtaie, A. Abbaspour, M. Fotuhi-Firuzabad, and P. Dehghanian, "Optimized probabilistic phev demand management in the context of energy hubs," *IEEE Transactions on Power Delivery*, vol. 30, no. 2, pp. 996–1006, 2015.
- [102] M. Moeini-Aghtaie, A. Abbaspour, M. Fotuhi-Firuzabad, and P. Dehghanian, "Phev's centralized/decentralized charging control mechanisms: Requirements and impacts," in *The 45th North American Power Symposium (NAPS)*, pp. 1–6, 2013.
- [103] M. S. Misaghian, M. Saffari, M. Kia, A. Heidari, P. Dehghanian, and B. Wang, "Electric vehicles contributions to voltage improvement and loss reduction in microgrids," in *North American Power Symposium (NAPS)*, pp. 1–6, 2018.
- [104] B. Wang, P. Dehghanian, and D. Zhao, "Chance-constrained energy management system for power grids with high proliferation of renewables and electric vehicles," *IEEE Transactions on Smart Grid*, pp. 1–13, 2020.
- [105] B. Wang, D. Zhao, P. Dehghanian, Y. Tian, and T. Hong, "Aggregated electric vehicle load modeling in large-scale electric power systems," *IEEE Transactions on Industry Applications*, pp. 1–14, 2020.
- [106] P. Jamborsalamati, M. Hossain, S. Taghizadeh, A. Sadu, G. Konstantinou, M. Manbachi, and P. Dehghanian, "Enhancing power grid resilience through an IEC61850-based ev-assisted load restoration," *IEEE Transactions on Industrial Informatics*, vol. 16, pp. 1799–1810, March 2020.
- [107] B. Wang, P. Dehghanian, D. Hu, and S. Wang, "Adaptive operation strategies for electric vehicle charging stations," in *IEEE Industry Applications Society (IAS) Annual Meeting*, pp. 1–7, 2019.
- [108] E. National Academies of Sciences, Medicine, *et al.*, *Enhancing the resilience of the Nation's electricity system*. National Academies Press, 2017.
- [109] B. Zhang, P. Dehghanian, and M. Kezunovic, "Optimal allocation of PV generation and battery storage for enhanced resilience," *IEEE Transactions on Smart Grid*, vol. 10, no. 1, pp. 535–545, 2017.
- [110] M. Nazemi, M. Moeini-Aghtaie, M. Fotuhi-Firuzabad, and P. Dehghanian, "Energy storage planning for enhanced resilience of power distribution networks against earthquakes," *IEEE Transactions on Sustainable Energy*, vol. 11, pp. 795–806, April 2020.
- [111] P. Dehghanian, S. Aslan, and P. Dehghanian, "Quantifying power system resiliency improvement using network reconfiguration," in *IEEE 60th International Midwest Symposium on Circuits and Systems (MWSCAS)*, pp. 1–5, 2017.
- [112] P. Interconnection, "Pjm's evolving resource mix and system reliability," *March*, vol. 30, p. 2017, 2017.

- [113] B. H. Obama, “Critical infrastructure security and resilience,” *Presidential Policy Directive/PPD-21*, 2013.
- [114] M. Chaudry, P. Ekins, K. Ramachandran, A. Shakoor, J. Skea, G. Strbac, X. Wang, and J. Whitaker, “Building a resilient uk energy system,” 2011.
- [115] H. H. Willis and K. Loa, “Measuring the resilience of energy distribution systems,” *RAND Corporation: Santa Monica, CA, USA*, 2015.
- [116] A. Berkeley, M. Wallace, and C. COO, “A framework for establishing critical infrastructure resilience goals,” *Final Report and Recommendations by the Council, National Infrastructure Advisory Council*, 2010.
- [117] C. Office, “Keeping the country running: natural hazards and infrastructure,” 2011.
- [118] M. McGranaghan, M. Olearczyk, and C. Gellings, “Enhancing distribution resiliency: Opportunities for applying innovative technologies,” *EPRI: Palo Alto, CA, USA*, 2013.
- [119] M. Panteli, D. N. Trakas, P. Mancarella, and N. D. Hatziargyriou, “Power systems resilience assessment: Hardening and smart operational enhancement strategies,” *Proceedings of the IEEE*, vol. 105, no. 7, pp. 1202–1213, 2017.
- [120] C. DoD, “Department of defense global information grid architectural vision,” 2007. Accessed: 2019.
- [121] J. Emanuelson, “E1, E2 and E3.” [Online] Available at: <http://www.futurescience.com/emp/E1-E2-E3.html>, Accessed: 2019.
- [122] J. Venable, “Electromagnetic Pulse Would Devastate Our Power Grid,” 2018. The Daily Signal, [Online].
- [123] E. S. William Radasky, “Intentional Electromagnetic Interference (IEMI) and Its Impact on the U.S. Power Grid,” 2010. Accessed: 2019.
- [124] T. Harris, “How e-bombs work,” 2003. [Online] Available at: <https://science.howstuffworks.com/e-bomb.htm>, Accessed: 2019.
- [125] K. Berent, “Electromagnetic Pulse (EMP) Grid Resiliency Project,” tech. rep., Electric Power Research Institute, 2016.
- [126] Executive Office of the President, “National electric grid security and resilience action plan,” 2016. [Online] Available at: <https://www.hsd1.org/?abstract&did=797486>, Accessed: 2019.
- [127] National Coordinating Center for Communications (NCC), “Electromagnetic Pulse (EMP) Protection and Resilience Guidelines for Critical Infrastructure and Equipment,” 2019. [Online] Available at: https://www.dhs.gov/sites/default/files/publications/19_0307_CISA_EMP-Protection-Resilience-Guidelines.pdf, Accessed: 2019.

- [128] E. Savage, J. Gilbert, and W. Radasky, “The Early-Time (E1) High-altitude Electromagnetic Pulse (HEMP) and Its Impact on the US Power Grid,” *Report Meta-R-320 for Oak Ridge National Laboratory*, 2010.
- [129] U.S. Food and Drug Administration, “Electromagnetic Compatibility (EMP).” <https://www.fda.gov/radiation-emitting-products/radiation-safety/electromagnetic-compatibility-emc>. Accessed: 2018.
- [130] S. Miyata, Y. Kayano, and H. Inoue, “Em radiation through aperture of metallic enclosure with a pcb inside,” in *2008 Asia-Pacific Symposium on Electromagnetic Compatibility and 19th International Zurich Symposium on Electromagnetic Compatibility*, pp. 658–661, IEEE, 2008.
- [131] D. of Defence, “Mil-std-188/125, military standard: High-altitude electromagnetic pulse (hemp) protection for ground-based c4i facilities performing critical,” 1998. Accessed: 2019.
- [132] D. of Defense Interface Standard MIL-STD-461-G: 2015, “Requirements for the control of electromagnetic interference characteristics of subsystems and equipment,” Dec. 2015. Accessed: 2020.
- [133] D. I. Standard, “Electromagnetic environmental effects requirements for systems,” tech. rep., DOD MIL-STD-464C, 2010.
- [134] H. Shen, Z. Wang, and W. Zheng, “Pcb level si simulation based on ibis model for high-speed fpga system,” in *2009 9th International Conference on Electronic Measurement & Instruments*, pp. 4–74, IEEE, 2009.
- [135] T. Burghart, H. Rossmann, and G. Schubert, “Evaluating the rf-emissions of automotive cable harness,” in *2004 International Symposium on Electromagnetic Compatibility (IEEE Cat. No. 04CH37559)*, vol. 3, pp. 787–791, IEEE, 2004.
- [136] M. Schwark, A. Junge, and R. Keibel, “Vhf interference measurements on cable harnesses in passenger cabins of airplanes,” *IEEE Transactions on Electromagnetic Compatibility*, vol. 50, no. 3, pp. 536–541, 2008.
- [137] H. Rebholz and S. Tenbohlen, “A fast radiated emission model for arbitrary cable harness configurations based on measurements and simulations,” in *2008 IEEE International Symposium on Electromagnetic Compatibility*, pp. 1–5, IEEE, 2008.
- [138] S. Alexandersson and H. Bangtsson, “Analytic prediction of electromagnetic behaviour,” in *2008 International Symposium on Power Electronics, Electrical Drives, Automation and Motion*, pp. 338–343, IEEE, 2008.
- [139] M. P. Robinson, T. M. Benson, C. Christopoulos, J. F. Dawson, M. Ganley, A. Marvin, S. Porter, and D. W. Thomas, “Analytical formulation for the shielding effectiveness of enclosures with apertures,” *IEEE transactions on Electromagnetic Compatibility*, vol. 40, no. 3, pp. 240–248, 1998.

- [140] S. Ali, D. S. Weile, and T. Clupper, "Effect of near field radiators on the radiation leakage through perforated shields," *IEEE transactions on electromagnetic compatibility*, vol. 47, no. 2, pp. 367–373, 2005.
- [141] M. Li, J. Nuebel, J. L. Drewniak, R. E. DuBroff, T. H. Hubing, and T. P. Van Doren, "Emi from cavity modes of shielding enclosures-fdtd modeling and measurements," *IEEE Transactions on Electromagnetic Compatibility*, vol. 42, no. 1, pp. 29–38, 2000.
- [142] C. H. Kraft, "Modeling leakage through finite apertures with tlm," in *Proceedings of IEEE Symposium on Electromagnetic Compatibility*, pp. 73–76, IEEE, 1994.
- [143] C.-H. Liang and D. Cheng, "Electromagnetic fields coupled into a cavity with a slot-aperture under resonant conditions," *IEEE Transactions on Antennas and Propagation*, vol. 30, no. 4, pp. 664–672, 1982.
- [144] A. Renko, A. Arslan, S. Yuferev, and M. Uusimaki, "3d electromagnetic modeling and design flow in system level," in *2003 IEEE International Symposium on Electromagnetic Compatibility, 2003. EMC'03.*, vol. 2, pp. 1077–1080, IEEE, 2003.
- [145] F. Sabath, "Classification of electromagnetic effects at system level," in *2008 International Symposium on Electromagnetic Compatibility-EMC Europe*, pp. 1–5, IEEE, 2008.
- [146] M. Apra, M. D'Amore, K. Gigliotti, M. S. Sarto, and V. Volpi, "Lightning indirect effects certification of a transport aircraft by numerical simulation," *IEEE Transactions on Electromagnetic Compatibility*, vol. 50, no. 3, pp. 513–523, 2008.
- [147] P. D. Kannu and M. J. Thomas, "Lightning-induced voltages in a satellite launch-pad protection system," *IEEE transactions on electromagnetic compatibility*, vol. 45, no. 4, pp. 644–651, 2003.
- [148] C. Christopoulos, A. Mallik, P. Naylor, and P. Johns, "Computer modelling for vehicle electromagnetic compatibility," in *IEE Colloquium on Vehicle Electromagnetic Compatibility*, pp. 5–1, IET, 1988.
- [149] C. Wenqing, S. Donglin, S. Wei, and H. Yanchun, "The behavioral simulation of emi system by dna method at the system level," in *2008 IEEE International Symposium on Electromagnetic Compatibility*, pp. 1–3, IEEE, 2008.
- [150] N. Instruments, "Simulation and analysis guide," 2019. Accessed: 2019.
- [151] X. B.-B. Z. Qibin Z, Yize S, "Simulation and protection of lightning electromagnetic pulse in non-metallic nacelle of wind turbine," pp. 1–10, 2019. Accessed: 2020.
- [152] K. M.-Z. M. Samak MMEA, Bakar AAA, "Comprehensive Numerical Analysis of Finite Difference Time Domain Methods for Improving Optical Waveguide Sensor Accuracy," 2016. Accessed: 2019.

- [153] D. H. Boteler and R. J. Pirjola, “Modelling geomagnetically induced currents produced by realistic and uniform electric fields,” *IEEE Transactions on Power Delivery*, vol. 13, pp. 1303–1308, Oct 1998.
- [154] T. J. Overbye, T. R. Hutchins, K. Shetye, J. Weber, and S. Dahman, “Integration of geomagnetic disturbance modeling into the power flow: A methodology for large-scale system studies,” in *2012 North American Power Symposium (NAPS)*, pp. 1–7, Sep. 2012.
- [155] R. A. Walling, “Potential impacts of harmonics on bulk system integrity during geomagnetic disturbances,” in *2013 IEEE Power Energy Society General Meeting*, pp. 1–5, July 2013.
- [156] V. D. Albertson, J. M. Thorson, R. E. Clayton, and S. C. Tripathy, “Solar-induced-currents in power systems: Cause and effects,” *IEEE Transactions on Power Apparatus and Systems*, vol. PAS-92, pp. 471–477, March 1973.
- [157] Xuzhu Dong, Yilu Liu, and J. G. Kappenman, “Comparative analysis of exciting current harmonics and reactive power consumption from gic saturated transformers,” in *2001 IEEE Power Engineering Society Winter Meeting. Conference Proceedings*, vol. 1, pp. 318–322, Jan 2001.
- [158] X. Kong and Y. Xie, “An active e-field sensor based on laser diode for EMP measurement,” in *2014 XXXIth URSI General Assembly and Scientific Symposium (URSI GASS)*, pp. 1–4, Aug 2014.
- [159] J. G. Kappenman, V. D. Albertson, and N. Mohan, “Current transformer and relay performance in the presence of geomagnetically-induced currents,” *IEEE Transactions on Power Apparatus and Systems*, vol. PAS-100, pp. 1078–1088, March 1981.
- [160] P. Ripka, K. Draxler, and R. Styblikova, “Measurement of dc currents in the power grid by current transformer,” *IEEE Transactions on Magnetics*, vol. 49, pp. 73–76, Jan 2013.
- [161] T. Breckenridge, T. Cumming, and J. Merron, “Geomagnetic induced current detection and monitoring,” 2001.
- [162] C. C. S. Technology, “Cst studio suite.” <https://www.cst.com>. Accessed: 2019.
- [163] J. Legro, N. Abi-Samra, and F. Tesche, “Study to assess the effects of magnetohydrodynamic electromagnetic pulse on electric power systems. phase i, final report. volume 3,” tech. rep., Westinghouse Electric Corp., Pittsburgh, PA (USA). Advanced Systems, 1985.
- [164] “Electromagnetic compatibility (emc), part 2: Environment—section 9: Description of hamp environment—radiated disturbance,” *International Electrotechnical Commission, IEC61000-2-9*, 1996.

- [165] E. W. C. NEHRING, “Acsr – aluminum conductor steel reinforced.” [Online] Available at: <http://www.nehringwire.com/aluminum/bare-aluminum-and-acsr/acsr-aluminum-conductor-steel-reinforced>, Accessed: 2019.
- [166] J. Oakley, “Simulation of electromagnetic pulses (emp),” May 14, 2019. Accessed: 2019.
- [167] J. L. Gannon, A. Swidinsky, and Z. Xu, *Geomagnetically Induced Currents from the Sun to the Power Grid*. Wiley Online Library, 2019.
- [168] T. J. Overbye, K. S. Shetye, T. R. Hutchins, Q. Qiu, and J. D. Weber, “Power grid sensitivity analysis of geomagnetically induced currents,” *IEEE Transactions on Power Systems*, vol. 28, no. 4, pp. 4821–4828, 2013.
- [169] Geospatial time-varying surface electric fields developed from National Science Foundation, Award Number 1520864; T. J. Overbye, PhD, Texas A&M University, Principal Investigator; J. Gannon, PhD, Computational Physics, Inc., Contributor, Accessed: 2019.
- [170] F. M. T. O. R. N. L. P. S. T. P. E. D. J. R. Legro, N. C. Abi-Samra, “Study to assess the effects of magnetohydrodynamic electromagnetic pulse on electric power systems: Phase i, final report,” 1985. Accessed: 2020.
- [171] T. J. Overbye, “Pserc tutorial: High altitude electromagnetic pulse (hemp) impacts on the grid,” 2016. Accessed: 2020.
- [172] J. Allen, H. Sauer, L. Frank, and P. Reiff, “Effects of the march 1989 solar activity,” *Eos, Transactions American Geophysical Union*, vol. 70, no. 46, pp. 1479–1488, 1989.
- [173] N. Chandler, “How faraday cages work.” [Online] Available at: <https://science.howstuffworks.com/faraday-cage.htm>, Accessed: 2019.
- [174] Meteolabor, “Lighting and EMP protection devices,” 2016. [Online] Available at: http://www.meteolabor.ch/fileadmin/user_upload/pdf/SuccessStory/EMP-Standard.pdf, Accessed: 2019.
- [175] Meteolabor, “MAK modular attachment kit,” 2019. [Online] Available at: http://www.meteolabor.ch/fileadmin/user_upload/pdf/SuccessStory/Meteolabor-MAK-Catalog-R2-2019_e_d.pdf.
- [176] “The Worlds First Entire Home EMP protection Device | EMP Shield.” [Online] Available at: <https://empshield.com>, Accessed: 2019.
- [177] U.S. Department of Homeland Security, “Strategy for protecting and preparing the homeland against threats of electromagnetic pulse and geomagnetic disturbances,” 2018. [Online] Available at: <https://www.hsd1.org/?abstract&did=817225>, Accessed: 2019.

- [178] ETS-Lindgren, “Solutions for electromagnetic pulse (EMP),” 2018.
[Online] Available at: http://www.ets-lindgren.com/sites/etsauthor/General_Brochures/EMP_General_brochure.pdf, Accessed: 2019.
- [179] Y.-N. Li and Z.-L. Tan, “front-end electromagnetic protection module based on vhf communication,” in *2018 International Conference on Electronics Technology (ICET)*, pp. 142–146, IEEE, 2018.
- [180] “Environmental management plan (emp).” [Online] Available at: <https://newmachineparts.blogspot.com/2015/12/environmental-management-plan-emp.html>, Accessed:2020.
- [181] “Emp protection construction.” [Online] Available at: <http://www.dynamicshielding.com/emp-protection/emp-protection-construction>, Accessed:2020.
- [182] M. P. Robinson, T. M. Benson, C. Christopoulos, J. F. Dawson, M. Ganley, A. Marvin, S. Porter, and D. W. Thomas, “Analytical formulation for the shielding effectiveness of enclosures with apertures,” *IEEE transactions on Electromagnetic Compatibility*, vol. 40, no. 3, pp. 240–248, 1998.
- [183] M. Kazerooni, H. Zhu, and T. J. Overbye, “Mitigation of geomagnetically induced currents using corrective line switching,” *IEEE Transactions on Power Systems*, vol. 33, pp. 2563–2571, May 2018.
- [184] H. Zhu and T. J. Overbye, “Blocking device placement for mitigating the effects of geomagnetically induced currents,” *IEEE Transactions on Power Systems*, vol. 30, no. 4, pp. 2081–2089, 2014.
- [185] A. H. Etemadi and A. Rezaei-Zare, “Optimal placement of gic blocking devices for geomagnetic disturbance mitigation,” *IEEE Transactions on Power Systems*, vol. 29, no. 6, pp. 2753–2762, 2014.
- [186] B. Kovan and F. de León, “Mitigation of geomagnetically induced currents by neutral switching,” *IEEE Transactions on Power Delivery*, vol. 30, pp. 1999–2006, Aug 2015.